



**Karolinska  
Institutet**

Department of Laboratory Medicine, Clinical Research Center, Experimental  
Cancer Medicine

## **GENETIC AND METABOLIC STUDIES TOWARDS PERSONALIZED CONDITIONING REGIMEN PRIOR TO STEM CELL TRANSPLANTATION**

AKADEMISK AVHANDLING

som för avläggande av medicine doktorexamen vid Karolinska Institutet  
offentligen försvaras i R64, Karolinska Universitetssjukhuset, Huddinge

**Fredagen den 5 September, 2014, kl 09:30**

av

**Ibrahim El-Serafi**  
MD

*Principal Supervisor:*

Prof. Moustapha Hassan  
Karolinska Institutet  
Department of Laboratory Medicine  
Division of Clinical research center

*Co-supervisor(s):*

Ass. Prof. Zuzana Potáčová  
Karolinska Institutet  
Department of Laboratory Medicine  
Division of Clinical research center

Dr. Ylva Terelius  
Medivir AB  
Department Discovery research

*Opponent:*

Prof. Jeannine McCune  
University of Washington  
Department of Pharmacy

*Examination Board:*

Prof. Curt Pettersson  
Uppsala University  
Department of Medicinal Chemistry  
Division of Analytical Pharmaceutical Chemistry

Prof. Marja-Liisa Dahl  
Karolinska Institutet  
Department of Laboratory Medicine  
Division of Clinical pharmacology

Ass. Prof. Inger Johansson  
Karolinska Institutet  
Department of Physiology and Pharmacology  
Division of Pharmacogenetics

Stockholm 2014

## ABSTRACT

Hematopoietic stem cell transplantation (HSCT) is a curative treatment for several malignant and non-malignant diseases. The busulphan (Bu)/cyclophosphamide (Cy) combination is one of the most common conditioning regimens given prior to HSCT.

The general aim of the present thesis is to investigate the molecular mechanisms underlying the metabolism of the Bu/Cy conditioning regimen in order to personalize the treatment and improve the clinical outcome.

To follow the metabolic pathway of busulphan, a new gas chromatography-mass spectrometry (GC-MS) method was developed and validated for the quantification and detection of busulphan and its four major metabolites.

Incubation of the first core metabolite of busulphan, tetrahydrothiophene (THT), with human liver microsomes or recombinant enzymes has resulted in the formation of subsequent metabolites. The highest initial THT disappearance rate and the highest  $CL_{int}$  value were observed with FMO3 followed by several CYPs indicating that FMO3 and, to a lesser extent, CYPs are involved in the metabolic pathway of busulphan. Moreover, FMO3 inhibition significantly ( $P < 0.05$ ) affected Bu and THT kinetics in mice. In patients, *FMO3* expression was significantly ( $P < 0.05$ ) up-regulated during Bu treatment.

In order to personalize oral Bu dosage, a reliable limited sampling model was developed and evaluated in both adult and pediatric patients.

To understand the role of cyclophosphamide in the conditioning regimen, the gene expression profile over two days of Cy treatment was investigated, where 299 genes were found to be specifically affected by the treatment. Cyclophosphamide down-regulated the expression of several genes mapped to immune/autoimmune activation and graft rejection including *CD3*, *CD28*, *CTLA4* and *IL2R*, and up-regulated immune-related receptor genes, e.g. *IL1R2*, *IL18R1*, and *FLT3*.

Significant ( $P < 0.01$ ) up-regulation, with high inter-individual variation, of the cytochrome P450 oxidoreductase (*POR*) gene was also observed during Cy treatment. *In vitro*, different batches of CYP2B6.1, with different ratios of POR/CYP, showed positive correlation between the intrinsic clearance ( $V_{max}/K_m$ ) and the POR/CYP ratio for the Cy 4-hydroxylation.

Further analysis of the above mentioned patients, prior to Cy treatment, revealed that *CYP2J2* mRNA expression was significantly ( $P < 0.01$ ) higher compared to healthy controls. *CYP2J2* expression was further up-regulated during Cy treatment, with high inter-individual variation. Repeated treatment with Cy resulted in an increased 4-OH-Cy/Cy ratio, indicating auto-induction of Cy-metabolism.

The viability of HL-60 cells, lacking CYP2B6 but expressing *CYP2J2*, was reduced after incubation with Cy. Inhibition of *CYP2J2* reduced 4-OH-Cy formation and improved HL-60 cell survival. Cy incubation with recombinant *CYP2J2* confirmed that *CYP2J2* is involved in Cy bioactivation.

In summary, the present results have improved our understanding of the Bu/Cy metabolism. This knowledge may help to interpret several interactions, high inter-individual variability, adverse effects and unexpected toxicity observed during and/or after the conditioning regimen. This certainly will help in developing new strategies for personalized medicine and thus improve clinical outcome.

From Department of Laboratory Medicine  
Clinical Research Center – Experimental Cancer Medicine  
Karolinska Institutet, Stockholm, Sweden

**GENETIC AND METABOLIC STUDIES  
TOWARDS PERSONALIZED  
CONDITIONING REGIMEN PRIOR TO  
STEM CELL TRANSPLANTATION**

Ibrahim El-Serafi



**Karolinska  
Institutet**

Stockholm 2014

All previously published papers were reproduced with permission from the publisher.

Cover picture shows a ribbon representation of human microsomal CYP2B6, generated by *Neera Borkakoti*, using Maestro (Schrodinger) on the X-ray coordinates available in the public protein structure database RCSB.

Published by Karolinska Institutet

Printed by US-AB Universitetservice

© Ibrahim El-Serafi, 2014

ISBN 978-91-7549-589-7

*To my lovely family ♥*



“Research is not a job, research is a life style”

*Moustapha Hassan*





## ABSTRACT

Hematopoietic stem cell transplantation (HSCT) is a curative treatment for several malignant and non-malignant diseases. The busulphan (Bu)/cyclophosphamide (Cy) combination is one of the most common conditioning regimens given prior to HSCT.

The general aim of the present thesis is to investigate the molecular mechanisms underlying the metabolism of the Bu/Cy conditioning regimen in order to personalize the treatment and improve the clinical outcome.

To follow the metabolic pathway of busulphan, a new gas chromatography-mass spectrometry (GC-MS) method was developed and validated for the quantification and detection of busulphan and its four major metabolites.

Incubation of the first core metabolite of busulphan, tetrahydrothiophene (THT), with human liver microsomes or recombinant enzymes has resulted in the formation of subsequent metabolites. The highest initial THT disappearance rate and the highest  $CL_{int}$  value were observed with FMO3 followed by several CYPs indicating that FMO3 and, to a lesser extent, CYPs are involved in the metabolic pathway of busulphan. Moreover, FMO3 inhibition significantly ( $P < 0.05$ ) affected Bu and THT kinetics in mice. In patients, *FMO3* expression was significantly ( $P < 0.05$ ) up-regulated during Bu treatment.

In order to personalize oral Bu dosage, a reliable limited sampling model was developed and evaluated in both adult and pediatric patients.

To understand the role of cyclophosphamide in the conditioning regimen, the gene expression profile over two days of Cy treatment was investigated, where 299 genes were found to be specifically affected by the treatment. Cyclophosphamide down-regulated the expression of several genes mapped to immune/autoimmune activation and graft rejection including *CD3*, *CD28*, *CTLA4* and *IL2R*, and up-regulated immune-related receptor genes, e.g. *IL1R2*, *IL18R1*, and *FLT3*.

Significant ( $P < 0.01$ ) up-regulation, with high inter-individual variation, of the cytochrome P450 oxidoreductase (*POR*) gene was also observed during Cy treatment. *In vitro*, different batches of CYP2B6.1, with different ratios of POR/CYP, showed positive correlation between the intrinsic clearance ( $V_{max}/K_m$ ) and the POR/CYP ratio for the Cy 4-hydroxylation.

Further analysis of the above mentioned patients, prior to Cy treatment, revealed that *CYP2J2* mRNA expression was significantly ( $P < 0.01$ ) higher compared to healthy controls. *CYP2J2* expression was further up-regulated during Cy treatment, with high inter-individual variation. Repeated treatment with Cy resulted in an increased 4-OH-Cy/Cy ratio, indicating auto-induction of Cy-metabolism.

The viability of HL-60 cells, lacking CYP2B6 but expressing *CYP2J2*, was reduced after incubation with Cy. Inhibition of *CYP2J2* reduced 4-OH-Cy formation and improved HL-60 cell survival. Cy incubation with recombinant *CYP2J2* confirmed that *CYP2J2* is involved in Cy bioactivation.

In summary, the present results have improved our understanding of the Bu/Cy metabolism. This knowledge may help to interpret several interactions, high inter-individual variability, adverse effects and unexpected toxicity observed during and/or after the conditioning regimen. This certainly will help in developing new strategies for personalized medicine and thus improve clinical outcome.



## LIST OF SCIENTIFIC PAPERS

- I. Gas chromatographic- Mass spectrometry method for the detection of busulphan and its metabolites in plasma and urine  
**IBRAHIM EL-SERAFI**, Ylva Terelius, Brigitte Twelkmeyer, Ann-Louise Hagbjörk, Zuzana Hassan and Moustapha Hassan  
*Journal of Chromatography B*, 2013, Volume 913 – 914, Page 98 – 105
- II. Flavin-containing monooxygenase 3 (FMO3) is important in busulphan metabolic pathway  
**IBRAHIM EL-SERAFI**, Seán Naughton, Maryam Saghafian, Manuchehr Abedi-Valugerdi, Jonas Mattsson, Ann-Louise Hagbjörk, Parvaneh Afsharian, Ylva Terelius, Ali Moshfegh, Zuzana Potáčová and Moustapha Hassan  
(*Manuscript*)
- III. Comparison of algorithms for oral busulphan area under the concentration-time curve limited sampling estimate  
Fredrik Sjöo, **IBRAHIM EL-SERAFI**, Jon Enestig, Jonas Mattsson, Johan Liwing and Moustapha Hassan  
*Clinical Drug Investigation*, 2014, Volume 34, Issue 1, pp 43-52
- IV. Cyclophosphamide alters the gene expression profile in patients treated with high doses prior to stem cell transplantation  
**IBRAHIM EL-SERAFI**, Manuchehr Abedi-Valugerdi, Zuzana Potáčová, Parvaneh Afsharian, Jonas Mattsson, Ali Moshfegh and Moustapha Hassan  
*PLoS ONE*, 2014, Volume 9, Issue 1, e86619
- V. The role of human CYP2B6 polymorphism and cytochrome P450 oxidoreductase in the bioactivation of cyclophosphamide  
**IBRAHIM EL-SERAFI**, Parvaneh Afsharian, Ali Moshfegh, Moustapha Hassan and Ylva Terelius  
(*Submitted*)
- VI. CYP2J2 is a new key enzyme in cyclophosphamide bioactivation  
**IBRAHIM EL-SERAFI**, Mona Fares, Manuchehr Abedi-Valugerdi, Parvaneh Afsharian, Ali Moshfegh, Ylva Terelius, Zuzana Potáčová and Moustapha Hassan  
(*Submitted*)

## RELATED PUBLICATIONS NOT INCLUDED IN THE THESIS

- I. Pharmacokinetics and biodistribution of the cyclin-dependent kinase inhibitor - CR8- in mice  
Hattem Sallam, **IBRAHIM EL-SERAFI**, Laurent Meijer and Moustapha Hassan  
*BMC Pharmacology and Toxicology* 2013, 14:50
- II. Biodegradable polymeric vesicles containing magnetic nanoparticles, quantum dots and anticancer drugs for drug delivery and imaging.  
Fei Ye, Åsa Barrefelt, Heba Asem, Manuchehr Abedi-Valugerdi, **IBRAHIM EL-SERAFI**, Maryam Saghafian, Khalid Abu-Salah, Salman Alrokayan, Mamoun Muhammed, Moustapha Hassan  
*Biomaterials* 2014 Apr;35(12):3885-94
- III. Posaconazole Concentrations in Human Tissues after Allogeneic Stem Cell Transplantation.  
Ola Blennow, Erik Eliasson, Tommy Pettersson, Anton Pohanka, Attila Szakos, **IBRAHIM EL-SERAFI**, Moustapha Hassan, Olle Ringdén, and Jonas Mattsson  
*Antimicrob Agents Chemother* 2014 Aug;58(8):4941-4943. Epub 2014 Jun 2.
- IV. Quantitative method for the determination of posaconazole in mouse organ tissues using liquid chromatography-mass spectrometry  
**IBRAHIM EL-SERAFI** \*, Tommy Pettersson\*, Ola Blennow, Jonas Mattsson, Erik Eliasson, Anton Pohanka, and Moustapha Hassan  
*Accepted. Journal of Analytical & Bioanalytical Techniques* 2014.

# CONTENTS

1	Introduction .....	1
1.1	Hematological malignancy.....	2
1.2	Hematopoietic stem cell transplantation.....	3
1.2.1	Conditioning regimen .....	3
1.3	Cytostatics.....	5
1.3.1	Busulphan .....	5
1.3.2	Cyclophosphamide.....	5
1.4	Metabolism of cytostatics.....	6
1.4.1	Cytochrome P450.....	6
1.4.2	Glutathione conjugation.....	7
1.4.3	Busulphan metabolism.....	8
1.4.4	Cyclophosphamide metabolism.....	10
1.5	Significance .....	13
2	Aim of the thesis.....	15
2.1	General aim.....	15
2.2	Specific aims.....	15
3	Patients and methods.....	17
3.1	Chemicals .....	17
3.2	Patient population.....	18
3.2.1	Blood sampling .....	18
3.2.2	RNA extraction and cDNA preparation .....	19
3.2.3	Gene array and genotyping .....	19
3.2.4	Real time PCR.....	19
3.3	Studies in mice.....	21
3.4	Studies in HL-60 cell line.....	22
3.5	Studies in microsomes.....	23
3.5.1	Busulphan metabolism.....	23
3.5.2	Cyclophosphamide metabolism.....	23
3.6	Measurement of busulphan and its metabolites.....	25
3.6.1	Busulphan .....	25
3.6.2	Tetrahydrothiophene and sulfolane .....	25
3.6.3	Tetrahydrothiophene 1-oxide and 3-hydroxysulfolane.....	25
3.7	Measurement of cyclophosphamide and its active metabolite.....	26
3.8	Validation of the method for quantification of busulphan and its metabolites .....	26
3.8.1	Stock solutions .....	27
3.8.2	Conduct of validation.....	27
3.8.3	Clinical application .....	27
3.9	Limited sampling model development .....	28
3.9.1	Model building .....	28

3.9.2	Assay methodology.....	31
3.9.3	Computer program .....	32
3.9.4	Statistical analysis .....	32
3.10	Data analysis.....	33
4	Results .....	35
4.1	Busulphan .....	35
4.1.1	Method development and validation .....	35
4.1.2	Enzymes involved in busulphan metabolic pathway .....	38
4.1.3	Development of busulphan limited sampling model .....	42
4.2	Cyclophosphamide .....	45
4.2.1	Identification of differentially expressed genes and gene clusters related to cyclophosphamide treatment.....	45
4.2.2	The role of POR in cyclophosphamide bioactivation .....	51
4.2.3	The role of CYP2J2 in cyclophosphamide bioactivation .....	55
5	Discussion.....	61
6	Conclusion.....	71
7	Future perspectives.....	72
8	Acknowledgements .....	73
9	References .....	77

## LIST OF ABBREVIATIONS

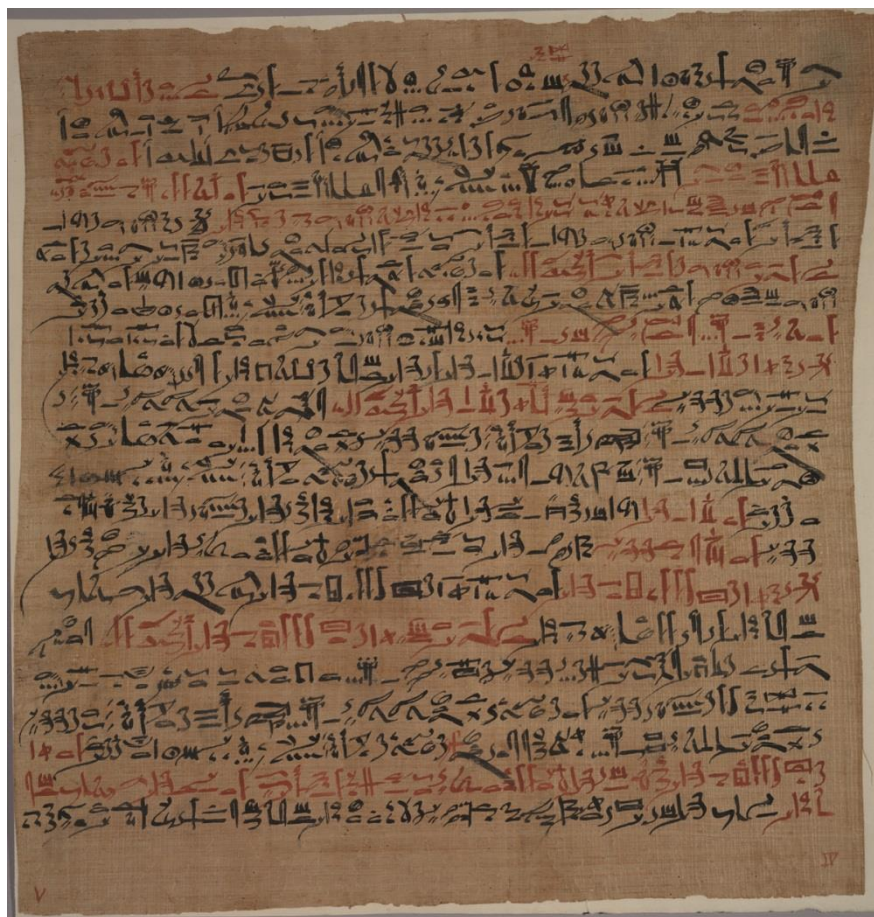
3-OH-sulfolane	3-hydroxy-sulfolane
4-OH-Cy	4-hydroxy-cyclophosphamide
ACN	Acetonitrile
AUC	Area under the concentration-time curve
AML	Acute Myeloid Leukemia
Bu	Busulphan
cDNA	Complementary DNA
$CL_{int}$	The intrinsic clearance
Cy	Cyclophosphamide
CYP	Cytochrome P450
DPBS	Dulbecco's phosphate buffered saline
DMSO	Dimethyl sulfoxide
FMO	Flavin-containing monooxygenase
GC	Gas chromatography
GC-MS	Gas chromatography- Mass spectrometry
GSH	Glutathione
GST	Glutathione S-transferase
GVHD	Graft-versus-host disease
HLM	Human liver microsomes

HPLC	High performance liquid chromatography
HSCT	Hematopoietic stem cell transplantation
$IC_{50}$	Half-maximal inhibitory concentration
$K_m$	Michaelis constant
LLOQ	Lower limit of quantification
LSM	Limited sampling model
MUD	Matched unrelated donor
$\beta$ -NADPH	$\beta$ -Nicotinamide adenine dinucleotide phosphate
PCR	Polymerase chain reaction
POR	Cytochrome P450 oxidoreductase
PTU	Phenylthiourea
QC	Quality control
qRT-PCR	Quantitative real time PCR
SIM	Selective ion monitoring
SNP	Single nucleotide polymorphism
$V_0$	Initial rate
$V_{max}$	Maximum production rate of metabolite
TBI	Total body irradiation
TDM	Therapeutic drug monitor
THT	Tetrahydrothiophene



# 1 INTRODUCTION

Cancer is a group of diseases which is characterized by out of control cell growth. Cancer is a disease as old as man. The oldest evidence of cancer was found in human bones in ancient Egyptian mummies dated several thousand years B.C. The Edwin Smith Surgical Papyrus (shown below), dated to 1,600 B.C., was an updated version from another papyrus dated to approximately 3,000–2,500 B.C. It can most probably be attributed to Imhotep (the Egyptian physician-architect), and provides authentic accounts of breast cancer. A case was deemed incurable if the disease was “cool to touch, bulging and spread all over the breast” It was also recorded that there was “No treatment” for the disease and only superficial breast ulcers were removed surgically by cauterization [1].



The first anticancer drugs were prepared from plants by the Romans (300 B.C.). Ginger root was used to treat skin cancer. Dioscorides (40 - 90 A.D.) reported the use of red clover and autumn crocus for cancer treatment [2]. Later on, arsenic was used by Avicenna (980 - 1037 A.D.) as the first systemic treatment for cancer.

Surgery has remained the first choice for cancer treatment for many centuries, despite the fact that ancient surgeons reported that cancer had come back after its removal. After invention of anesthesia in the late 19<sup>th</sup> century, surgeons Bilioth, Handley and Halsted succeeded to remove entire tumors including the lymph nodes [1].

In 1896, Wilhelm Conrad Roentgen reported the discovery of a new type of ray called “X-ray” which means an unknown ray. Three years later, radiation was used both in cancer diagnosis and therapy [1]. Roentgen was awarded the first Nobel Prize in physics in 1901.

During World War I, E. Krumbhaar served as a medical officer conducting autopsies on victims of mustard gas. Together with his wife, H. Krumbhaar, who also served in World War I, they wrote “Blood and Bone Marrow in Mustard Gas Poisoning”. During World War II, nitrogen mustard was developed and later was applied for the treatment of lymphoma.

Nitrogen mustard was the first alkylating agent that damaged DNA and killed the rapidly growing cancer cells. Shortly after the introduction of nitrogen mustard gas in the treatment of cancer, a folic acid analogue, aminopterin, was reported to block DNA replication. Aminopterin was later replaced by methotrexate, a drug commonly used until today [3]. In the mid-20<sup>th</sup> century, several anti-neoplastic drugs were developed for use in cancer chemotherapy [4].

After World War II, Japanese physicians noticed that the bone marrow in people exposed to atomic bombs was destroyed by radiation. This observation together with the studies on how to protect human beings from the devastating effects of radiation has led to the development of hematopoietic stem cell transplantation (HSCT). HSCT was facilitated by killing the old bone marrow using high doses of radiation.

However, any of the available treatments alone, i.e. surgery, chemo- or radiotherapy, did not cure all patients. Therefore, cancer treatment based on the combination of surgery and cytostatics and/or radiation was developed and has become standard treatment for several cancer types [1]. However, in spread disease involving several organs, such as metastatic solid cancer and hematological malignancies, chemotherapy remains the dominating treatment.

## **1.1 HEMATOLOGICAL MALIGNANCY**

Hematological malignancies comprise a heterogeneous group of cancer diseases that involves hematopoietic and lymphatic tissue. The World Health Organization (WHO) has developed a consensus-based classification system for hematopoietic and lymphoid neoplasms with distinct entities defined by their morphological, clinical and biological features [5]. Hematological malignancies are classified into three distinct categories according to the type of affected progenitor cells: lymphoma, myeloma and leukemia.

Many treatment protocols have been introduced in the treatment of hematological malignancies in order to induce remission and to achieve a cure. However, in some patients palliative treatment aims only to slow down the disease progression. The curative treatment of hematological diseases has been intensified over the years due to improvements in supportive care including antibiotic, antifungal and transfusion therapy. Nevertheless, in some patients the recurrent or primary resistant disease does not allow for a cure. Those patients may be offered hematopoietic stem cell transplantation.

## **1.2 HEMATOPOIETIC STEM CELL TRANSPLANTATION**

The first successful stem cell transfusion was performed by Nobel Prize winner E. Donnall Thomas in 1957 [6]. HSCT is a curative treatment for malignancies such as leukemia, lymphomas and some solid tumors, and non-malignancies such as metabolic disorders and aplastic anemia [7]. Unfortunately, several acute and chronic complications such as graft-versus-host disease (GVHD), infections and sinusoidal obstruction syndrome (SOS) may occur and hamper treatment success.

There are several major types of HSCT based on the relationship between the patient and the donor:

1. Autologous: The patient is transplanted with his or her own stem cells, which were previously harvested and cryopreserved during remission. It may also be considered as a rescue treatment following high-dose chemotherapy with profound myelosuppressive effect.
2. Syngeneic: The patient is transplanted from an identical twin.
3. Allogeneic: The source of stem cells is a human leukocyte antigen (HLA) matched family member or matched unrelated donor (MUD).
4. Haploidentical: The donor is the patient's partially HLA matched relative, usually a parent.

Hematopoietic stem cells may be harvested from bone marrow, peripheral blood or umbilical cord blood. HSCT consists of four phases: conditioning regimen, stem cell infusion, aplastic/neutropenic phase and post-engraftment period.

### **1.2.1 Conditioning regimen**

The conditioning regimen is one of the most important steps in HSCT. Conditioning contributes to elimination of the malignant cells, provides a free space for the donor cells and suppresses the host immune system in order to avoid graft rejection. Conditioning regimens can be divided into either total body irradiation (TBI)-based (TBI and cytostatics) or chemotherapy-based (combinations of cytostatics without TBI). In the best of worlds, TBI and cytostatics would exert minimal toxic effects on normal host cells and tissues [8].

When HSCT was first used, radiotherapy was used as the sole conditioning regimen. However, radiotherapy was associated with many acute and chronic complications such as stomatitis, enteritis and infection-related death. Even rarer complications were reported. In the early 1970's, two patients developed a recurrence of leukemia post-transplantation in donor-derived cells after TBI [9].

In addition, TBI has also been associated with late complications that have occurred years after HSCT, such as secondary malignancies, cataracts, CNS damage in pediatric patients, impaired growth, and endocrine dysfunction [10]. Development of cytostatic agents contributed to the use of cytostatics in conditioning regimen and reduced use of radiotherapy. In the beginning, cyclophosphamide (Cy) was added to TBI regimen to reduce TBI-related side effects. However, studies on the effect of Cy/TBI conditioning in children have shown growth impairment to be a late side effect of TBI [11, 12].

Later, busulphan (Bu) was added to Cy, instead of TBI, based on studies reporting that Bu results in less severe delayed effects than TBI [9, 13]. Bu/Cy regimen proved to be as good as TBI based regimens, especially in children and adults with myeloid leukemia. Conditioning regimens are divided into three categories: myeloablative (MA), non-myeloablative (NMA) and reduced-intensity (RIC) [14].

**Myeloablative conditioning** involves the administration of high doses of TBI and/or cytostatics, which will cause myeloablation and permanent irreversible pancytopenia. The conditioning has to be followed by HSCT. Bu/Cy and Cy/TBI regimens represent myeloablative conditioning and are frequently used prior to HSCT [14].

**Non-myeloablative conditioning** causes minimal cytopenia. The patient's own hematopoiesis will recover without donor stem cell infusion. NMA regimens are immunoablative and result in full engraftment of donor lymphohemopoietic stem cells when followed by an infusion of granulocyte colony-stimulating factor mobilized peripheral blood stem cells. NMA requires large numbers of donor T-lymphocytes and CD34+ cells in order to facilitate engraftment [14].

**Reduced-intensity conditioning regimen** is a conditioning regimen with intermediate intensity between MA and NMA. In RIC regimen; the dose of TBI or cytostatics is reduced by at least 30% compared to MA regimen, however, the conditioning causes cytopenia that should be followed by HSCT.

The conditioning regimen is selected with regards to the diagnosis, disease stage, patient age, patient health status, comorbidities and risk of transplantation-related complications.

### **1.3 CYTOSTATICS**

Cytostatics are classified into several groups based on their mechanisms of action: alkylating agents, antimetabolites, antitumor antibiotics, mitosis inhibitors, topoisomerase inhibitors, enzymes and hormonal agents.

Alkylating agents is one of the oldest groups of drugs used in cancer treatment. They act by attaching an alkyl group to the guanine base of DNA at the O6 or N7 atom of the imidazole ring. This reaction forms covalent bonds with amino, phosphate and carboxyl groups. This kind of damage can trigger apoptosis when the cellular machinery fails to repair it.

Alkylating agents include nitrogen mustard, chlorambucil, melphalan, cyclophosphamide, ifosfamide, thiotepa, busulphan and hexamethylmelamine. They are the corner stone in cancer treatment and used in the treatment of hematological as well as solid tumors including breast cancer, leukemia, lymphoma, lung cancer and ovarian cancer.

As mentioned above, Bu/Cy became a common conditioning regimen prior to HSCT as early as over 25 years ago. This combination is considered to be equivalent to a Cy/TBI regimen, but avoids some of the side effects of radiation [15, 16].

#### **1.3.1 Busulphan**

Busulphan is an old cytostatic that has been on the market since 1959. It is a cell cycle non-specific alkylating agent, its chemical designation is 1,4-butanediol dimethanesulfonate. As an alkylating agent, it attaches an alkyl group to the number 7 nitrogen atom of the imidazole ring of the guanine base in DNA. This leads to guanine adenine inter- and intra-strand crosslinks and triggers apoptosis [17].

#### **1.3.2 Cyclophosphamide**

Cyclophosphamide is another DNA-alkylating agent. Like busulphan, Cy attaches the alkyl group to the guanine base of DNA at the number 7 nitrogen atom of the imidazole ring [18]. Cy is one of the most common drugs for conditioning before stem cell transplantation either in combination with other drugs or with TBI. It is also used as an immunosuppressive drug in the treatment of rheumatoid arthritis, systemic lupus erythematosus and other autoimmune diseases. Cy affects both T- and B-lymphocytes, and thus affects both humoral and cellular-mediated immunity [19]. Due to its immunosuppressive effect, Cy has recently been used post-grafting to prevent rejection and GVHD [20].

## 1.4 METABOLISM OF CYTOSTATICS

The cytostatics, for the body are considered to be foreign substances or xenobiotics, and are thus subjected to different enzymatic reactions in order to be excreted from the body. In general, the main aim of these reactions is to make the drugs more hydrophilic which facilitates excretion. The liver is the main organ involved. Some drugs may also be excreted unchanged.

Metabolism of cytostatics occurs in two phases. In phase I, the major reaction involved is hydroxylation, which is catalyzed mainly by cytochrome P450 (CYP). Some other phase I reactions are desulfuration, deamination, dehalogenation, epoxidation, peroxygenation, and reduction. The phase I reactions usually convert the drugs to less active or inactive compounds. However, for several drugs, such as cyclophosphamide, the reaction converts an inactive prodrug to a biologically active metabolite instead [21].

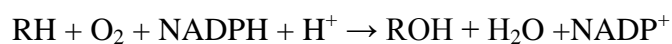
In phase II, the compounds produced in phase I reaction, or compounds that already possess polar substituents such as hydroxyl- or amino-groups, are converted by specific enzymes to various more polar metabolites by conjugation with polar molecules like glutathione, glucuronic acid, sulfate, sugars or amino acids [21].

### 1.4.1 Cytochrome P450

Cytochrome P450 (CYP) is a superfamily of enzymes that are primarily membrane-associated hemoproteins, located in the cell in the inner membrane of mitochondria or in the endoplasmic reticulum. CYPs are involved in the metabolism of many drugs and xenobiotics. They are present in many tissues, but the highest quantity is found in the liver and the small intestine.

Most of the CYPs are inducible and the induction is mainly due to an increase in mRNA transcription. For instance, the administration of phenobarbital or other drugs causes hypertrophy of the smooth endoplasmic reticulum and a three- to four-fold increase in the amount of CYP within 4-5 days. Certain cases of induction involve stabilization of mRNA, enzyme stabilization, or other mechanisms (e.g., an effect on translation). However, certain drugs can also inhibit CYP activities [22, 23].

The most common reaction catalyzed by CYP is a monooxygenase reaction, which is the insertion of one atom of oxygen into an organic substrate while the other oxygen atom is reduced to water:



This reaction is recognized as a Phase I reaction and is important in the metabolism of xenobiotics, including drugs, carcinogens, pesticides and pollutants. Some endogenous compounds, like steroids, fatty acids, and retinoids are also metabolized by CYPs.

Cytochrome P450 oxidoreductase (POR) is an enzyme that is commonly involved in the reaction. Electrons for this reaction are transferred from NADPH to POR and then to CYP. Cytochrome *b<sub>5</sub>* is another hemoprotein which can act as an electron donor in some situations.

In humans, CYP comprises 57 genes and more than 58 pseudogenes divided into 18 families and 43 subfamilies [24]. Many CYPs exist in polymorphic forms (genetic variants), that differ in their catalytic activity. This may explain the inter-individual variations in drug response reported among patients. The most common enzymes reported to be involved in drug metabolism are CYP1A1, CYP1A2, CYP2A6, CYP2B6, CYP2C8, CYP2C9, CYP2C19, CYP2D6, CYP2E1, CYP3A4 and CYP4A11 [23].

### **1.4.2 Glutathione conjugation**

Glutathione (GSH) is a non-essential tripeptide consisting of glutamic acid, cysteine and glycine. It has an unusual peptide linkage between the amino group of cysteine and the carboxyl group of the glutamate side chain. The sulfhydryl (thiol) group (SH) of cysteine serves as a proton donor and is responsible for the biological activity of glutathione.

Glutathione exists in reduced (GSH) and oxidized (GSSG) states. In the reduced state, the thiol group of cysteine is able to donate a reducing equivalent ( $H^+ + e^-$ ) to other unstable molecules, such as reactive oxygen species. By donating an electron, glutathione itself becomes reactive, and readily reacts with another reactive glutathione to form a dimer glutathione disulfide (GSSG). Such a reaction is possible due to the high concentration of glutathione in cells. The reaction is often catalyzed by glutathione S-transferases (GSTs) which are present mainly in liver cytosol. GSH can be regenerated from GSSG by the enzyme glutathione reductase [25].

GSH is the major endogenous antioxidant produced by cells. Beside its role in the conjugation of drugs and other xenobiotics, it participates in the neutralization of free radicals and reactive oxygen compounds, as well as maintaining exogenous antioxidants such as vitamins C and E in their reduced (active) forms.

GSH is essential for the immune system to exert its full potential. It also plays a fundamental role in numerous metabolic and biochemical reactions such as DNA synthesis and repair, protein synthesis, prostaglandin synthesis, amino acid transport and enzyme activation [26].

### 1.4.3 Busulphan metabolism

Busulphan is predominantly metabolized in the liver by conjugation with glutathione (GSH) [27-30]. Cytosolic GSTs have been identified as the enzymes responsible for this conjugation. GSTA1 is the most active glutathione transferase in catalyzing Bu-GSH conjugation in human liver and in the small intestine of young children, while GSTM1 and GSTP1 are less active [31, 32].

The conjugation of busulphan with glutathione results in the formation of a sulfonium ion which is an unstable intermediate product and is broken down to tetrahydrothiophene (THT). Oxidation products of THT, such as THT 1-oxide, sulfolane and 3-hydroxy sulfolane make up the majority of identified Bu metabolites (Figure 1). Several minor metabolites of Bu have been detected, but yet not identified [27-30].

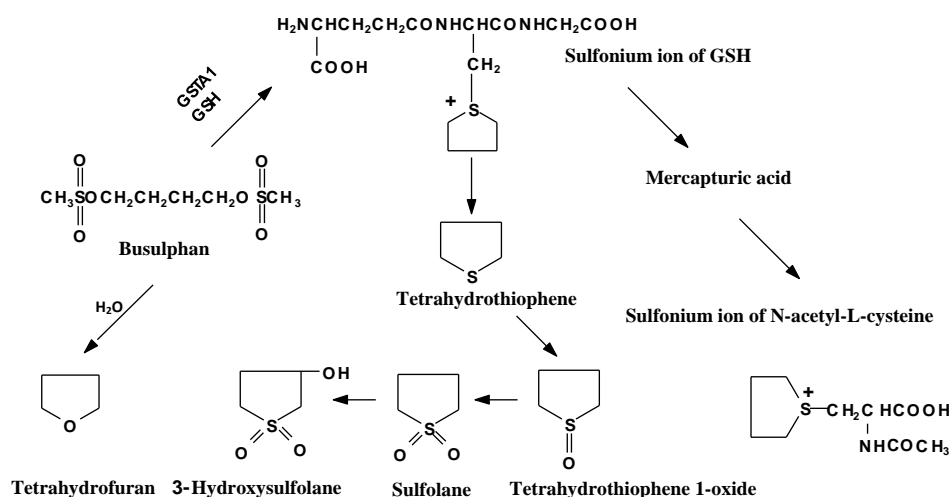


**Figure 1:** Metabolic pathway of busulphan

Several drugs such as itraconazole, metronidazole, phenytoin and ketobemidone have been reported to affect Bu plasma concentrations during conditioning regimen [33-35]. Our group has observed that the antimycotic drugs, voriconazole and posaconazole, also affect Bu plasma levels (unpublished results). Moreover, our group reported that the time interval between Bu and Cy during conditioning regimen affected the frequency of liver toxicity and the pharmacokinetics of Cy [36]. Several attempts have been made to identify other enzymes involved in Bu metabolism besides conjugation with GSH. In this study, we are investigating the role of flavin-containing monooxygenase 3 (FMO3) as well as CYPs in the



metabolism of Bu via its core metabolite THT. We hypothesize that these enzymes are involved in THT oxidation to THT-1-oxide and thus affect the overall Bu kinetics (Figure 2).

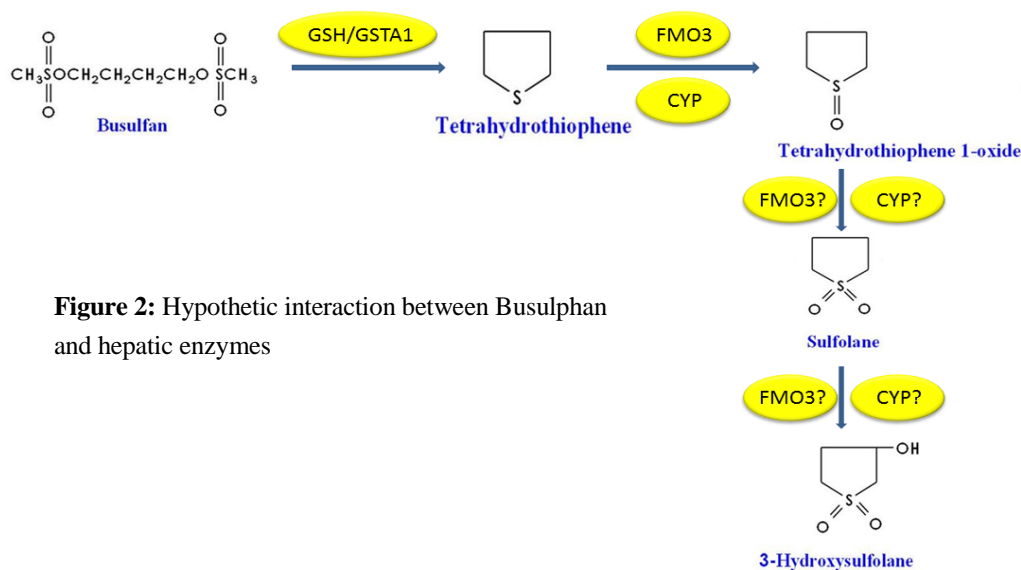


**Figure 2:** Hypothetic interaction between Busulphan and hepatic enzymes

FMOs consist of a group of hepatic microsomal enzymes involved in the metabolism of xenobiotics [37, 38]. They are mainly responsible for the breakdown of compounds containing nitrogen, sulfur and phosphorus while using NADPH as a cofactor. Five active forms have been identified in humans, FMO1 - FMO5. The most common liver enzyme is FMO3 [39].

Recently, FMO3 was reported to be involved in the metabolism of many drugs, such as voriconazole, ketoconazole, methimazole, tamoxifen, codeine and nicotine [40-42]. Voriconazole is an antifungal drug which is used to treat or prevent fungal infections or their recurrence, and thus, sometimes given during busulphan conditioning due to the high risk of infection in the immunocompromised patients. It was reported that 25% of voriconazole is metabolized by FMO3 [40], which might explain the high busulphan plasma concentrations found in patients treated by voriconazole shortly before or during conditioning.

All enzymes involved in the Bu pathway have not been identified yet. Thus, the effect of enzyme polymorphisms on the drug kinetics has not been extensively studied, and the only way to personalize Bu dosage is currently based on the therapeutic drug monitoring (TDM) strategy. Bu is characterized by a narrow therapeutic index and wide inter- and intra-patient variability of pharmacokinetic parameters. Overdosing may cause high toxicity. Before HSCT, a standard total dose of Bu given orally is 16 mg/kg. The total dose is administered over four days divided into 1 to 4 daily doses. The Bu exposure (measured as the area under the concentration-time curve, AUC) varies up to 5-7 fold in patients receiving conditioning regimen [43, 44]. Substantial inter-patient variation in pharmacokinetic parameters is due to differences in Bu metabolism [45-48].

TDM is a common strategy for maintaining Bu exposure within the target AUC in order to reduce Bu side effects and retain treatment efficacy. Target AUC ranges depend on the type of HSCT; 3600-5400ng<sub>h</sub>/ml in partially matched or unrelated recipients and 1200-5400ng<sub>h</sub>/ml in allogeneic matched sibling patients [47, 49, 50]. TDM uses Bu concentrations from serial blood samples to calculate AUC and guide dose adjustments to achieve the target AUC.

TDM in patients undergoing stem cell transplantation is complicated by the collection of blood samples in a short time span from anemic patients and young children. Analysis and evaluation have to be carried out rapidly in order to allow early dose adjustment. The full pharmacokinetic estimation of AUC is based on a series of about 10 blood samples. Several attempts have been made to develop limited sampling models (LSMs) and to reduce the number of samples for the benefit of patients and nurses, as well as reducing costs [51-53]. The correlation between the AUC estimated using limited sampling models and the AUC obtained from full pharmacokinetics depends on several factors such as the patient population. Developments in computer software currently offer new possibilities for TDM modeling.

Several methods for analysis of Bu and several methods for analysis of its metabolites have been reported. However, the advantage of simultaneous analysis of the parent compound and its metabolites was challenging. Analysis of Bu and its metabolites using a single solid method would facilitate kinetic and metabolic pathways investigations of Bu.

#### **1.4.4 Cyclophosphamide metabolism**

Cyclophosphamide is a prodrug that is metabolized by cytochrome P450 to 4-hydroxycyclophosphamide (4-OH-Cy) which is the main active metabolite (90% of the total Cy) [54]. Subsequently, 4-OH-Cy is metabolized to phosphoramidate mustard and acrolein. The latter is responsible for urotoxicity. An alternative pathway is *N*-dechloroethylation in which Cy is metabolized to an inactive metabolite, *N*-dechloroethyl-Cy, and the neurotoxic metabolite chloroacetaldehyde (Figure 3) [55-57].

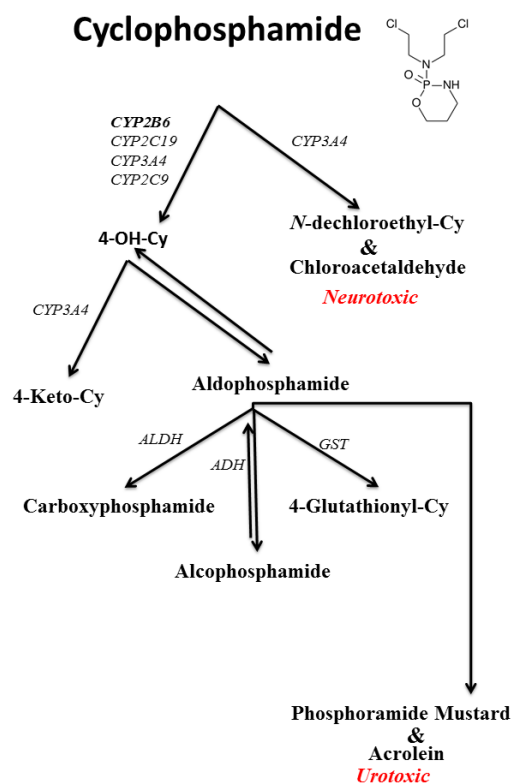


**Figure 3:** Metabolic pathway of cyclophosphamide

CYP2B6 is the main enzyme responsible for Cy bioactivation [55, 58] while other enzymes like CYP3A4, CYP3A5, CYP2C9 and CYP2C19 are also involved in its metabolism [59, 60].

The gene for CYP2B6 is located in the middle of chromosome 19 [61]. CYP2B6 is mainly expressed in the liver; however, it has been detected in extra-hepatic tissues such as intestine, kidney, brain, lung and skin [62-65]. CYP2B6 has been reported to be involved in the metabolism of many drugs, such as Cy, ifosfamide, diazepam and efavirenz as well as in the synthesis of endogenous compounds like cholesterol and steroids [63, 66, 67].

*CYP2B6* polymorphism has been reported to affect the kinetics of several drugs. For example; the mirtazapine concentration was higher in patients with *CYP2B6*\*6/\*6 [68]. Also the frequencies of different alleles differ among populations. Ribaudo *et al.* have shown that *CYP2B6*\*9 is more frequent among African-American individuals compared to Caucasian-American individuals, which resulted in a two-fold longer plasma half-life of efavirenz in homozygotes for this allele [69].

A high inter-individual variation in Cy kinetics including elimination half-life and clearance has been reported [55, 70]. Several investigators have shown high inter-individual variation in expression and catalytic activity of CYP2B6 which can be due to the genetic polymorphism of this enzyme [71-73].

In total, more than fifty different alleles containing point mutations have been identified to date (28-Nov-2013) (<http://www.cypalleles.ki.se/cyp2b6.htm>). Most of these mutations are silent but five of them result in amino-acid substitutions in exons 1, 4, 5 and 9 [63].

Some of the common alleles such as *CYP2B6*\*2, *CYP2B6*\*4, *CYP2B6*\*5, *CYP2B6*\*6, *CYP2B6*\*7 and *CYP2B6*\*9 have been reported to affect Cy kinetics by either decreased liver protein expression or altered function of the enzyme [63, 74-76]. In addition, some more rare SNPs have been reported to result in absent or non-functional enzyme [77].

In contrast, some studies have reported that *CYP2B6* genetic polymorphism doesn't alter the Cy metabolism or the 4-OH-Cy formation *in vivo* or *in vitro* [58-60]. Moreover; Yao *et al.* suggested that clinical factors such as patient age and cancer grade may contribute to the inter-individual variation in Cy kinetics [78].

The clinical efficacy of Cy either alone or in combination with other cytostatics or radiotherapy has been studied previously [79, 80]. However, the contribution of Cy to HSCT outcome and, more importantly, the mechanisms by which Cy exerts its effect on immune cells has not yet been fully elucidated.

In the past decade, the advent of DNA microarray technology together with the availability of the complete nucleotide sequence of the human genome have allowed elucidation of the molecular mechanisms in several diseases [81, 82] or treatment regimens [83, 84]. However, the effect of high dose cyclophosphamide on different genes and the gene expression profile has not been studied yet.

Cytochrome P450 oxidoreductase (POR) is a membrane-bound enzyme in the endoplasmic reticulum that is involved in electron transfer from NADPH to CYP. POR is important in the metabolism of drugs and xenobiotics and thus, allelic variants and variability in expression may have clinical implications [85, 86].

POR deficiency may lead to serious alteration of the normal development such as disordered steroidogenesis, abnormal genitalia, bone abnormalities and William's syndrome [87-89]. Recently, POR variants have been found to affect CYP-catalyzed metabolism of drugs and xenobiotics. *POR* polymorphism affects the activities of CYPs such as CYP3A4, 2C9, 3A5, 2D6, 1A2 and 2C19 that are mainly dependent on POR-mediated electron transfer by changing the electron transfer capacity from POR to CYPs [90-93]. POR variants have altered the *CYP2B6* dependent activity in bupropion metabolism and *S*-mephenytoin *N*-demethylation [94, 95]. *POR*\*28 is the only polymorphism so far reported to increase CYP activity *in vivo* [96].

Variations in *POR* gene expression *in vivo* and how POR affects Cy kinetics has not been fully elucidated yet.

CYP2J2 is another CYP involved in the metabolism of xenobiotics. It is encoded by the *CYP2J2* gene which has been mapped to the short arm of chromosome 1 in humans and chromosome 4 in mice [97].

CYP2J2 is active mainly in the intestine and cardiovascular system [98-100]. CYP2J2 has been reported to metabolize several drugs, particularly in extrahepatic tissues. High CYP2J2 activity in the intestine could contribute to the first-pass metabolism of some drugs [101-103]. Moreover, Matsumoto *et al.* have demonstrated that CYP2J2 is dominant in the pre-systemic elimination of astemizole in human and rabbit small intestine [103].

In the human heart, CYP2J2 is responsible for the epoxidation of endogenous arachidonic acid to four regioisomeric epoxyeicosatrienoic acids (EETs) released in response to some stimuli like ischemia [104]. Transgenic mice overexpressing *CYP2J2* have been shown to have less extensive infarcts and more complete recovery after ischemia [105-107]. These mice were also better protected against global cerebral ischemia associated with increased regional cerebral blood flow [108].

Recently, CYP2J2 has been also related to malignancy. Chen *et al.* have reported that *CYP2J2* is highly expressed in human- and mouse- derived malignant hematological cell lines (K562, HL-60, Raji, MOLT-4, SP2/0, Jurkat, and EL4 cells) as well as in peripheral blood and bone marrow cells of leukemia patients [109]. In these patients, high expression of *CYP2J2* was associated with accelerated proliferation and attenuated apoptosis. *CYP2J2* overexpression also enhanced malignant xenograft growth [109].

*CYP2J2* is also overexpressed in ovarian cancer and lung cancer metastasis [110, 111] and its inhibition by terfenadine-related compounds has been shown to suppress the proliferation of human cancer cells both *in vitro* and *in vivo* [112]. The expression of *CYP2J2* in HL-60 cells can explain why Cy exerts cytotoxic effects in these cells despite lack of CYP2B6 [113]. The role of CYP2J2 in Cy bioactivation has not been elucidated yet.

## 1.5 SIGNIFICANCE

Hematopoietic stem cell transplantation is a curative treatment for several diseases. However, HSCT is a complex and complicated procedure accompanied by a high risk of acute and late serious complications. Multiple drugs are used as prophylactic treatment to prevent and/or to treat complications. However, drug-drug interactions may also contribute to the development of complications and eventually increase morbidity and mortality.

Conditioning regimen plays an essential role in HSCT. The busulphan/cyclophosphamide regimen is one of the most commonly used conditioning regimens in both adults and pediatric patients. Despite the long clinical use of both drugs, there is still scant information concerning their metabolism, their pharmacodynamics, the effect of gene regulation and

(most of all) their mechanism of action. There is also still no satisfactory explanation for the high inter- and intra-individual variation seen in clinical settings.

There is a need for more extensive knowledge regarding:

- The enzymes involved in busulphan and cyclophosphamide metabolism.
- Genes that are affected by the treatment.
- The importance of polymorphism in these genes in regard to treatment efficacy and toxicity.
- The impact of up- or down-regulation of these genes on the pharmacodynamics of the drug.
- Dose adjustment based on individual genetic factors.
- The pharmacological activity of the metabolites.
- The pharmacokinetics and pharmacodynamics (PK/PD) in correlation to side effects on an individual basis.
- Reliable models that can be used for dose adjustment in relation to age/disease/patient gender.

This knowledge will certainly help to personalize medicine based on individual genetic information, as well as enhancing dosage schedule and/or dose adjustment. Moreover, it will enable clinicians to choose drugs with fewer potential interactions. This knowledge may play a central role in the improvement of the conditioning regimen prior to HSCT and hence improve its clinical outcome. The improvement in clinical results may be seen in terms of fewer side effects, improved patient life quality, longer survival and less relapse rate, which will benefit both the individual and society as a whole.

## **2 AIM OF THE THESIS**

### **2.1 GENERAL AIM**

To study the molecular mechanisms involved in the metabolism of the Bu/Cy conditioning regimen in order to avoid drug interactions and personalize the treatment before HSCT and hence, increase treatment efficacy, reduce adverse effects and improve the clinical outcome.

### **2.2 SPECIFIC AIMS**

- 1- To develop an analytical method for the concomitant detection and quantification of busulphan and its main metabolites in different biological fluids.
- 2- To identify other enzymes involved in busulphan metabolism and their effect on busulphan kinetics.
- 3- To establish a limited sampling model for the calculation of busulphan pharmacokinetics based on a practical limited sampling protocol in combination with a reliable algorithm.
- 4- To study the contribution of cyclophosphamide to the outcome of HSCT and the molecular mechanisms by which cyclophosphamide exerts its effect on immune cells.
- 5- To investigate the role of human *CYP2B6* polymorphism and POR in cyclophosphamide bioactivation.
- 6- To investigate the role of *CYP2J2* in cyclophosphamide bioactivation.





## 3 PATIENTS AND METHODS

### 3.1 CHEMICALS

The following compounds were purchased with a purity > 96%: busulphan and 3-hydroxysulfolane (Sigma-Aldrich, Steinheim, Germany); Cyclophosphamide, Phenylthiourea (PTU), telmisartan, dansylhydrazine, and dimethyl sulfoxide (DMSO) (Sigma-Aldrich, Stockholm, Sweden);  $\beta$ -nicotinamide adenine dinucleotide phosphate reduced form ( $\beta$ -NADPH), tetrahydrothiophene and sulfolane (Sigma-Aldrich, St. Louis, USA); tetrahydrothiophene 1-oxide (Sigma-Aldrich, Tokyo, Japan); sodium iodide (Merck, Darmstadt, Germany); nicotine (Merck, Hohenbrunn, Germany); 3-methylsulfolane (TCI, Tokyo, Japan); resazurin (R&D Systems Inc., Minneapolis, USA); antithymocyte globulin (ATG, Thymoglobulin, Genzyme, Cambridge, MA, USA); Dulbecco's phosphate buffered saline (DPBS) (Life technologies, Stockholm, Sweden). 1,5-bis(methanesulfonyl) pentane was prepared in our laboratory (Karolinska University Hospital-Huddinge, Sweden) [114]. Maphosphamide was kindly provided by Professor Ulf Niemeyer, Baxter Oncology GmbH (Frankfurt, Germany).

All solvents were of analytical grade with purity > 99%: methanol, acetonitrile, *n*-heptane (Merck, Darmstadt, Germany); dichloromethane (Fluka, Seeze, Germany) and ethyl acetate (Sigma-Aldrich, Steinheim, Germany).

QuickPrep Total RNA Extraction Kit was purchased from GE Life Sciences, Uppsala, Sweden, TaqMan Reverse Transcriptase-complementary DNA (cDNA) Kit from Applied Biosystems, Roche, NJ, USA and NimbleGen microarrays from Roche Diagnostics Scandinavia, Bromma, Sweden.

TaqMan genotyping polymerase chain reaction (PCR) primers were purchased from Applied Biosystems (Stockholm, Sweden) as follows:

A- Gene expression primers (Catalogue# 4331182): *FMO3* (assay ID; Hs00199368\_m1), *CYP2J2* (assay ID; Hs00951113\_m1), *ANGPTL1* (assay ID; Hs00559786\_m1) and *c-JUN* (assay ID; Hs01103582\_s1) and the housekeeping gene *GAPDH* (assay ID; Hs02758991\_g1).

B- Single nucleotide polymorphism (SNP) genotyping (catalogue #4362691): *CYP2J2* SNPs (rs72547599, rs1056595, and rs66515830) and *POR\*28* SNP (rs1057868).

QuantiNova probe PCR kit for genotyping (catalogue # 208252) was from Qiagen (Stockholm, Sweden), while TaqMan genotyping master mix (catalogue #4371355) and TaqMan fast universal master mix (catalogue # 4352042) were from Applied Biosystems (Stockholm, Sweden).

## 3.2 PATIENT POPULATION

Patients undergoing HSCT at the Center for Allogeneic Stem Cell Transplantation (CAST), Karolinska University Hospital, Huddinge, Sweden were included in the study. The study was approved by the ethical committee of Karolinska Institutet (616/03) and informed consent was obtained from the patients. Patient characteristics are presented in Table 1.

Twelve patients received Bu/Cy conditioning regimen before HSCT. Busulphan was administered orally at a dose of 2 mg/kg twice daily for 4 consecutive days followed by i.v. infusion of cyclophosphamide at a dose of 60 mg/kg/day once daily for 2 consecutive days.

Eleven patients were conditioned with Cy/TBI regimen. They received an i.v. infusion of Cy 60 mg/kg/day once daily for two consecutive days followed by fractionated TBI in a total dose of 12 Gy (3 Gy daily for 4 days), except one patient who received only 6 Gy in total.

All patients with matched unrelated donors (MUD) were treated with ATG (antithymocyte globulin) at a total dose of 6 mg/kg given at day -4 through -1 during the conditioning regimen. The only exception was a patient with CD52+ leukemia and a sibling donor who received Alemtuzumab 30 mg x 1.

GVHD prophylaxis consisted of cyclosporine (CsA) in combination with four doses of methotrexate (MTX) [115]. During the first month, blood CsA levels were maintained at 100 ng/mL in patients with sibling donors and at 200 - 300 ng/mL in patients with MUD. In the absence of GVHD, CsA was successively discontinued in patients with sibling donors after three to four months and in patients with MUD after six months.

Acute and chronic GVHD were diagnosed on the basis of clinical symptoms and/or biopsies (skin, liver, gastrointestinal tract, or oral mucosa) according to standard criteria [116]. The patients were treated for grade I acute GVHD with prednisone, starting at a dosage of 2 mg/kg/day, which was successively lowered after the initial response. Chronic GVHD was initially treated with CsA and steroids. In most cases, daily prednisone at 1 mg/kg per day and daily CsA at 10 mg/kg per day were used [117].

### 3.2.1 Blood sampling

Blood samples for RNA determination were collected in PAX tubes (BD, Stockholm, Sweden). During the Bu/Cy conditioning regimen, samples were collected prior to the start of Bu treatment and after the last dose of Bu. In patients conditioned with Cy/TBI, blood samples were collected before start and 6 h after termination of Cy infusion on both treatment days. The samples were numbered consecutively from 1 to 4.

For the analysis of Cy and 4-OH-Cy kinetics, blood samples were collected before the first infusion of Cy and at 0.5, 1, 2, 4, 6 and 8 h after its termination, as well as before the second infusion of Cy and 6 h after its termination. Blood (2.5 mL) was collected in prechilled heparinized tubes (BD, Stockholm, Sweden) and immediately centrifuged at 3000 x g for 3 min at 4°C. Plasma (0.5 mL) was transferred to new tubes containing 0.5 mL prechilled

ACN, vortexed for 30 s, and centrifuged at 3000 x g for 3 min. The supernatant and remaining plasma were stored at -80°C until analysis.

### **3.2.2 RNA extraction and cDNA preparation**

RNA was extracted from mononuclear cells using QuickPrep Total RNA Extraction Kit according to the manufacturer's instructions and was quantified by measuring the absorbance at 260 and 280 nm. cDNA was obtained by reverse transcription using the TaqMan Reverse Transcriptase-cDNA Kit. All samples were stored at -150°C.

### **3.2.3 Gene array and genotyping**

Purified mRNA was analyzed using global gene expression, NimbleGen microarrays (Roche Diagnostics Scandinavia, Bromma, Sweden). Data were analyzed using GeneSpring GX (Agilent, CA, USA). Expression data of the probes and genes were normalized using quantile normalization and the Robust Multichip Average algorithm, respectively. Gene expression was determined by ANOVA to be significantly differentially expressed if the selection threshold of a false discovery rate (FDR) was < 5% and the fold change in SAM output result was > 1.3. The complete data set for patients conditioned with Cy and TBI can be accessed in the Gene Expression Omnibus (GEO) database with accession number GSE51907 [118].

Pathway identification and reporting was performed using IPA software (Ingenuity, Qiagen, CA, USA) and Kyoto Encyclopedia of Genes and Genomes software (KEGG) (Kyoto University Bioinformatics Centre, Japan).

### **3.2.4 Real time PCR**

TaqMan gene expression assay was performed by means of the FAM dye labeling system according to the manufacturer's instructions. The assay was performed for the selected highly expressed genes, *FMO3* expression in patients treated with Bu and *ANGPTL1*, *c-JUN*, *POR* and *CYP2J2* in patients treated with Cy. All results were normalized against *GAPDH* as a housekeeping gene. Twelve samples from healthy controls were run in parallel.

Patient samples were scanned using TaqMan genotyping PCR primers for *CYP2J2* SNPs (rs72547599, rs1056595 and rs66515830) and *POR\*28* SNP (rs1057868). cDNA samples (10 ng) containing 1x TaqMan SNP Genotyping were amplified by means of the VIC and FAM dye-labeling system, according to the manufacturer's instructions, in a 384-well plates (10 µL total volume) for *CYP2J2* (7500 Fast Real-Time PCR System, Applied Biosystems Life Technologies, Stockholm, Sweden) and a 72 rotor (20 µL total volume) for *POR\*28* (Rotor Gene Real-Time PCR System, Qiagen, Stockholm, Sweden). Post-PCR end-point reading was performed and genotypes were assigned using the manual calling option in the allelic discrimination applications.

**Table 1:** Patients clinical data

	Diagnosis	Age, (years)	Conditioning regimen	CD 34 dose/Kg	Disease status, at HSCT	Outcome	Cause of death
P 1	AML	47	Bu + Cy + ATG	8,1 x10(6)	CR1	Alive	N/A
P 2	CML	57	Bu + Cy + ATG	15,3 x10(6)	CR	Alive	N/A
P 3	AML	2	Bu + Cy + ATG	4,85 x10(6)	CR1	Alive	N/A
P 4	Thalassemia Major	13	Bu + Cy + ATG	8,05 x10(6)	N/A	Alive	N/A
P 5	CML	14	Bu + Cy	4,8 x10(6)	CP1	Alive	N/A
P 6	MDS-AML	50	Bu + Cy + ATG	9,36 x10(6)	CR1	Alive	N/A
P 7	Sickle cell anemia	13	Bu + Cy	3,39 x10(6)	N/A	Alive	N/A
P 8	AML	35	Bu + Cy + ATG	8,75 x10(6)	CR1	Alive	N/A
P 9	CML	55	Bu + Cy + ATG	8,19 x10(6)	CP2	† 9 moths	Multi organ failure
P 10	Kostmann + MDS	12	Bu + Cy + ATG	4,48 x10(6)	N/A	† 10 moths	Sudden Death
P 11	AML	54	Bu + Cy	3,7 x10(6)	CR1	Alive	N/A
P 12	MDS	14	Bu + Cy + Mel + ATG	7,9 x10(6)	PR	Alive	N/A
P 13	AML	51	Cy+fTBI+ATG	10.6x10(6)	Refractory	Alive	N/A
P 14	Pre-B ALL	26	Cy+fTBI+ATG	13.5x10(6)	CR2	† 35 months	Relapse
P 15	B-CLL	57	Cy+fTBI (6 Gy)+ Alemtuzumab	14.7x10(6)	Transformed	† 10 months	Relapse
P 16	AML	31	Cy+fTBI+ATG	2x10(6)	CR2	† 6 months	Pneumonia
P 17	T-cell lymphoma	41	Cy+fTBI+ATG	9.3x10(6)	Relapse	† 51 days	Invasive fungal infection
P 18	Pre-B ALL	25	Cy+fTBI+ATG	7.3x10(6)	CR2	Alive	N/A
P 19	T-cell lymphoma	38	Cy+fTBI	2.9x10(8)	PR	† 19 months	Relapse
P 20	T-ALL	10	Cy+fTBI+ATG	6.48x10(8)	CR1	† 12 months	Relapse
P 21	T-ALL	26	Cy+fTBI+ATG	0.5x10(5) 0.2x10(5)	CR2	† 11 months	Relapse
P 22	T-ALL	14	Cy+fTBI+ATG	19.9x10(6)	CR2	Alive	N/A
P 23	ALL	19	Cy+fTBI+ATG	13.5x10(6)	CR3	† 9 months	Relapse & pneumonia

*Abbreviations:* ALL, acute lymphoblastic leukemia; AML, acute myeloid leukemia; ATG, antithymocyte globulin; B, B lymphocyte; CML, chronic myeloid leukemia; CLL, chronic lymphoblastic leukemia; MDS, myelodysplastic syndrome; CD 34, bone marrow-derived stem cells; CR, complete remission; Bu, busulphan; Cy, cyclophosphamide; Mel, melphalan; fTBI, fractionated total body irradiation; HSCT, hematopoietic stem cell transplantation; P, patient; PR, partial remission; T, T lymphocyte; †, survival time.

One patient with recent fungal infections required continuous prophylaxis with voriconazole even during the Bu/Cy conditioning regimen. Busulphan was administered at a dose of 2 mg/kg twice daily for four days. This clinical setting gave us an opportunity to study the effect of FMO3 on Bu kinetics. Blood samples were drawn at 0, 1, 2, 4, 6, and 8 h for the first and fifth dose and at 0, 4, 6 and 8 h for the third dose. Plasma was separated by centrifugation at 1200 x g and stored at -20°C until analysis of Bu and THT [119].

For the development of the busulphan limited sampling model, adult and pediatric patients diagnosed with malignant hematological disease and treated with busulphan as part of their conditioning regimen were studied. Oral busulphan was administered in a dose of 2 mg/kg twice daily for four days, preceding cyclophosphamide treatment (Table 2). All adult and adolescent patients, as well as parents of pediatric patients, consented to participation in this protocol.

**Table 2:** Patients characteristics for LSM

Group	Mean age (range)	Diagnosis (n)	Gender (male/female)
<b>Initial patient group, (23 patients)</b>	38 (13-59)	AML (12), CML (9), Ewing sarcoma (1), Pre-B ALL (1)	10/13
<b>Pediatric evaluation group, (20 patients)</b>	6 (0.1-13)	AML/MDS (10), Neuroblastoma (6), MPD (1), Hurler (1), JMML (1), Fanconi/MDS (1)	8/12
<b>Adult evaluation group, (23 patients)</b>	43 (18-67)	AML (18), MDS (3), CML (2)	10/13

*Abbreviations:* ALL, acute lymphoblastic leukemia; AML, acute myeloid leukemia; CML, chronic myeloid leukemia; JMML, juvenile myelomonocytic leukemia; MDS, myelodysplastic syndrome.

### 3.3 STUDIES IN MICE

Male C57BL/6N mice (6-8 weeks old) were purchased from Charles River (Koln, Germany). The mice were allowed to acclimatize to their surroundings for 2 weeks with a 12 h dark/12 h light cycle. Mice were fed with standard laboratory chow and water *ad libitum*. An ethical permit (S119-12) was obtained from the Stockholm South Animal Research Review Board.

To assess Bu and THT kinetics, Bu was injected i.p. (25 mg/kg) dissolved in DMSO [120]. THT was prepared and injected in a similar way and administered in an equimolar dose of 8.8 mg/kg, since it has a lower molecular weight compared to Bu. At appropriate time points (10 min, 30 min, 1 h, 2 h, 4 h, 6 h and 8 h after administration), blood samples were collected and mice were sacrificed.

To assess the role of FMO3 in Bu kinetics, a similar experiment was carried out after treatment with the FMO3 inhibitor, phenylthiourea (PTU), [121] administered as an i.p.

injection. PTU was dissolved in DMSO and injected (3 mg/kg) once daily for 3 days followed by Bu and THT injection on the 4th day. The mice were sampled and sacrificed as described above.

To investigate the effect of THT accumulation on Bu metabolism, a third group of mice were injected with double dose of THT (17.6 mg/kg) at the same time with Bu and in order to simulate the THT accumulation. Mice were sampled and sacrificed according the same schedule as reported above. Plasma was separated from the blood samples and stored at -20°C.

All experiments have been run in (at least) triplicate including negative controls (NaCl injection) and controls treated with PTU alone. Bu and THT were measured as described previously [119].

### **3.4 STUDIES IN HL-60 CELL LINE**

HL-60 cells were purchased from DSMZ (Braunschweig, Germany). Cells were cultured in 96-well BD BioCoat black culture plates (Stockholm, Sweden) using Roswell Park Memorial Institute (RPMI) 1640 medium, supplemented with 10% heat inactivated fetal bovine serum (FBS), penicillin (100 U/mL), and streptomycin (100 µg/mL).

Cells in the exponentially growing phase (passage 6) were incubated in a humidified incubator at 37°C with a 5% CO<sub>2</sub>/95% O<sub>2</sub> atmosphere. Cells were seeded at a density of 10.000 cells/well. In order to assess cytotoxicity of the Cy and the CYP2J2 inhibitor, telmisartan, [122] cells were incubated with Cy in concentrations of 0.2 - 20 mM for 6 - 96 h or with telmisartan in concentrations of 2.5 - 40 µM for 48 h.

To study the effect of telmisartan on Cy-induced cytotoxicity, HL-60 cells were preincubated with telmisartan in concentrations of 2.5, 5, or 10 µM for 2 h. Then, Cy in a final concentration of 9 mM and cells were incubated for a further 48 h. Controls were incubated in drug-free medium (negative control).

At appropriate time points, the cell samples were aliquoted for different assays. One aliquot was added to precooled ACN for analysis of 4-OH-Cy, the other aliquot was used to assess cell viability using the resazurin assay. Resazurin in a 10% final concentration was added to the cell suspensions. The cells were then incubated for an additional 2 h at 37°C and fluorescence was detected at 590 nm following excitation at a wavelength of 544 nm using a FLUOstar Optima system (BMG LABTECH, Ortenberg, Germany). Experiments were performed in triplicate.

## 3.5 STUDIES IN MICROSOMES

### 3.5.1 Busulphan metabolism

To study the involvement of microsomal enzymes in Bu metabolism, pools of human liver microsomes (HLM) (Cypex, Dundee, UK) were incubated with THT in concentrations of 10 - 500  $\mu\text{M}$  at protein concentrations of 0.125 - 1 mg/mL. Microsomes were incubated at 37°C in 200  $\mu\text{L}$  of 50 mM potassium phosphate buffer, pH 7.4, and started with NADPH to a final concentration of 1 mM. The reaction was terminated at appropriate time points by adding one volume of ice cold dichloromethane.

To determine the main enzyme involved in THT oxidation, parallel HLM incubations were performed after heat inactivation of FMO3 at 45°C for 10 min or inhibition of CYPs with carbon monoxide (CO) (AGA Gas, Enköping, Sweden).

To corroborate our results, 11 batches of microsomes from *baculovirus* infected insect cells expressing human CYPs and POR, were incubated with 25  $\mu\text{M}$  THT. The enzymes expressed were FMO3, CYP1A1, CYP1A2, CYP2B6, CYP2C8, CYP2C9, CYP2C19, CYP2D6, CYP2E1, CYP3A4 and CYP4A11 (BD Biosciences, Stockholm, Sweden). The microsomes were incubated for 0, 5, 15, 30 and 60 min at a protein concentration of 0.35 mg/mL for FMO3 microsomes, or at 35 pmol CYP/mL for the other enzymes.

All microsomes were incubated in triplicates and negative controls were run in parallel. Negative controls consisted of incubations using the same conditions, but excluding either NADPH, microsomes or THT, or by adding dichloromethane before NADPH addition. THT disappearance and the formation of metabolites were measured using GC-MS [119].

### 3.5.2 Cyclophosphamide metabolism

The linearity of the reactions with time, CYP and Cy concentrations were determined before measuring apparent enzyme kinetic constants.

For assessment of the role of POR in Cy bioactivation, microsomes containing human CYP2B6.1 and human POR coexpressed in *Escherichia coli* and supplemented with purified human cytochrome *b5* were purchased from Cypex Ltd. (Dundee, UK). Batches with variable, up to approximately 18-fold differences in POR/CYP ratios were available. Microsomes containing human POR only from the same vendor were used as a control (Table 3).

Microsomes with the same amounts of CYP (40 pmol/mL) and variable amounts of POR and POR/CYP ratios were incubated for 15 min in two independent experiments at 37°C, in a total volume of 100  $\mu\text{L}$  containing 50 mM potassium phosphate buffer, pH 7.4, and started with NADPH to a final concentration of 1 mM. Nine substrate concentrations (0, 0.15, 0.25, 0.5, 1, 2, 4, 8 and 10 mM) were used for the determination of apparent  $K_m$  and  $V_{max}$ . The

reactions were stopped by adding 100  $\mu$ L of ice-cold ACN. The mixtures were vortexed and centrifuged at 3000 x g for 5 min to remove precipitated protein.

Negative control incubations were run in parallel without cyclophosphamide, without NADPH, or without microsomes. Microsomes containing POR alone were incubated in parallel under the same conditions after adjusting the POR amount to be equal to the highest CYP2B6.1 batch.

For further confirmation of our results, Cy (0.75 mM) was incubated under the linearity conditions with 3 batches having the same POR amounts (356 nmol/min/mL) and variable amounts of CYP and POR/CYP ratios. The formation of 4-OH-Cy was assessed using HPLC with fluorescent detector [123, 124].

**Table 3:** Characterizations of commercial recombinant microsomes containing human CYP2B6.1

Batch No.	Batch 1	Batch 2	Batch 3	POR
Catalogue No.	CYP/EZ016	CYP/EZ041***	CYP020	CYP004
Lot. No	C2B6LR002/A	C2B6BR016A	C2B6R005	RED004
Company	Cypex	Cypex	Cypex	Cypex
P450 concentration*	1	1	1	N/A
Protein concentration**	10	10	10.6	12.7
Specific P450 content #	100	100	94	N/A
Cytochrome c reductase activity##	77	890	1302	2437

\*P450 concentration (nmol/mL), \*\*Protein concentration (mg/mL), #Specific P450 content (pmol/mg protein), ##Cytochrome c reductase activity (nmol/min/mg protein). \*\*\* Batch 2 also contained a supplement of purified human cytochrome *b*<sub>5</sub>. N/A; Not applicable.

To study the role of CYP2J2 in Cy bioactivation, microsomes from *Escherichia coli* coexpressing human CYP2J2 and CYP reductase were obtained from Cypex (Dundee, UK). The specific CYP content was 127 pmol/mg protein and the reductase activity was 429 nmol/(min·mg) protein. Microsomes were incubated for 1 h at 37°C with Cy in concentrations of 0 - 50 mM in 100  $\mu$ L of 50 mM potassium phosphate buffer, pH 7.4, and started with NADPH to a final concentration of 1 mM. The reaction was terminated by adding an equal volume of ice-cold ACN. Incubations were performed in triplicates and negative controls were run in parallel. 4-OH-Cy formation was measured using HPLC with fluorescence detector [123, 124].



## 3.6 MEASUREMENT OF BUSULPHAN AND ITS METABOLITES

### 3.6.1 Busulphan

Samples were extracted according to the method reported previously by Hassan *et al.* [125]. Briefly, 500  $\mu\text{L}$  of plasma and urine were diluted with 500  $\mu\text{L}$  of  $\text{H}_2\text{O}$ . Fifty microliters of the internal standard (1,5-bis(methanesulfonyl)pentane; 38.5  $\mu\text{M}$ ) were added, followed by the addition of 1 mL of sodium iodide (8M) and 400  $\mu\text{L}$  of *n*-heptane. The tubes were placed under magnetic stirring in a water bath (70 °C) for 45 min. During the reaction, busulphan and 1,5-bis(methanesulfonyl)pentane were converted to 1,4-diiodobutane and 1,5-diiodopentane respectively and extracted to *n*-heptane [126]. The percentage of the conversion of busulphan and 1,5-bis(methanesulfonyl)pentane to 1,4-diiodobutane and 1,5-diiodopentane was over 90% [125]. The organic phase was transferred into either GC-MS or GC tubes.

### 3.6.2 Tetrahydrothiophene and sulfolane

Samples (180  $\mu\text{L}$ ) were added to 10  $\mu\text{M}$  nicotine (20  $\mu\text{L}$ ) as an internal standard before extraction. The matrix was extracted by liquid-liquid extraction with dichloromethane (equal volumes 200  $\mu\text{L}$ ) for 30 s of high speed vortexing. After extraction and centrifugation at 16000 x *g* for 10 min, the organic phase was transferred into GC-MS tubes.

### 3.6.3 Tetrahydrothiophene 1-oxide and 3-hydroxysulfolane

Samples (180  $\mu\text{L}$ ) were added to 10  $\mu\text{M}$  of 3-methylsulfolane (20  $\mu\text{L}$ ) as an internal standard. The matrix was lyophilized (< 1 mbar at 40°C under  $\text{N}_2$  stream) to dryness, the residue was dissolved in 10  $\mu\text{L}$  water and 200  $\mu\text{L}$  of ethyl acetate for extraction. Samples were vortexed for 30 s at high speed and centrifuged at 16000 x *g* for 10 min. The organic phase was transferred to GC-MS tubes.

The GC-MS system consisted of a Hewlett Packard 5890 Series II gas chromatograph equipped with an Agilent 6890 series auto-injector and a Hewlett Packard 5972 series mass selective detector (Santa Clara, CA, USA). This system was utilized for the measurement of busulphan and its metabolites (Study I, II). The column used was Rxi-1ms 100% dimethyl polysiloxane split fused silica non-polar phase, 30 m, 0.25 mm ID and 1.0  $\mu\text{m}$  df (Bellefonte, PA, USA). The carrier gas was helium and the pressure on the top of the column was 40 kPa with an inlet temperature of 50°C. A 2  $\mu\text{L}$  sample aliquot was injected splitless at a flow of 0.9 ml/min. The analysis was run in a gradient with an initial temperature of 40°C for 2.5 min followed by 20°C  $\text{min}^{-1}$  increase up to 100°C then 10°C  $\text{min}^{-1}$  increase up to 180°C and finally 50°C  $\text{min}^{-1}$  increase up to 240°C. The final temperature was maintained for 3 min. The injector temperature was 190°C while the detector temperature was 250°C [127]. Chromatograms and all the quantitative results were measured using Enhanced ChemStation software G1401BA version B.01.00 (Agilent, Santa Clara, CA, USA).

Gas chromatography (SCION 436-GC) with electron capture detector (ECD) connected to fused silica Column 15m X 0.25mm (Bruker Optics Scandinavia AB, Stockholm, Sweden)

was used for busulphan measurement in Study III. The injection temperature was 250°C, the column was operated isothermally at 145°C with a detector temperature of 300°C. The calibration curve was linear within the range 25 - 1500 ng/mL.

### **3.7 MEASUREMENT OF CYCLOPHOSPHAMIDE AND ITS ACTIVE METABOLITE**

Cyclophosphamide was measured in 1 mL patient plasma samples as described previously [128]. Plasma was extracted using diethyl acetate ester after the addition of ifosfamide as an internal standard. The organic layer was evaporated to dryness. Then, 30 µL aliquots of residue dissolved in mobile phase were injected into the HPLC.

The concentration of 4-OH-Cy was determined using fluorescence detection. 4-OH-Cy was fluorescence sensitive after adding dansylhydrazine and hydrochloric acid as described previously [123, 124]. The mixture was vortexed and incubated at 50°C for 5 min. 30 µL aliquots of the final sample supernatant were injected into the HPLC system.

High-performance liquid chromatography (HPLC) consisted of an LKB-2150 pump, Gilson-234 auto-injector with a 100-µL sample loop connected to an Extend-C18 column (150 × 4.6 mm × 3.5 µm) with a C18 guard column (Agilent, CA, USA). Integration was performed with a CSW32 (version 1.3) chromatographic station (DataApex Ltd., Prague, Czech Republic).

For Cy measurements, the mobile phase consisted of ACN/0.05 M potassium phosphate buffer, pH 2.8 (24:76 v/v) and the flow rate was 1 mL/min. Cy was detected by a Milton Roy UV Spectro-Monitor 310 detector (Pont-Saint-Pierre, France) at a wavelength of 195 nm.

For 4-OH-Cy measurements, the mobile phase consisted of ACN/phosphate buffer, pH 3.5 (1:2 v/v), and a flow rate of 1.6 mL/min. A Shimadzu RF-10XL fluorescence detector (Tokyo, Japan) was used to detect 4-OH-Cy. Detection was performed at excitation and emission wavelengths of 350 and 550 nm, respectively.

### **3.8 VALIDATION OF THE METHOD FOR QUANTIFICATION OF BUSULPHAN AND ITS METABOLITES**

This analytical method for the detection and quantification of busulphan and its main metabolites in different biological fluids was developed:

Mass spectrometry was operated in selective ion monitoring (SIM) mode at the following ions:  $m/z$  310 for busulphan after conversion to 1,4-diiodobutane,  $m/z$  60 and 88 for THT,  $m/z$  55 and 104 for THT 1-oxide,  $m/z$  56 and 120 for sulfolane and  $m/z$  44 and 136 for 3-OH sulfolane. For compounds used as internal standards,  $m/z$  324 for 1,5-bis(methanesulfonyl)pentane after conversion to 1,5-diiodopentane,  $m/z$  162 for nicotine

and  $m/z$  134 for 3-methylsulfolane was used. The parent compounds and the highest daughter ions were detected.

### 3.8.1 Stock solutions

Frozen plasma samples were thawed at room temperature and vortexed before use, while urine samples were freshly collected on the same day. The analysis was performed for each analyte separately (3 injections) and was also evaluated after mixing the analytes and injecting once. All stock solutions were prepared as 1 mM solutions (THT, THT 1-oxide, sulfolane and 3-OH sulfolane) in phosphate buffer pH 7.4, while busulphan was dissolved in ACN). Sample final concentrations were prepared from the stocks by serial dilution. For the recovery study, all compounds were prepared as stock solutions (1 mM) in the appropriate solvent and subsequently serially diluted in the same solvent prior to use.

### 3.8.2 Conduct of validation

The bioanalytical validation has been carried out according to the international guidelines recommended by Shah *et al.* [129, 130]. A standard curve was defined by a set of calibration standards ranging from 0.5  $\mu\text{M}$  to 50  $\mu\text{M}$  for all compounds except for 3-OH sulfolane, which was 1.25  $\mu\text{M}$  - 50  $\mu\text{M}$ . Samples for the standard curve were randomized through the entire run. At least three standard curves per analyte were assayed over a three day period in both plasma and urine. The quantification analysis was based on the ratio peak area analyte/peak area IS and equal weighting in a linear regression analysis equation. Three quality controls (QC) covering the whole range of the standard curve (2, 15 and 30  $\mu\text{M}$ ) were run in triplicate over three days in both plasma and urine to determine the inter- and intra-day reproducibility. Blank samples for all compounds were run in parallel and were compared with the lower limit of quantification (LLOQ) for each compound. Stability of the analytes in biological fluids and through the analytic process was established with two different concentrations of QC [129, 130].

### 3.8.3 Clinical application

In order to evaluate the applicability of the method for measuring Bu and its metabolites in clinical samples, we studied the plasma and urine samples from a patient undergoing HSCT. The patient was treated with high dose busulphan (2 mg/kg twice daily) for four days. Blood samples were withdrawn according to standard protocol for dose adjustment of busulphan. Samples were collected at 0, 0.5, 1, 2, 3, 4, 6, 8 and 10 h after the first and the fifth dose and at 0, 1, 3 and 6 h for doses 3 and 7. Blood was collected in EDTA vacutainer tubes, plasma was separated by centrifugation at 3000  $\times g$  for 5 min and stored at  $-20^{\circ}\text{C}$  until analysis as described above. Urine samples were collected at 6, 12, 24, 48 and 72 h and stored at  $-20^{\circ}\text{C}$  until assay.

## 3.9 LIMITED SAMPLING MODEL DEVELOPMENT

### 3.9.1 Model building

In the present investigation, we have employed the following models: multiple regression models, compartment models, and plain curve fitting models. The present model was developed using 23 patients and validated in 20 pediatric and 23 adult patients (Table 2).

#### 3.9.1.1 Multiple regression models

The strategy of analyzing the correlation between AUC and each concentration sample from a full sample set using a multiple regression procedure has been described previously [15]. The concentration samples found to have the strongest correlation with AUC were retained, while the other concentrations were declined. Stepwise regression was used to construct a linear equation (Equation 1):

$$\text{AUC} = K_0 + K_1 \cdot C_1 + K_2 \cdot C_2 + \dots + K_n \cdot C_n$$

(Equation 1)

$K_n$  is the calculated constant associated with the  $n$  sample and  $C_n$  is the plasma concentration of busulphan in the  $n$  sample.

The number of concentration samples is limited to  $n$  and the sampling times after dose administration must be identical in all subjects. The formula is verified using a new sample and the correlation is often satisfactory, provided the same population is studied at the same center using the same treatment protocol [131, 132]. This equation is simple, and it is easy to implement the model in clinical practice [133].

#### 3.9.1.2 Compartment models

Drug dynamics within the body in the present model were approximated by kinetically defined compartments. Mathematical formulas describe plasma concentration over time based on absorption, elimination, and distribution rates in compartment models. One or two compartments are most commonly used. Due to the distribution properties of busulphan it is reasonable to implement a one-compartment model for this drug [134]. The formula for calculating AUC then takes the form (Equation 2):

$$\text{AUC} = \int_{t=0}^{t=\infty} \frac{F \text{ Dose } k_{abs}}{V_d(k_{abs} - k_{el})} (e^{-k_{el}t} - e^{-k_{abs}t}) dt$$

(Equation 2)

$F$  is the bioavailability,  $\text{Dose}$  the drug dose administered,  $k_{abs}$  is the absorption rate constant,  $k_{el}$  is the elimination rate constant,  $t$  is the time, and  $V_d$  is the volume of drug distribution.

By fitting the absorption rate  $k_{abs}$ , elimination rate  $k_{el}$ , and the absorbed dose ( $F \cdot \text{dose}$ ), drug distribution ratio  $F \cdot \text{Dose} / V_d$ , it is possible in theory to calculate the exact AUC. In practice, problems arise from unusual absorption patterns and noisy data that affect the drug concentrations. In particular, the absorption rate is not constant, which may affect the validity of the formula and could result in a major deviation of the AUC estimate. Moreover, the estimate is very sensitive to even single errors in concentration measurements.

### 3.9.1.3 Non-compartment curve fitting models

In the present model, the third strategy was to fit a mathematical formula to the plasma concentrations. Several methods have been devised, some involving elaborate calculations such as splines or piecewise polynomial interpolation. The simple numeric trapezoidal rule or trapezoidal rule with log trapezoidal rule during the elimination phase is, however, most commonly used. It is hard to find convincing evidence for the benefit of utilizing complicated calculations. A comparison of 11 numerical curve fitting models found that an interpolation with piecewise parabolas through the origin for concentration intervals until the second concentration or  $C_{max}$ , with log trapezoidal rule for the remaining intervals, showed the most promising results [135]. This method was chosen for study because it can produce a negative curvature. Purves argued that an interpolation method with negative curvature would presumably be more adequate during the absorption phase after an oral dose than a method, such as the common trapezoidal rule, with zero curvature. Among the methods compared were the Lagrange and cubic spline methods. Both were deprecated due to large variance in their estimates [135]. The AUC using the proposed interpolation for  $n$  samples is calculated in equation 3:

AUC=

$$\int_{t_0}^{t_2} (a_1 t^2 + b_1 t) dt + \sum_{i=2}^{i_p-1} \int_{t_i}^{t_{i+1}} (a_i t^2 + b_i t) dt + \sum_{i=p}^{n-1} \frac{(t_{i+1}-t_i)(C_{i+1}-C_i)}{\log\left[\frac{C_{i+1}}{C_i}\right]}$$

(Equation 3)

$P$  is the peak plasma sample concentration,  $t_i$  is the time point  $i$ ,  $C_i$  is the drug concentration in sample  $i$  and  $n$  is the total number of samples.

The equation  $a_i t^2 + b_i t$  describes a parabola through origo (PTO) and  $(t_i, C_i)$ ;  $(t_{i+1}, C_{i+1})$

### 3.9.1.4 Implementation of Models

Specific models must be designed to compare the respective strategies. It can be argued that there are flaws in the specific model implementation rather than in the strategy itself; however, we have carefully strived to produce the best possible models, in respect to accuracy and efficiency.

### 3.9.1.5 Implementation of multiple linear regression model

Linear model (Equation 4) was utilized for estimating the AUC using limited sampling at our facility. The model was validated and developed by us and is accordingly well adapted to local circumstances. It originates from studies of busulphan pharmacokinetics in 20 children who underwent HSCT for either leukemia or inherited disorders. Based on three plasma concentrations (1, 3, and 6 h) after administration of one busulphan dose, a linear model with high correlation ( $r = 0.998$ ) was devised using multiple linear regression [52] (Equation 4):

$$\text{AUC} = 1.69 \times C_1 + 1.45 \times C_2 + 7.28 \times C_3$$

(Equation 4)

$C_1$  is the concentration at 1 h,  $C_2$  is the concentration at 3 h and  $C_3$  is the concentration at 6 h.

### 3.9.1.6 Implementation of compartment model

Several compartment models have been devised for busulphan kinetics. Two compartments may be used in a model of drug distribution for a more accurate simulation of the actual kinetics in humans. The specifics of the drug determine how much is gained in accuracy from introducing the complexity of a two compartment model. Basically, sparse input data reduce the feasibility of using a complex model with several deduced parameters. Further, several studies have demonstrated that a one compartment model provides a good approximation of busulphan kinetics in the human body [134].

A lag time for the absorption phase can be added to account for a delay before the drug starts appearing in plasma. Using few samplings with just one or two samples during the absorption phase impede determination whether a concentration results from a slow absorption and small lag time or the opposite. Moreover, lag time has a limited effect on AUC estimate [136]. Consequentially using lag time has been excluded.

For fitting the parameters of the model to the measured plasma concentrations, Levenberg - Marquardt algorithm was employed. It outperforms simple gradient descent and other conjugate gradient descent methods in a wide variety of problems [53].

CenterSpace™ Software (Corvallis, OR, USA) in the NMath library for the .NET platform was used for calculating the implementation of the algorithm. The model has the same time points for sampling as the regression model developed earlier. To make the Levenberg - Marquardt algorithm converge with reasonable regularity, at least four plasma concentrations are needed from each patient. The first ten patients have been tested using a recently introduced method for finding the most predictive design points in a model [137].

The analysis was done with R using an implementation of the algorithm provided by the authors of the method. The last concentration at 8 h was found to be the most predictive concentration sample for AUC. Sampling at 8 h was accordingly added for both the compartment model and the non-compartment curve fitting model. From some datasets it is

not possible to construct a compartment model due to mathematical reasons, and the model fails. In this study the model has failed in three adult patients but in none of the pediatric patients.

#### *3.9.1.7 Implementation of non-compartment curve fitting model*

In our department we have used estimates of total AUC for  $t_0 \rightarrow \infty$  for decisions regarding dose adjustment. The comparison by Purves described earlier inspired us to look more closely at the possibility of using piecewise formulas with a PTO until or one step beyond  $C_{max}$  and then the piecewise log trapezoidal rule [135]. However, the formula has been adapted to four concentrations, which we consider to be the least number of concentrations necessary to get a meaningful implementation of this strategy. An estimate for the AUC tail area from the last concentration to infinity has been added. Since the algorithm involves repeated conditional calculations, it is practical to utilize a computer program. A graphic representation of the resulting plasma concentration simulation is possible because the model involves integration of an actual curve. However, the algorithm fails if it is not possible to calculate the tail area which happens if the  $C_{max}$  is not reached before the last sample is taken. In our study, this occurred in four adult patients and in one pediatric patient.

#### *3.9.1.8 Combining the non-compartment curve fitting model with the compartment model*

The two LSMs represent different strategies for interpreting the same data and the results of both deviate from estimates using standard rich sampling, but not in the same way. This led to the idea that a strategy of combining the methods, using the average of the two LSMs estimates could perform better than either model alone. Moreover, calculations using either model will fail to produce a result for some data. The risk that both calculations will fail is far lesser and did not occur for any of our patients. If one LSM strategy calculation fails, it is still possible to use the estimate from the other LSM. The performance of this strategy was tested and compared using the different single LSM modeling strategies.

### **3.9.2 Assay methodology**

Adult and pediatric patients were recruited at the Center for Allogeneic Stem Cell Transplantation (CAST) at Karolinska University Hospital, Huddinge as mentioned previously.

Blood samples were collected before and at 0.5, 1, 2, 3, 4, 6, 8, and 10 h after the administration of Bu. Blood was collected (1.5 mL/sample) in heparinized vacutainer tubes. Samples were centrifuged at 3000 x g for 5 min and plasma was separated and transferred to new tubes. Busulphan was extracted and quantified using GC-ECD as described previously.

### 3.9.3 Computer program

The principal features of the program and an in-depth description of the other parts of the program can be freely obtained from the main author contact as cited in the contact information [138].

#### 3.9.3.1 Area under the concentration–time curve and simulated plasma concentration curve

The four measured plasma concentrations are used for calculating the resulting AUC estimates of the compartmental and modified Purves models and the resulting average is shown one graph at a time for illustration of the simulated plasma concentration curve. Figure 4 shows a screen dump from an example session to illustrate the presentation of data.

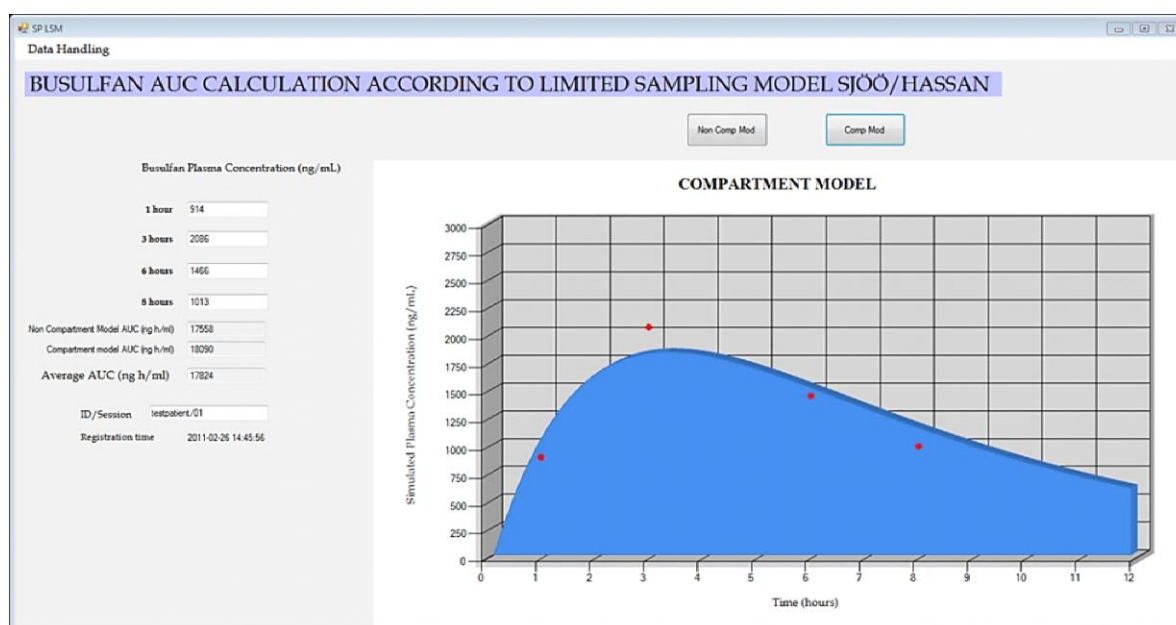


**Figure 4:** Picture from AUC2 program showing the Graphic User Interface for calculations of AUC

### 3.9.4 Statistical analysis

The intraclass correlation coefficient (ICC) assesses agreement as well as consistency (precision). The ICC is based on analysis of variance calculations and, depending on the data, different models are used. The presented case of the ICC is based on a mixed-model analysis of variance (Equation 5). The equation for the agreement parameter  $q$  is seen in Equation 6. This parameter can be estimated from an analysis of variance table and the sum of squares obtained from this analysis, as described in Eq. 5:



$$ICC = \frac{BMS - EMS}{BMS + (k - 1)EMS + \frac{k}{n}(MMS - EMS)}$$

(Equation 5)

*BMS* is between-patients mean square, *EMS* is the residual error mean square, *MMS* is the methods mean square, *k* is number of methods compared (in this case 2 each comparison) and *n* is the number of patients (23).

$$P = \frac{\sigma_P^2}{\sigma_P^2 + \sigma_M^2 + \sigma_I^2 + \sigma_E^2}$$

(Equation 6)

*P* is the correlation,  $\sigma_P^2$  is the variance of patients,  $\sigma_M^2$  is the variance of methods,  $\sigma_I^2$  is the variance of patient-method interaction and  $\sigma_E^2$  is the variance of the residual error.

### 3.10 DATA ANALYSIS

Kinetics estimations were performed using Microsoft Excel and WinNonLin software (standard edition, version 2.0). All statistical analyses and graphs were carried out using GraphPad Prism (version 4.0, GraphPad Software, Inc.) and SigmaPlot (version 12.5, Systat software, Inc).



## 4 RESULTS

### 4.1 BUSULPHAN

#### 4.1.1 Method development and validation

##### 4.1.1.1 Choice of a solvent

Extraction solution may significantly affect the extracted amount, peak shape and column efficiency [139]. Different solvents have been tested with all the compounds to reach the maximum recovery, highest sensitivity for the analyzed compound expressed as the lowest LLOQ and best peak shape. We have tested solvents hexane, pentane, toluene and diethyl ether. Finally, three solvents and three methods of extraction were selected for five compounds to reach the best results.

##### 4.1.1.2 Quantitative analysis of the analytes in biological fluids

###### 4.1.1.2.1 Sensitivity and selectivity

Matrix effect bias for both plasma and urine has been discussed as a major problem in quantification methods using GC-MS, but using SIM mode has reduced this effect. Five samples of each compound have been run over three days in both plasma and urine. The LLOQ was 0.5  $\mu\text{M}$  for all compounds except for 3-OH sulfolane for which the LLOQ was 1.25  $\mu\text{M}$ . Blank samples have been run in parallel to the LLOQ samples and no carry over was observed. This is probably due to the extensive washing procedure between samples (x 5 solvent and x 5 acetone). Results for LLOQ are shown in Table 4. All the results were within 20% of the expected value.

**Table 4:** LLOQ in biological fluids.

	Plasma			Urine		
	Mean	SD	RSD%	Mean	SD	RSD%
<b>Busulphan 0.5 <math>\mu\text{M}</math></b>	0.483	0.087	18.01	0.585	0.114	19.49
<b>THT 0.5 <math>\mu\text{M}</math></b>	0.469	0.064	13.65	0.510	0.069	13.53
<b>THT 1-oxide 0.5 <math>\mu\text{M}</math></b>	0.567	0.094	16.58	0.545	0.080	14.68
<b>Sulfolane 0.5 <math>\mu\text{M}</math></b>	0.568	0.106	18.66	0.422	0.080	18.96
<b>3-OH-sulfolane 1.25 <math>\mu\text{M}</math></b>	1.413	0.074	5.24	1.071	0.138	12.89

n = 15 per analyte; SD, standard deviation, RSD, relative standard deviation.

###### 4.1.1.2.2 Recovery

The recovery was determined by comparing the concentrations of two QC samples after extraction from plasma and urine with the same concentration dissolved in solvent and injected directly to GC-MS in triplicate. Sulfolane showed the best recovery (93.2%) while THT had the lowest recovery value (17.1%). The recoveries of THT 1-oxide and 3-hydroxy sulfolane were 44.4 and 48.2%, respectively, while for the internal standards nicotine and

3-methylsulfolane the recoveries were 93.5 and 70%, respectively. The recoveries of busulphan and its internal standard (1,5-bis(methanesulfonyl)pentane) were 91 and 92%, respectively, which is in good agreement with the results reported previously [125].

#### 4.1.1.2.3 Accuracy and precision

Accuracy and precision were assessed from the analysis of three standard curves and three QCs in triplicate using both biological fluids. The standard curve was linear over the concentration range 0.5-50  $\mu\text{M}$  for busulphan, THT, THT 1-oxide and sulfolane and 1.25-50  $\mu\text{M}$  for 3-OH sulfolane. The standard curves were run for each compound and all calibration curves contained between 5-7 standard points.  $R^2$  for all curves was between 0.995 and 0.999.

The accuracy and precision were determined for all five analytes in triplicate for inter- and intra-day variations over three consecutive days. The QC results showed a standard deviation < 15% for all values obtained including low, medium and high QCs compared to the nominal values (Table 5).

Calibration standards and QCs were prepared freshly everyday by dilution of individual aliquots of stock solution(s). The final percentage of the biological matrix in the quality control samples was at least 80%.

**Table 5:** Quality controls in biological fluids.

		Plasma			Urine		
		Mean	SD	RSD%	Mean	SD	RSD%
<b>Busulphan</b>	<b>Low 2<math>\mu\text{M}</math></b>	1.875	0.243	12.960	2.267	0.234	10.322
	<b>Med 15<math>\mu\text{M}</math></b>	17.20	1.613	9.378	13.456	0.40	2.973
	<b>High 30<math>\mu\text{M}</math></b>	32.267	1.956	6.062	30.444	1.862	6.116
<b>THT</b>	<b>Low 2<math>\mu\text{M}</math></b>	1.778	0.188	10.574	2.166	0.11	5.078
	<b>Med 15<math>\mu\text{M}</math></b>	14.144	1.368	9.672	12.814	0.858	6.696
	<b>High 30<math>\mu\text{M}</math></b>	30.2	2.506	8.298	25.5	3.359	13.173
<b>THT 1-oxide</b>	<b>Low 2<math>\mu\text{M}</math></b>	2.133	0.292	13.690	1.867	0.166	8.891
	<b>Med 15<math>\mu\text{M}</math></b>	15.372	1.742	11.332	14.516	1.292	8.901
	<b>High 30<math>\mu\text{M}</math></b>	31.878	3.026	9.492	30.211	1.518	5.025
<b>Sulfolane</b>	<b>Low 2<math>\mu\text{M}</math></b>	1.831	0.073	3.987	1.879	0.248	13.199
	<b>Med 15<math>\mu\text{M}</math></b>	15.056	1.102	7.319	13.678	1.445	10.564
	<b>High 30<math>\mu\text{M}</math></b>	30.944	1.053	3.403	28.111	3.195	11.366
<b>3-OH-sulfolane</b>	<b>Low 2<math>\mu\text{M}</math></b>	2.14	0.286	13.364	2.244	0.270	12.032
	<b>Med 15<math>\mu\text{M}</math></b>	17.144	1.579	9.210	13.625	1.807	13.262
	<b>High 30<math>\mu\text{M}</math></b>	33.333	3.228	9.684	29.556	1.884	6.374

n = 9 per analyte; SD, standard deviation; RSD, relative standard deviation.

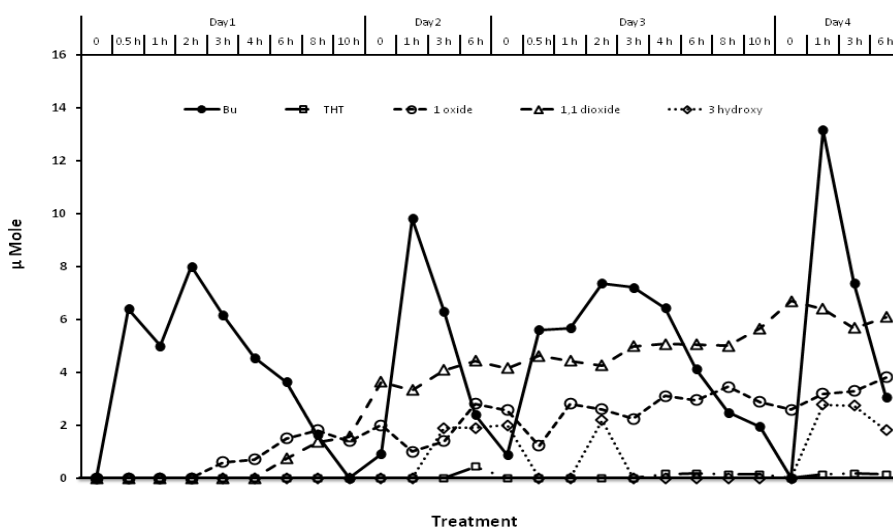
#### 4.1.1.2.4 Sample stability

Stability of the analytes in the sample extracts has been studied. Two QCs have been run in triplicate after extraction from both plasma and urine. The analytes were stable during the extraction process, extract storage and chromatography. Since all the compounds are not light sensitive, they have been stored on a bench in daylight.

The stability of the analytes was also examined prior to extraction in plasma and urine. The results showed that all compounds were stable at 4°C and -20°C for 24 h. However, after 24 h at room temperature, the concentration of THT was decreased by about 38% in urine. THT was more stable in plasma, in which the observed decrease was only 17%. Busulphan concentrations decreased by about 34% in plasma, but were stable in urine. THT 1-oxide, sulfolane and 3-OH sulfolane were stable in both plasma and urine at room temperature for 24 h. Our results indicate that samples containing THT and busulphan should be stored immediately at 4°C or -20°C, while for the other analytes storage at room temperature until 24 h is acceptable.

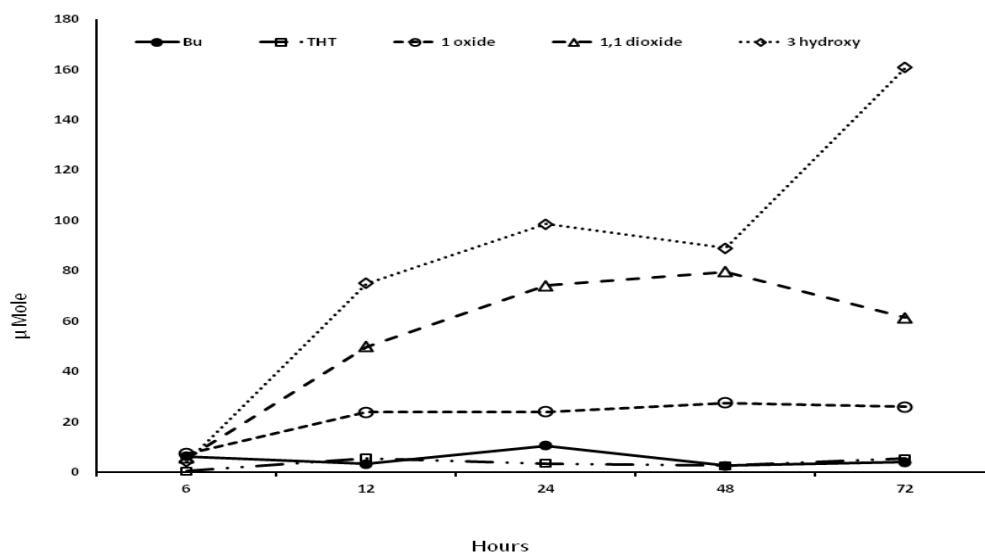
#### 4.1.1.3 *Clinical application*

Figure 5 shows busulphan concentrations in patient plasma collected using complete sampling protocol for the first and fifth doses. First AUC was estimated to be 7240 ng/mL\*min. Following dose adjustment aiming to achieve the target AUC, the estimated AUC was 8151 and 11604 ng/mL\*min for doses 5 and 7, respectively. The levels of THT were rather low indicating its rapid metabolism (oxidation). A continuous increase in both THT 1-oxide and sulfolane concentrations indicates further oxidation steps, while the low levels of 3-OH sulfolane indicate the elimination of the metabolite through the kidneys as presented in figure 6.



**Figure 5:** Busulphan and its metabolites in patient plasma during four days of high dose treatment.

The most polar compound out of busulphan major metabolites, 3-OH sulfolane, gave the highest yield in urine, followed by sulfolane and to a lesser extent THT 1-oxide. The levels of busulphan and THT were very low due to their lipophilicity. These results show that 3-OH sulfolane is the last oxidized metabolite which is excreted into the urine due to its hydrophilic nature (Figure 6).



**Figure 6:** Busulphan and its metabolites in patient urine during four days of high dose treatment.

## 4.1.2 Enzymes involved in busulphan metabolic pathway

### 4.1.2.1 Patient *FMO3* gene expression

Mononuclear cells from peripheral blood of patients undergoing conditioning regimen before HSCT were investigated. A significant up-regulation ( $P < 0.05$ , t-test) of *FMO3* was found after Bu conditioning. *FMO3* up-regulation followed the same pattern as that observed for *GSTA1* ( $P < 0.05$ , t-test) (Figure 7). These results have been confirmed by real time PCR for *FMO3* gene expression and normalized against *GAPDH*.

Clinical data including age, diagnosis, stem cell dose, relapse, remission, mortality and complications were collected (Table 1). No correlation between diagnosis and/or other clinical data and the results of *FMO3* expression was observed.

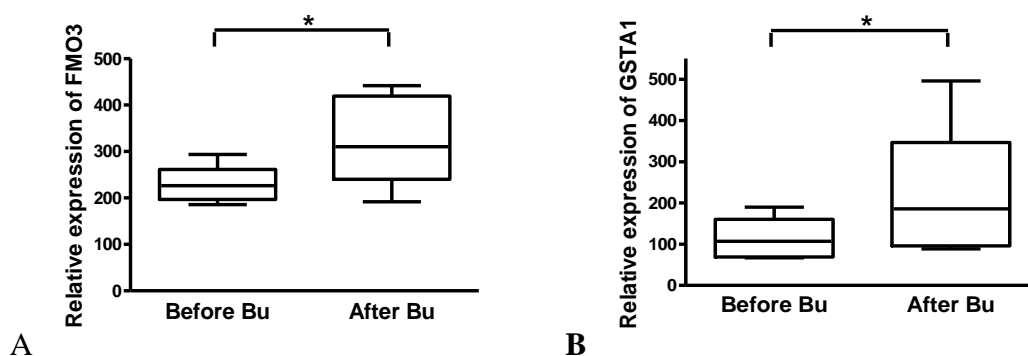


**Figure 7:** Up-regulation for *FMO3* (A) and *GSTA1* (B) mRNA during Bu conditioning

#### 4.1.2.2 Microsomal incubations with THT

Incubation of THT with HLM showed rapid decrease of THT concentrations and gradual formation of the subsequent metabolites. Up to 72% of THT has been metabolized after 1 h incubation. This percentage decreased to 48% when FMO3 was inhibited, while it was 67% after CYPs inhibition. These results have shown that THT is metabolized by the microsomal enzymes and FMO3 is the main enzyme in this process.

THT incubation with recombinant microsomes confirmed these results, since 96% of THT has been metabolized by recombinant FMO3 in 15 min in association with the formation of subsequent metabolites (Figure 8). When THT was incubated with recombinant CYPs, great variations in THT decrease was observed. CYP2B6, CYP2C8, CYP2C9, CYP2C19, CYP2D6, CYP2E1, CYP3A4 and CYP4A11 were the most important enzymes involved in THT metabolism.

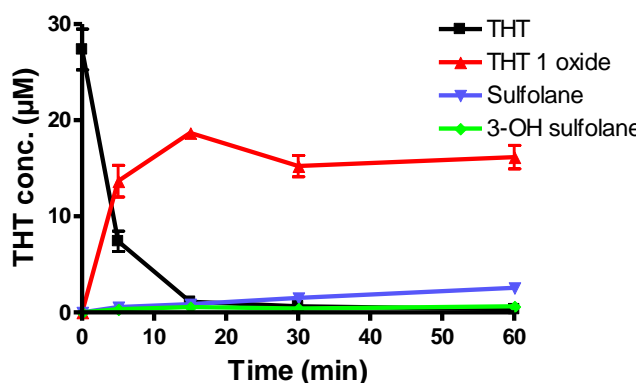


**Figure 8:** Kinetics of THT and its metabolites after incubation with recombinant *FMO3*. 96% of THT has been metabolized in 15 min. This disappearance was accompanied by the metabolites formation.

FMO3 had the highest initial THT disappearance rate ( $v_0$ ) (6.87 nmol/min/mL) followed by CYPs 3A4, 4A11 and 2C9. FMO3 also had highest  $CL_{int}$  value (0.26  $\mu$ L/min/mg protein) followed by CYPs 3A4, 4A11 and 2C8.

Comparing CYPs based on the initial THT disappearance rate ( $v_0$ )/(POR/CYP ratio), CYP2C8 had the highest rate for THT metabolism (5.03 nmol/min/mL/(POR/CYP ratio)) followed by CYPs 2C9, 2C19, 2E1 and 3A4. All results for enzymes kinetics are listed in table 6.

**Table 6:** Apparent kinetics for THT disappearance by recombinant human enzymes

Enzyme	$CL_{int}$ value ( $\mu\text{L}/\text{min}/\text{mg}$ protein)	$v_0$ (nmol/min/mL)	$v_0 / (\text{POR}/\text{CYP ratio})$ (nmol/min/mL/(POR/CYP ratio))
FMO3	0.26	6.87	---
CYP1A1	0.06	1.68	0.08
CYP1A2	0.05	1.24	0.08
CYP2B6	0.07	1.76	0.08
CYP2C8	0.09	2.45	5.03
CYP2C9	0.06	1.64	1.50
CYP2C19	0.06	1.51	0.53
CYP2D6	0.09	2.24	0.10
CYP2E1	0.06	1.41	0.38
CYP3A4	0.15	3.66	0.38
CYP4A11	0.11	2.52	0.20

FMO3 had the highest  $v_0$  and  $CL_{int}$  value while other CYPs showed lower activity such as 3A4, 4A11, 2C8 and 2C9. Comparing CYPs based on the initial THT ( $v_0$ )/(POR/CYP ratio); CYP2C8 had the highest rate for THT metabolism followed by CYPs 2C9, 2C19, 2E1 and 3A4.

#### 4.1.2.3 Mice treatments

Mice plasma were extracted for both Bu and THT as reported previously [119, 125] and quantified using GC-MS [119]. The estimated kinetics for busulphan after different treatments are presented in table 7. Treatment with FMO3 inhibitor, PTU, has increased Bu AUC and reduced its clearance. Simulation of THT accumulation by injecting THT at the same time with Bu had also the same effect on Bu kinetics compared to mice injected with Bu alone.

**Table 7:** Busulphan kinetics in mouse plasma

	Bu		Bu+PTU		Bu+THT	
	Mean	SEM	Mean	SEM	Mean	SEM
AUC ( $\mu\text{M}\cdot\text{h}$ )	44.29	5.79	65.33	1.27	65.51	8.57
$K_{0t}$ (h)	0.39	0.19	0.08	0.01	0.16	0.08
$K_{10}$ (h)	3.07	1.31	1.67	0.38	2.32	0.12
CL ( $\mu\text{M}\cdot\text{h}$ )	40.73	8.00	30.64	0.60	31.64	4.27
$C_{max}$ ( $\mu\text{M}$ )	7.47	0.98	25.54	6.26	16.51	2.72

Busulphan was injected into mice i.p. at different time points, after 3 days of i.p. injection of PTU and both Bu and THT (double dose).

PTU injection has significantly ( $P < 0.05$ , t-test) increased Bu plasma concentrations and its AUC. Moreover, simulated accumulation of THT by injecting THT concomitantly with Bu



has revealed, though to a lesser extent, higher levels of Bu compared to its levels in mice not injected with THT (Figure 9).

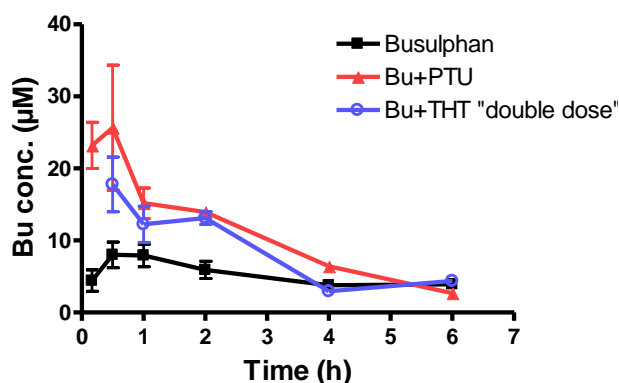


**Figure 9:** Busulphan concentrations in mouse plasma.

Busulphan was injected into mice i.p. at different time points, after 3 days of i.p. injection of PTU and both Bu and THT (double dose).

THT concentrations and AUC have significantly ( $P < 0.05$ , t-test) increased after PTU injection (Figure 10A). Also, THT concentrations and AUC were significantly ( $P < 0.05$ , t-test) higher in mice injected with Bu and PTU compared to mice injected with Bu alone (Figure 10B). THT concentrations in mice injected with Bu and PTU were almost at the same level as in mice injected with Bu and a double dose of THT.

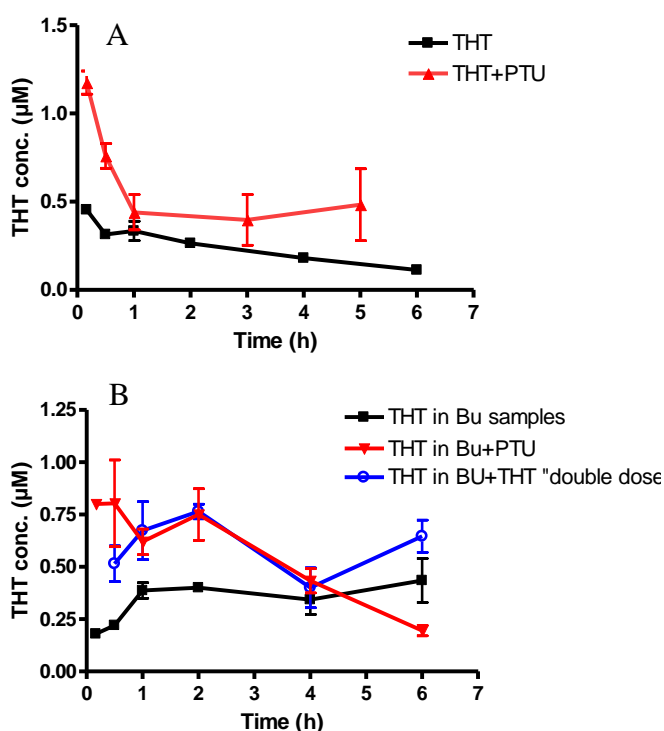


**Figure 10:** THT concentrations in the plasma of mice injected with THT or busulphan.

A- THT was injected i.p. at different time points. The same experiment was repeated after 3 days of i.p. injection of PTU.

B- Busulphan was injected to mice i.p. at different time points, after 3 days of i.p. injection of PTU and both Bu and THT (double dose).

#### 4.1.2.4 Clinical application

A patient treated concomitantly with busulphan and voriconazole had a much higher busulphan plasma concentrations than the levels usually observed after the same administered dose. The high levels of busulphan hampered the AUC calculation. THT levels were rather detectable from the first busulphan dose with higher accumulation and slower oxidation compared to what has previously been reported ( $P < 0.05$ , t-test) [119] (figure 11).

Voriconazole was stopped immediately after Bu first dose. Later busulphan concentrations were reduced to the expected values.

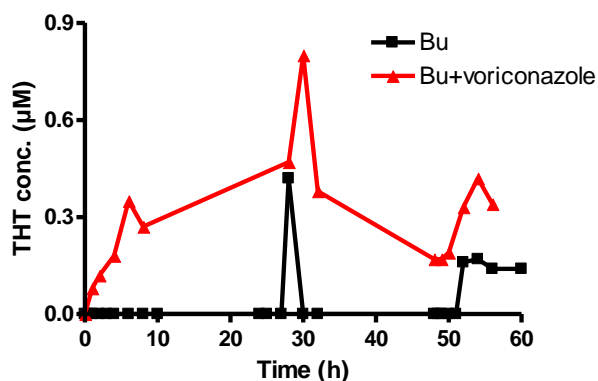


**Figure 11:** THT in patients treated with busulphan

THT was measured in a patient undergoing HSCT and conditioned with Bu. This patient was administered voriconazole at the same time. THT levels were detectable from the first dose of Bu with higher accumulation and slower oxidation compared to what has previously been reported [119].

### 4.1.3 Development of busulphan limited sampling model

#### 4.1.3.1 Log-log plot

A logarithmic scale was the most appropriate way for comparing ratios between AUC estimates. Figure 12 illustrates the three-sample linear LSMs and the combined use of the two LSMs on the y-axis and the reference WinNonlin adaptive compartment modeling with full sampling on the x-axis. Both LSMs correlated reasonably with the reference method; however, significant underestimation is much more common for the linear model, especially in the upper right corner with the highest AUC estimates. Overestimation seems to occur to a comparable extent for both LSMs. More LSM estimates for adults differ significantly from the reference compared with estimates for children, but the degree to which the “deviators” differ seems to be similar for both adults and children.

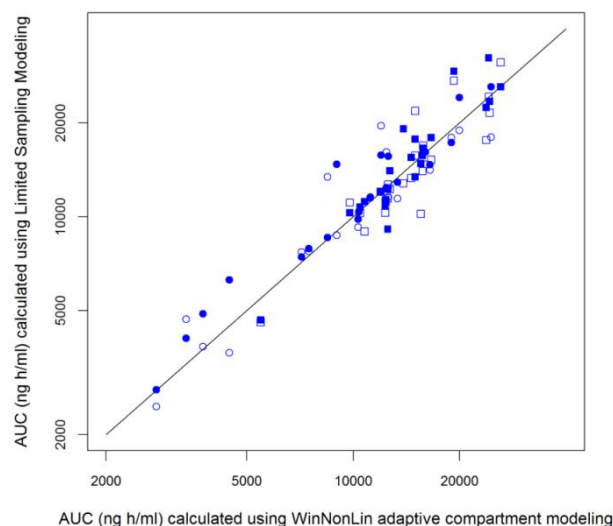


**Figure 12:** Comparison plot of the three-sample linear limited sampling models and the combined use of the two four-sample limited sampling models on the y-axis and the reference WinNonlin adaptive compartment modeling with full sampling on the x-axis. *Filled squares* represent combination estimates of limited sampling models and *empty squares* represent regression limited sampling models in adult patients. *Filled circles* represent combination estimates of limited sampling models and *empty circles* represent regression limited sampling models in pediatric patients under the concentration–time curve.

Dose reduction is often advocated if the AUC is above 12.000 ng h/mL. The plot shows that there may be a risk that a patient with an AUC in the range 12.000–20.000 ng h/mL measured with the reference method does not receive the appropriate dose reduction, especially when assessed with the regression model using three samples.

#### 4.1.3.2 The intraclass correlation coefficient

The ICC, based on a mixed-model analysis of variance, was calculated for the LSM as compared to reference. The results in table 8 show the performance of the respective methods both for the whole study population and for children/adults, respectively.

**Table 8:** ICC for the limited sampling models versus rich sampling AUC estimate. Calculations made using R and CRAN package irr.

	Multiple regression model	Modified Purves curve fitting model	Simplified compartment model	Average between PM and CM estimates. (*)
<b>All (n = 43)</b>	0.93 (0.89-0.96)	0.91 (0.84-0.95)	0.95 (0.88-0.97)	0.95 (0.90-0.97)
<b>Children (n = 20)</b>	0.94 (0.86-0.98)	0.89 (0.74-0.96)	0.96 (0.90-0.99)	0.96 (0.85-0.98)
<b>Adults (n = 23)</b>	0.89 (0.76-0.95)	0.93 (0.83-0.97)	0.89 (0.73-0.95)	0.92 (0.82-0.96)

Values are expressed as mean (range). CM; compartmental model, PM; Purves modified model, \*; While in no case did both the Purves model and the single-compartment model fail simultaneously, in some cases one of the methods failed to produce an area under the concentration–time curve estimate. In those cases, the available result from the successful estimate was used instead of an average.

The results confirm the findings in the log-log plot; however, it is obvious that the linear model performs much better for children than for adults.

Another way to compare AUCs is to compare back-transformed confidence intervals for the mean log AUC ratio between the method to be examined and reference. This is the preferred method for bioequivalence assessment between drugs, as demanded by regulatory authorities both in Europe and in the USA [140]. A two-sided 90 % confidence interval calculated in this manner for the respective LSM is listed in Table 9. This will primarily provide a measure of accuracy but not precision, since the interval width is mostly related to sample size.

**Table 9:** Ratios for limited sampling models versus rich sampling AUC estimate.

	<b>Multiple regression model</b>	<b>Modified Purves curve fitting model</b>	<b>Simplified compartment model</b>	<b>Average between PM and CM estimates. (*)</b>
<b>All (n = 43)</b>	1.01 (0.73-1.40)	0.96 (0.67-1.39)	0.93 (0.70-1.22)	0.94 (0.72-1.23)
<b>Children (n = 20)</b>	0.98 (0.69-1.39)	0.90 (0.59-1.39)	0.92 (0.70-1.18)	0.91 (0.70-1.18)
<b>Adults (n = 23)</b>	1.04 (0.77-1.40)	1.03 (0.80-1.33)	0.93 (0.68-1.27)	0.97 (0.75-1.27)

\* While in no case did both the Purves model and the single-compartment model fail simultaneously, in some cases one of the methods failed to produce an area under the concentration–time curve estimate. In those cases, the available result from the successful estimate was used instead of an average.

There is no statistical evidence that any of the methods used in this study systematically produces a higher or lower AUC than reference. Furthermore, the confidence intervals showed that it is unlikely that the mean AUC estimate difference from reference would render any of the limited sampling methods examined inadequate for use in clinical decision making.

#### 4.1.3.3 Mean error and root of mean squared error

The root of the mean squared error (RMSE) is a measure of precision and the mean error (ME) is a measure of bias. Using the average of the Purves modified model and compartmental model produces the best precision, except in a subgroup analysis of the adult patients (Table 10). However, a tendency to overestimate AUC is seen in all groups. Purves model shows the best result in the adult subgroup, but 4 of 23 adult patients could not be evaluated with the Purves model for mathematical reasons.

**Table 10:** Root of the mean squared error and mean error for limited sampling models versus rich sampling area under the concentration–time curve estimate.

	<b>Multiple regression model</b>	<b>Modified Purves curve fitting model</b>	<b>Simplified compartment model</b>	<b>Average between PM and CM estimates. (*)</b>
<b>All (n = 43)</b>	RMSE 3.02 MSE -54	RMSE 2.90 MSE 320	RMSE 3.81 MSE 1.60	RMSE 2.72 MSE 924
<b>Children (n = 20)</b>	RMSE 2.80 MSE 82	RMSE 3.22 MSE 728	RMSE 2.99 MSE 1.27	RMSE 2.12 MSE 969
<b>Adults (n = 23)</b>	RMSE 3.19 ME -173	RMSE 2.53 ME -87	RMSE 4.47 ME 1.93	RMSE 3.16 ME 884

\* While in no case did both the Purves model and the single-compartment model fail simultaneously, in some cases one of the methods failed to produce an area under the concentration–time curve estimate. In those cases, the available result from the successful estimate was used instead of an average.

## **4.2 CYCLOPHOSPHAMIDE**

### **4.2.1 Identification of differentially expressed genes and gene clusters related to cyclophosphamide treatment**

The overall patterns of gene expression in 11 patients treated with Cy have been assessed. The assessment was performed utilizing a hierarchical clustering analysis of the signal ratios of all arrays. The heat map representing array clustering based on normalized probe intensity showed a high inter-individual variation, as expected (Figure 13A). In the present study we observed variation in several thousands of genes during and after Cy treatment. However, after fold-change filtering (at least 2-fold compared to time 0, i.e. before treatment), differential expression of a group of 299 genes was identified as being specific for Cy treatment. By subjecting these genes to hierarchical clustering analysis, four clusters of up- and down-regulated genes which matched the chronological cascade of gene expression by cyclophosphamide treatment have been identified: highly down-regulated genes (cluster 1), highly up-regulated genes (cluster 2), early up-regulated but later normalized genes (cluster 3) and moderately up-regulated genes (cluster 4) (Figure 13B).

A

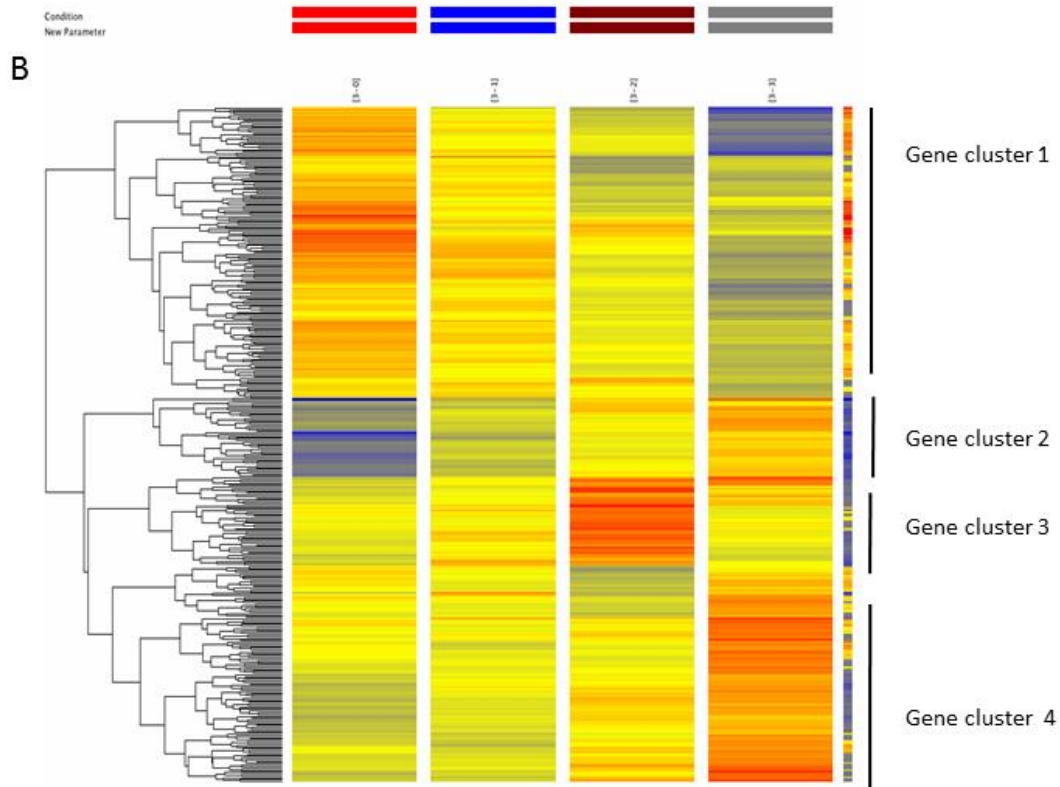
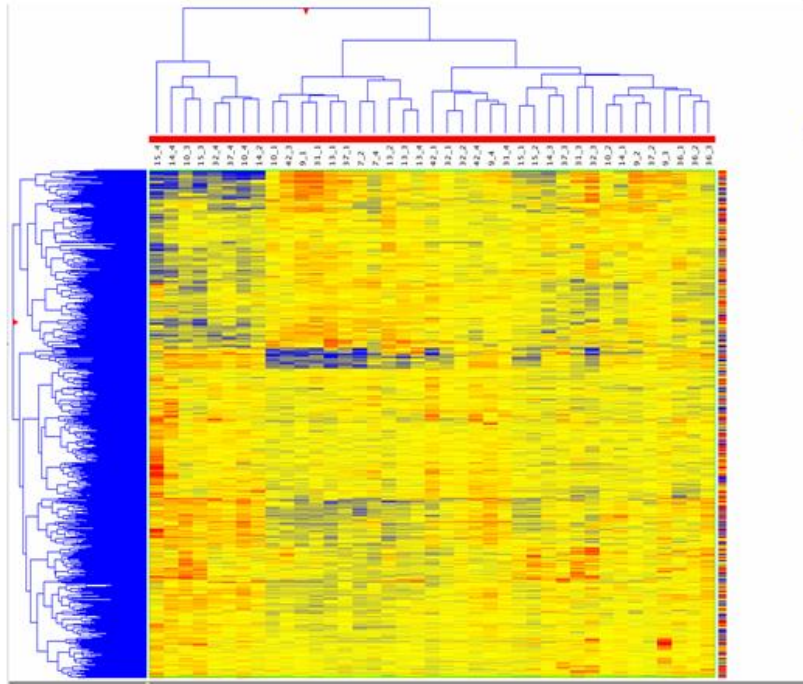


**Figure 13:** Heat map of patient gene expression during Cy treatment.

Genes expression for genes specific for Cy before and throughout the treatment (A). Four clusters of up- and down-regulated genes were identified as: highly down-regulated genes (cluster 1), highly up-regulated genes (cluster 2), early up-regulated but later normalized genes (cluster 3) and moderately up-regulated genes (cluster 4) as seen in B.

#### 4.2.1.1 Highly down-regulated genes (cluster 1)

The first cluster represents genes that were relatively up-regulated in all patients prior to cyclophosphamide treatment. However, this cluster was down-regulated at 6 h post administration followed by a pronounced decrease in expression at 30 h after the first dose (i.e. 6 h after the second dose; Figure 14A). This cluster possessed the highest number of genes (139 genes). The majority of these genes belonged to the immune system and its functions (Table 11). Moreover, further analysis of biological pathways related to these genes showed that a majority of immune- (e.g. T cell receptor signaling, natural killer cell mediated cytotoxicity and graft rejection), autoimmune- (e.g. autoimmune thyroid disease pathway, type 1 diabetes mellitus and rheumatoid arthritis) and inflammation- (e.g., GVHD and NF- $\kappa$ B signaling) related processes were down-regulated by the Cy treatment (Figure 15A).

#### 4.2.1.2 Highly up-regulated genes (cluster 2)

In contrast to cluster 1, this group of genes exhibited a constant and high up-regulation in response to Cy treatment (Figure 14B). In this cluster, 41 up-regulated genes were identified. The majority of these genes are involved in 3 important biological pathways involving cytokine-cytokine receptor interaction, transcriptional misregulation in cancer and hematopoietic cell lineage. Only one gene in this cluster was found to be related to the acute myeloid leukemia pathway (Table 11 and Figure 15B).

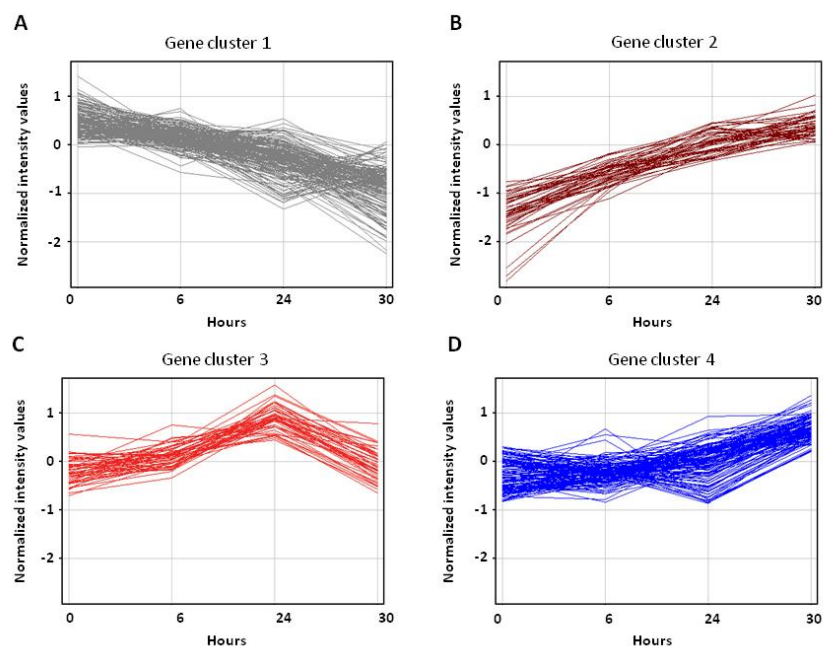


**Figure 14:** Gene clusters in relation to Cy treatment

The expression of Cy treatment specific genes at 6 h and 24 h after the first dose and 6 h after the second dose (30 h) was normalized to pre-treatment levels and divided to the following clusters: Cluster 1 showed highly down-regulated genes throughout the treatment (A); Cluster 2 showed highly up-regulated genes throughout the treatment (B); Cluster 3 showed early up-regulated but later normalized genes (C); Cluster 4 showed moderately up-regulated genes (D).

#### *4.2.1.3 Early up-regulated but later normalized genes (cluster 3)*

This group of genes exhibited remarkable up-regulation at an early time point in Cy treatment, but the expression was later normalized to the same level as before the start of treatment (Figure 14C). This cluster included 33 genes. An analysis of biological pathways related to these genes showed that although several pathways are involved (Table 11), only one gene in each pathway is affected by treatment with Cy (Figure 15C).

#### *4.2.1.4 Moderately up-regulated genes (cluster 4)*

Finally, treatment with Cy resulted in moderate up-regulation of a group of genes, mainly by the end of treatment (6 h after the second dose; Figure 14D). There were 90 genes in this cluster and the biological pathway analysis demonstrated that several pathways including cytokine-cytokine receptor interaction (4 genes), Jak-STAT signaling pathway (2 genes) and TGF-beta signaling pathway (2 genes) are related to this cluster (Table 11 and figure15D).



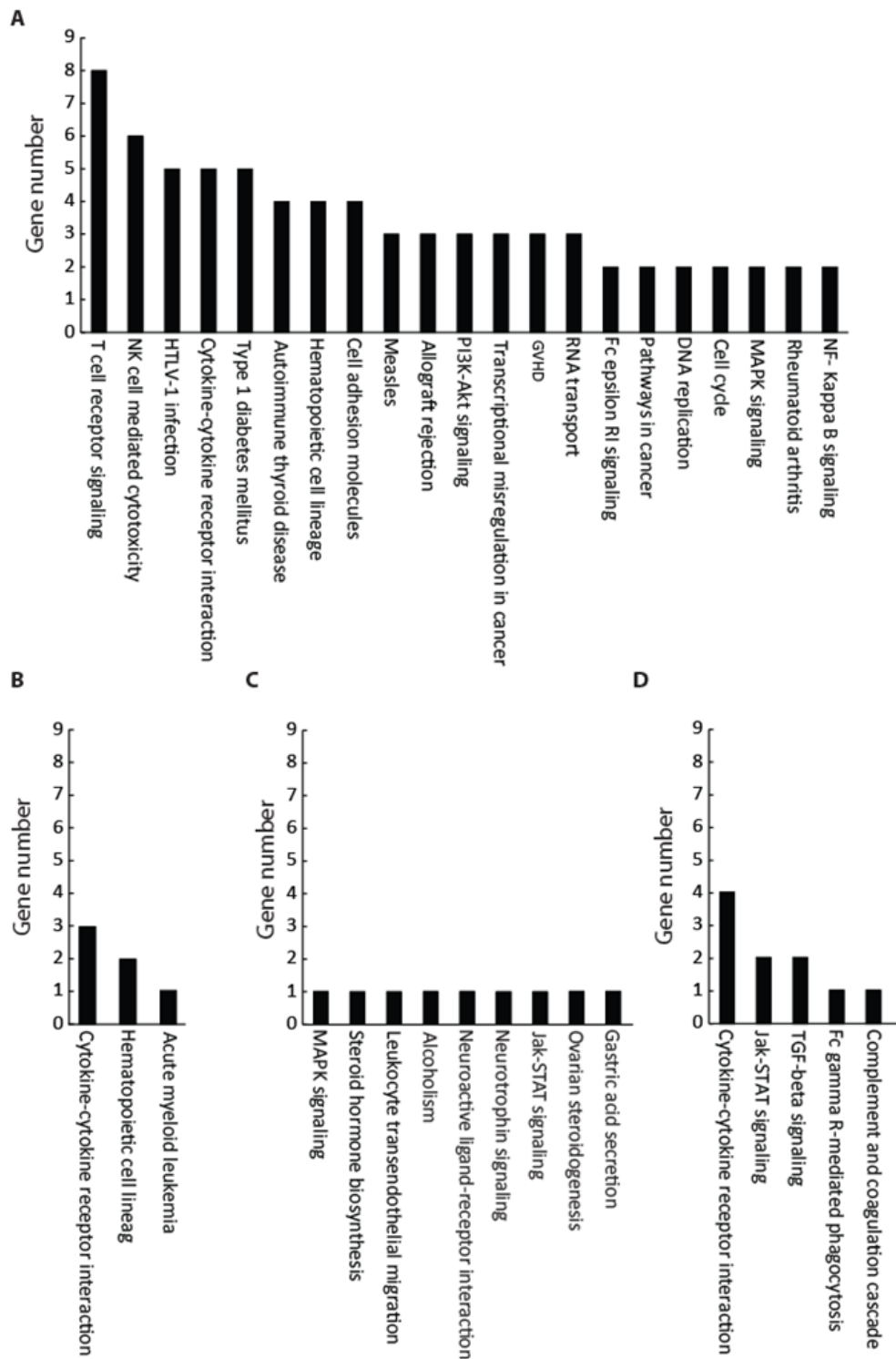


**Figure15:** The pathways related to each cluster and number of genes involved in each cluster

Cluster 1 for highly down-regulated genes throughout the treatment (A); the majority of them belonged to the immune system and its functions. Cluster 2 for highly up-regulated genes throughout the treatment (B); the majority of these genes are involved in 3 important biological pathways. Cluster 3 showed early up-regulated but later normalized genes (C); these genes were more related to biological pathway. Cluster 4 showed moderately up-regulated genes (D), involving several pathways such as cytokine-cytokine receptor interaction and Jak-STAT signaling pathway.

**Table 11:** Pathways reported in each cluster and genes involved in each of them

Cluster	Pathway	Genes
Cluster 1	T cell receptor signaling	<i>CTLA4, CD3e, CD3d, CD28, Lck, LAT, RasGRP1, NFAT</i>
	Natural killer cell mediated cytotoxicity	<i>Lck, LAT, NFAT, 2B4, GZMB, PRF1</i>
	HTLV-1 infection	<i>CD3, IL2R, NFAT, Ras, Lck</i>
	Cytokine-cytokine receptor interaction	<i>CX3CR1, CCR4, IL5RA, IL2RB, CSF1R</i>
	Type 1 diabetes mellitus	<i>INS, MHC-II, CD28, PRF1, GZMB</i>
	Autoimmune thyroid disease	<i>CTLA4, CD28, PRF1, GZMB</i>
	Hematopoietic cell lineage	<i>CD3, CD115, IL5RA, CD49</i>
	Cell adhesion molecules	<i>CD28, CTLA4, SPN, ITGA4</i>
	Measles	<i>CD3, CD28, IL2R</i>
	Allograft rejection	<i>CD28, PRF1, GZMB</i>
	PI3K-Akt signaling	<i>RTK, Cytokine R, ITG A</i>
	Transcriptional misregulation in cancer	<i>LMO2, PAX3, PAX7</i>
	Graft-versus-host disease	<i>CD28, PRF1, GZMB</i>
	RNA transport	<i>Exp5, Nup37, Nup205</i>
	Fc epsilon RI signalling	<i>FcεRIα, LAT</i>
	Pathways in cancer	<i>Ra1GDS, MCSFR</i>
	DNA replication	<i>Mcm4, Mcm7</i>
	Cell cycle	<i>Mcm4, Mcm7</i>
	MAPK signaling	<i>RasGRP1, Ras</i>
	Rheumatoid arthritis	<i>CD28, CTLA4</i>
NF- Kappa B signaling	<i>Lck, LAT</i>	
Cluster 2	Cytokine-cytokine receptor interaction	<i>FLT3, IL1R2, IL18R1</i>
	Hematopoietic cell lineage	<i>CD135, CD121</i>
	Acute myeloid leukemia	<i>AML1</i>
Cluster 3	MAPK signaling	<i>TrkA/B</i>
	Steroid hormone biosynthesis	<i>17beta-estradiol</i>
	Gastric acid secretion	<i>KCN</i>
	Alcoholism	<i>TrkB</i>
	Leukocyte transendothelial migration	<i>Thyl</i>
	Neuroactive ligand-receptor interaction	<i>ADR</i>
	Neurotrophin signaling	<i>TrkB</i>
	Jak-STAT signaling	<i>Sprouty</i>
	Ovarian steroidogenesis	<i>17β-HSD</i>
	MAPK signaling	<i>TrkA/B</i>
Cluster 4	Cytokine-cytokine receptor interaction	<i>IL13RA1, XEDAR, ACVR1B, BMPR2</i>
	Jak-STAT signaling	<i>CytokineR, SOCS</i>
	TGF-beta signaling	<i>BMPRII, ActivinR1</i>
	Fc gamma R-mediated phagocytosis	<i>Myosin X</i>
	Complement and coagulation cascade	<i>coagulation factor VIII</i>

#### 4.2.1.5 Disease-related common up-regulated genes

Hierarchical clustering analysis showed that 2 genes, angiotensin-like-1 (*ANGPTL1*) and c-JUN proto-oncogene (*c-JUN*), were considerably up-regulated prior to, during and after treatment with Cy in all tested patients. Furthermore, these results were confirmed by qRT-PCR (normalized to *GAPDH*). Figure 16A shows the results on qRT-PCR analysis of *ANGPTL1*. The gene expression was up-regulated from time 0 e.g. before Cy treatment and continued to be at a high expression level at 6 h after the first dose, before administration of the second dose and at 6 h after the second dose compared to control (healthy subjects). *c-JUN* gene expression was also found to be high expressed compared to healthy subjects (Fig. 16B).

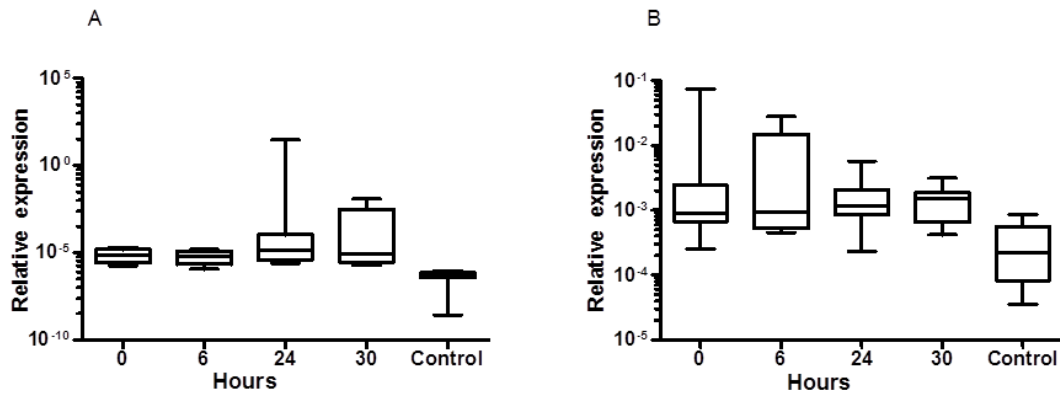


**Figure 16:** Effect of cyclophosphamide treatment on *ANGPTL1* and *c-JUN*

The relative expression of disease-related up-regulated genes, *ANGPTL1* (A) and *c-JUN* (B), compared to normal subjects as measured by qRT-PCR (normalized to *GAPDH*). Cy treatment did not affect the up-regulation of *ANGPTL1* and *c-JUN*.

## 4.2.2 The role of POR in cyclophosphamide bioactivation

### 4.2.2.1 Patients

The expression of the *POR* gene was significantly ( $P < 0.01$ , t-test) up-regulated before the administration of the second dose of Cy and 6 h after the second Cy infusion compared to their levels before conditioning. This finding has been expected as Cy bioactivation is CYP-dependent. However, high inter-individual variation in gene expression after Cy infusion was observed. This variation in gene expression may explain the high variation in Cy kinetics reported in patients (Figure 17A).

PCR results for *POR\*28* have shown that 6 out of 11 patients were carriers for this mutation (Figure 17B); 5 out of them had relatively high *POR* expression 24 h and 30 h after the first Cy infusion. However, 2 other non-mutated patients had also the same high *POR* expression.

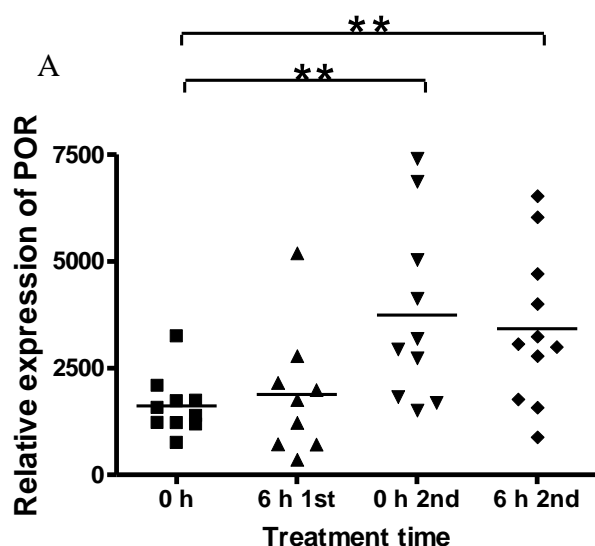


**Figure 17A:** Up-regulation of POR mRNA during Cy conditioning.

The gene expression of *POR* was significantly ( $P < 0.01$ , t-test) up-regulated 24 h after the first Cy infusion and 6 h after the second dose of Cy compared to its level before the start of Cy conditioning.

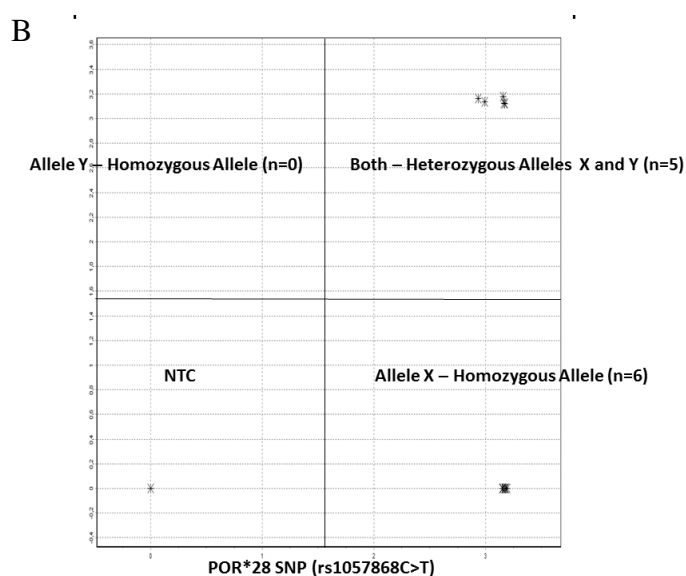


**Figure 17B:** Genotyping for *POR*\*28 polymorphism.

Genotyping PCR showed that 6 out of 11 patients were carriers for *POR*\*28 alleles. The other 5 patients didn't have this mutation. Negative control had NTC. NTC: non-template control.

#### 4.2.2.2 4-OH-Cy formation by CYP2B6.1 with variable *POR*

The enzyme kinetics for 4-OH-Cy formation in the microsomes containing human cDNA-expressed CYP2B6.1 with various ratios of POR/CYP were determined. Fitting the data from 2 independent experiments from each of 3 different batches of microsomes to Michaelis-Menten kinetics, the apparent  $K_m$  for CYP2B6.1 was almost constant in the 3 batches (2.95-4 mM) while the apparent  $V_{max}$  of 4-hydroxylation was proportional to the POR/CYP ratio ranging from 12.55 to 99.09 nmol/min/nmol CYP (Figure 18A). Comparing different enzyme kinetic models revealed that the best curve fit was obtained with a substrate inhibition model (Figure 18B).

Furthermore, the ratio of  $V_{max}/K_m$  was proportional to the POR/CYP ratio ranging between 3.12 and 33.66  $\mu\text{L}/\text{min}/\text{nmol}$  CYP (Figure 19). All kinetics values are presented in table 12. Microsomes containing only POR did not show 4-OH-Cy formation, which indicates that POR by itself cannot bioactivate Cy.

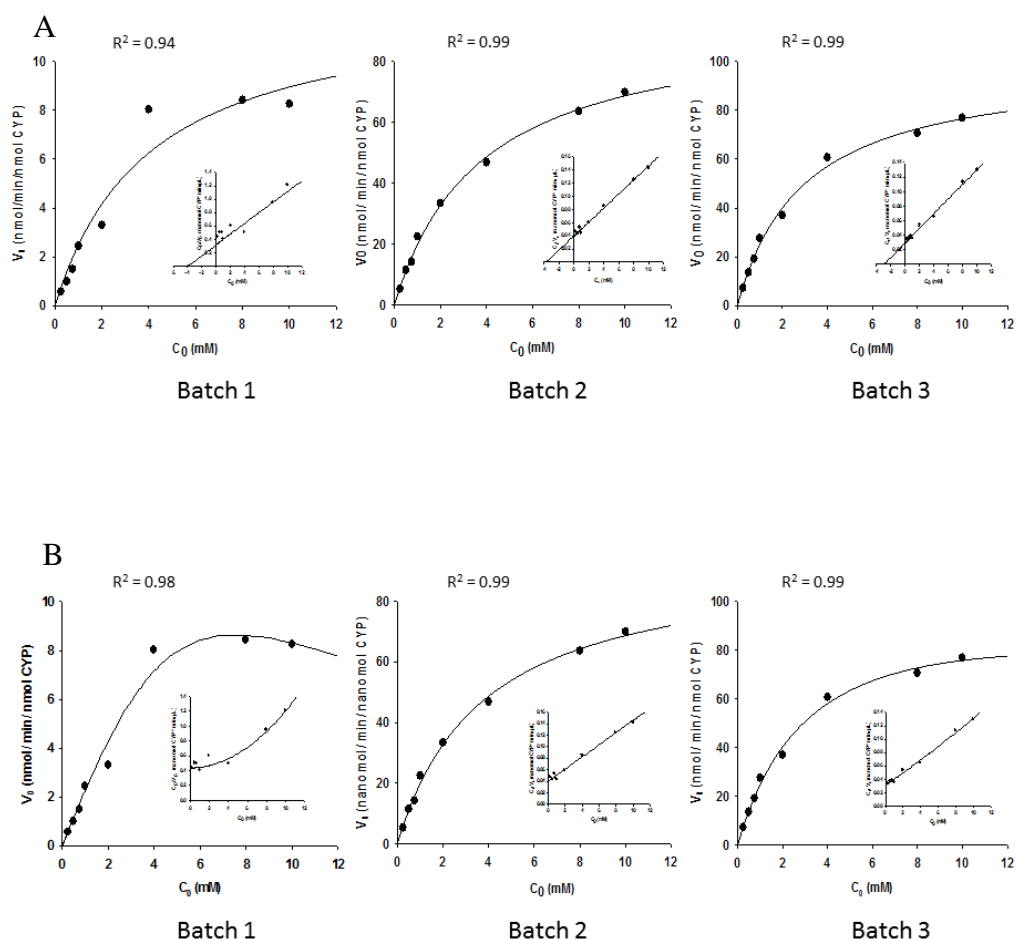


**Figure 18:** 4-OH-Cyclophosphamide kinetics after incubation with CYP2B6.1 batches with variable POR/CYP ratios

Cyclophosphamide was incubated with 3 batches of CYP2B6.1 containing variable POR/CYP ratios. The results shown are the average obtained with the three batches. Fitting the data to Michaelis-Menten kinetics gave an apparent  $V_{max}/K_m$  of 3.12, 25.13, 33.66  $\mu\text{L}/\text{min}/\text{nmol}$  CYP consequently (A). A substrate inhibition model, Hanes-Woolf plot (inset) had the best curve fit (B).

**Table 12:** Apparent kinetic constants for 4-OH-Cy by recombinant CYP2B6\*1 with different amount of CYP/POR ratios

	<b>Batch 1</b>	<b>Batch 2</b>	<b>Batch 3</b>
<b>POR/CYP (nmol/min/pmol CYP)</b>	0.77	8.90	13.80
<b><math>K_m</math> (mM)</b>	4.02	3.76	2.94
<b><math>V_{max}</math> (nmol/min/ nmol CYP)</b>	12.55	94.54	99.09
<b><math>V_{max}/K_m</math> (<math>\mu\text{L}/\text{min}/\text{nmol}</math> CYP)</b>	3.12	25.13	33.66

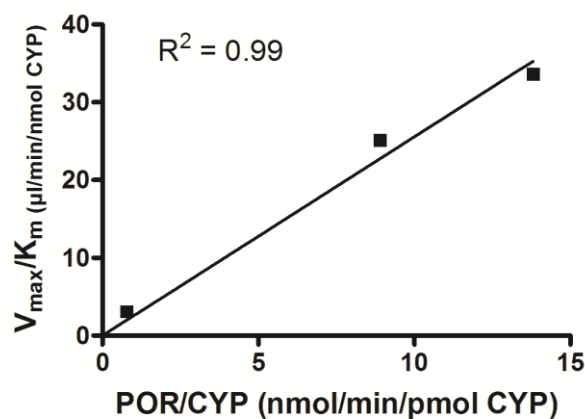


**Figure 19:** Cyclophosphamide clearance in correlation to POR/CYP ratios in different CYP2B6.1 batches

The ratio of  $V_{max}/K_m$  (3.12 - 33.66  $\mu\text{L}/\text{min}/\text{nmol CYP}$ ) was proportional to the POR/CYP ratio (0.77-13.8 nmol/min/pmol CYP) in several different CYP2B6.1 batches confirming the strong correlation between Cy kinetics and POR/CYP ratio.

For further confirmation of the results, the 3 batches were diluted to have the same POR amounts (356 nmol/min/mL) and variable amounts of CYP, and thus, POR/CYP ratio. Cy (0.75 mM) was incubated under the linearity conditions. The obtained results were compared to those from the previous experiment when the microsomes had the same CYP amount and variable amounts of POR and POR/CYP ratio. Both experiments showed the strong correlation between the POR/CYP ratio and the enzyme catalytic activity regardless the constant factor. These results corroborate that all experiments were done within the linear part of the reaction (Figure 20).

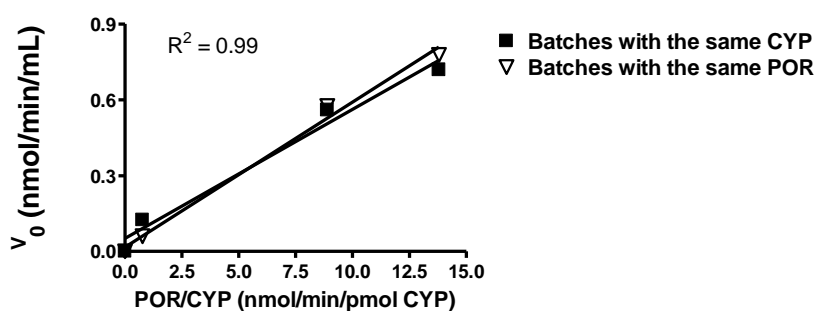


**Figure 20:** Initial Cy (0.75 mM) disappearance rate ( $v_0$ ) in CYP2B6.1 batches with variable POR/CYP ratios

Cyclophosphamide (0.75 mM) was incubated under the linearity conditions with CYP2B6.1 batches with variable POR/CYP twice. In first incubation, all batches had same CYP amount (40 pmol/mL) and variable amount of POR. In the second incubation all of the samples had same POR amounts (356 nmol/min/mL) and variable amounts of CYP. The POR/CYP ratio was the same in both incubations. Both experiments showed the strong correlation between the POR/CYP ratio and the enzyme catalytic activity.

### 4.2.3 The role of CYP2J2 in cyclophosphamide bioactivation

#### 4.2.3.1 CYP2J2 Gene Expression and Genotype in Patients

Mononuclear cells from peripheral blood of patients undergoing conditioning were investigated by gene array analysis. Patients were genotyped with regard to several CYPs, including CYP1A1, CYP1A2, CYP1B1, CYP2A6, CYP2A7, CYP2A13, CYP2B6, CYP2C8, CYP2C9, CYP2C18, CYP2C19, CYP2D6, CYP2E1, CYP2F1, CYP2J2, CYP3A4, CYP3A5, and CYP3A7. Significant up-regulation of mRNA expression was only detected for *CYP2J2*. The heat map for *CYP2J2* and other genes with similar expression pattern over 2 days of Cy treatment is presented in Figure 21.

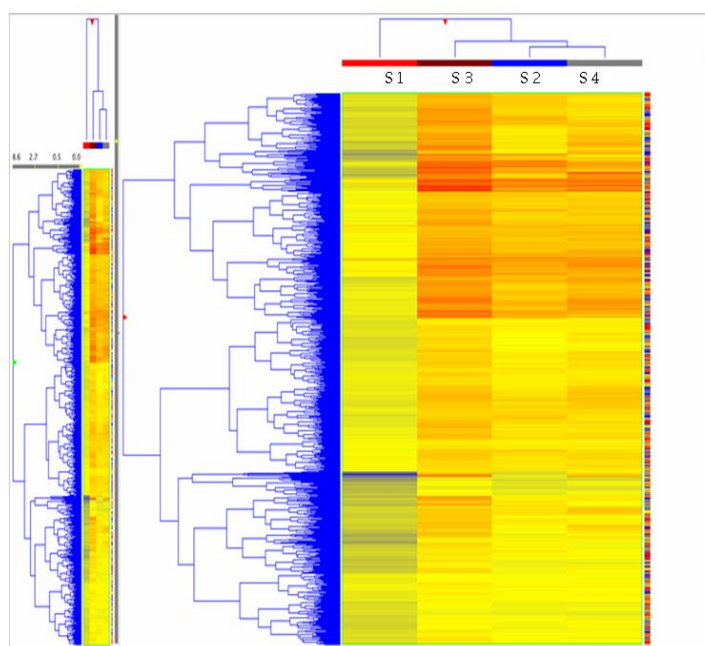


**Figure 21:** Heat map for gene expression including *CYP2J2* at baseline and during Cy treatment. S 1, baseline; S 2, 6 h after Cy administration on day 1; S 3, 24 h; S 4, 6 h after Cy administration on day 2. The majority of genes in each cluster had the same pattern of up- and down-regulation as observed for *CYP2J2*.

The heat map shows gene expression before conditioning (S 1), 6 h after Cy administration (S 2) on day 1, 24 h (S 3; before Cy infusion on day 2), and at 30 h (S 4; 6 h after the second Cy dose). The majority of genes in each cluster had the same pattern of up- and down-regulation as observed for *CYP2J2*. Expression of *CYP2J2* gene was significantly up-regulated 6 h after the first Cy infusion ( $P < 0.05$ , t-test). At S 4, *CYP2J2* expression was significantly reduced ( $P < 0.05$ , t-test) compared to measurements made at the S 2 time point, but were elevated compared with pretreatment (S 1) levels. These results for gene expression have been confirmed by qRT-PCR with high inter-individual variation (Figure 22).

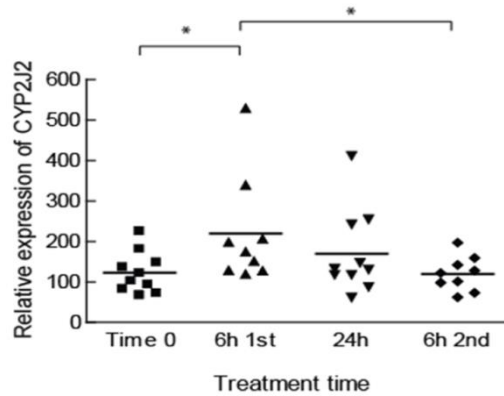


**Figure 22:** Expression of *CYP2J2* mRNA at baseline and during Cy conditioning.

The gene expression of *CYP2J2* was significantly ( $P < 0.05$ , t-test) up-regulated 6 h after the first Cy infusion. At the last sample (6 h after the second dose of Cy) *CYP2J2* was significantly ( $P < 0.05$ , t-test) down-regulated compared to the sample taken 6 h after the first dose of Cy. The high inter-individual variation in gene expression during Cy treatment might be due to different inducibility of the polymorphic forms of *CYP2J2*.

qRT-PCR experiments also demonstrated that *CYP2J2* gene expression was higher ( $P < 0.01$ , t-test) in samples from patients with hematological malignancies before treatment start compared to healthy controls (Figure 23).

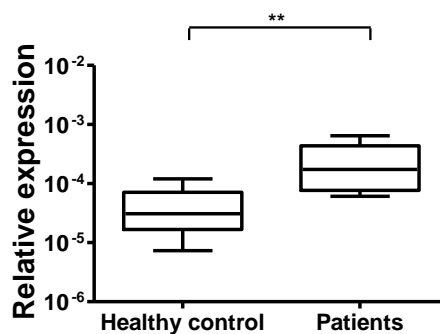


**Figure 23:** Expression of *CYP2J2* determined by qRT-PCR in healthy controls and cancer patients undergoing HSCT.

*CYP2J2* gene expression measured by qRT-PCR and normalized against GAPDH showed significantly ( $P < 0.01$ , t-test) higher levels in patients with hematological malignancies than in controls (healthy subjects) even prior to the start of Cy infusion.

Genotyping of the patients for *CYP2J2* SNP “rs1056596” (A/T) revealed that only one patient was carrier for this SNP and had a lower expression level of *CYP2J2* compared to other patients.

Pharmacokinetics for Cy and 4-OH-Cy were calculated (Table 13). Cy and 4-OH-Cy kinetics showed a significantly higher ( $P < 0.01$ , t-test) 4-OH-Cy/Cy ratio at S 4 compared with measurements recorded at time point S 2. The 4-OH-Cy: Cy concentration ratios 6 h after the first (S 2) and second (S 4) infusions are presented in Figure 24.



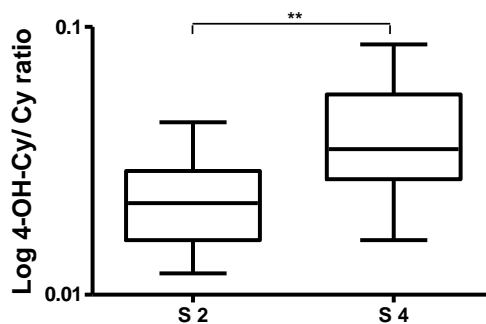


**Figure 24:** Log 4-OH-Cy/Cy concentration ratio at 2 time points.

The figure shows significantly ( $P < 0.01$ , t-test) higher levels of 4-OH-Cy/Cy ratio after the second infusion indicating auto-induction of CYP2B6-dependent Cy metabolism.

Clinical data, including diagnosis, type of donor, stem-cell dose, relapse, remission, mortality, and complications were collected. No correlation between clinical data and CYP2J2 results was observed.

**Table 13:** Pharmacokinetics of Cy and 4-OH-Cy Among Patients Undergoing HSCT

Patient	Cy			4-OH-Cy			4-OH-Cy/Cy AUC ratio
	AUC ( $\mu\text{g.h/mL}$ )	$C_{max}$ ( $\mu\text{g/mL}$ )	Half-life (h)	AUC (ng.h/mL)	$C_{max}$ (ng/mL)	Half-life (h)	
P 1	867.19	152.66	6.5	47501	1600.80	20.15	0.055
P 2	932.05	88.73	8.6	11531	1108.84	5.99	0.012
P 3	892.68	154.54	5.9	16675	1285.72	8.69	0.019
P 4	938.97	143.63	5.9	30432	1488.00	13.90	0.032
P 5	754.65	93.41	6.9	12165	977.39	7.39	0.016
P 6	1120.32	95.58	10.7	17870	1329.62	5.63	0.016
P 7	1310.99	118.39	8.7	13226	1216.67	4.24	0.010
P 8	808.97	113.08	5.5	8995	1330.53	4.69	0.011
P 9	654.13	76.81	6.5	6659	764.83	5.74	0.010
P 10	644.80	73.93	6.0	12870	1818.47	4.52	0.020
P 11	1020.95	105.76	8.6	17243	3252.19	3.68	0.017

Patients received an i.v. infusion of Cy (60 mg/(kg·day), once daily for 2 d) followed by fractionated TBI. Blood samples were withdrawn at baseline and at 0.5, 1, 2, 4, 6, 8, and 18 h after the first infusion of Cy. The results demonstrate high interindividual variation in the kinetics of Cy and its metabolite.

**Abbreviations:** 4-OH-Cy, 4-hydroxycyclophosphamide; AUC, area under the curve;  $C_{max}$ , peak plasma concentration; Cy, cyclophosphamide; P, patient.

#### 4.2.3.2 Role of CYP2J2 in Cy-induced HL-60 Cytotoxicity

Cy reduced cell viability of HL-60 cells in a concentration- and time-dependent manner as assessed by resazurin assay. The estimated half-maximal inhibitory concentration ( $IC_{50}$ ) was 3.6 mM. A concentration of 9 mM was selected for further Cy bioactivation experiments.

The CYP2J2 inhibitor, telmisartan, at a concentration less than or equal to 10  $\mu$ M did not affect viability of HL-60 cells. However, higher concentrations of telmisartan reduced cell viability in a concentration-dependent manner (Figure 25A). Telmisartan at a concentration of 10  $\mu$ M reduced the formation of 4-OH-Cy by approximately 50%. Moreover, preincubation of the cells with telmisartan (10  $\mu$ M) improved survival of cells treated with 9 mM Cy by 10% (Figure 25B). It is likely that telmisartan reduces Cy bioactivation and hence increases survival of HL-60 cells.

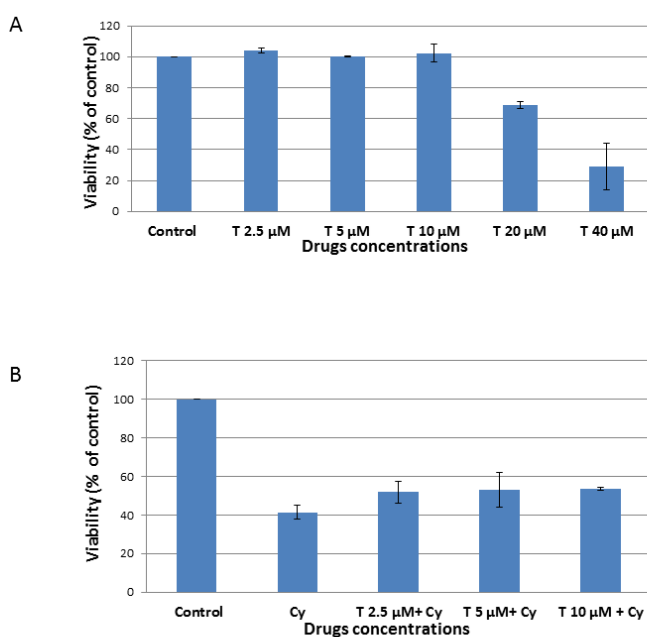


**Figure 25:** Effect of telmisartan (T) preincubation on Cy-induced cytotoxicity.

HL-60 cells were incubated with Cy for 6-96 h. The estimated  $IC_{50}$  was 3.6 mM. HL-60 cells were incubated with telmisartan (CYP2J2 inhibitor) for 48 h. Telmisartan has reduced HL60 cell viability in a concentration-dependent manner (A). Telmisartan at a concentration of 10  $\mu$ M or lower did not affect HL60 cell viability but reduced the formation of 4-OH-Cy by about 50%. HL-60 cells were pre-incubated with telmisartan at concentrations of 2.5, 5 or 10  $\mu$ M for 2 h, before adding Cy (9 mM) for an additional 48 h. HL-60 cells incubated with 9 mM Cy or 10  $\mu$ M telmisartan alone served as controls for drug toxicity. Controls treated with drug-free media have been incubated in parallel. Preincubation with telmisartan showed 10% improvement in the survival of cells treated with Cy compared to cells treated with Cy alone (B).

#### 4.2.3.3 Cy Metabolism by Recombinant CYP2J2

Incubation of Cy with microsomes containing recombinant human CYP2J2 showed that CYP2J2 is involved in Cy bioactivation. Fitting the data from 2 independent experiments performed on 2 different batches of microsomes to Michaelis-Menten kinetics (Figure 26A) gave an apparent  $K_m$  within the range of 3.7–6.6 mM, and an apparent  $V_{max}$  2.9–10.3 pmol/(min·pmol) CYP resulting in  $V_{max}/K_m$  of 0.5–2.3  $\mu\text{L}/(\text{min}\cdot\text{pmol})$  CYP. Comparing different enzyme kinetic models revealed that the curve of best fit was obtained with a substrate inhibition model (Figure 26B).

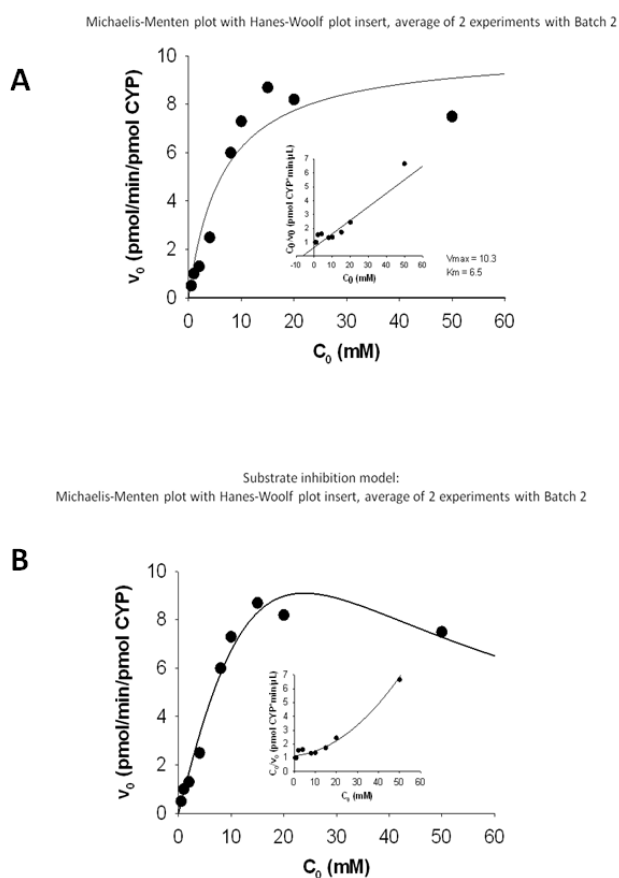


**Figure 26:** Michaelis-Menten plot with Hanes-Woolf plot (inset) of 4-OH-Cy kinetics after incubation with recombinant CYP2J2.

Cyclophosphamide was incubated with recombinant human CYP2J2. Fitting the data to Michaelis-Menten kinetics (A) gave an apparent  $K_m$  of 6.5 mM and an apparent  $V_{max}$  of 10.3 pmol/min/pmol CYP. The best curve fit was obtained with a substrate inhibition model (B).



## 5 DISCUSSION

HSCT is a curative treatment for several malignant and non-malignant diseases, but it also involves risk of life threatening toxicity related to conditioning regimen. Thus, better understanding of the mechanisms and toxicity of conditioning regimens is needed.

In this thesis, the molecular mechanisms involved in the metabolism of one of the most common myeloablative conditioning regimen, Bu/Cy, have been investigated in order to personalize the treatment prior to HSCT and hence avoid drug interactions, increase treatment efficacy and improve clinical outcome.

Busulphan metabolic pathway is not fully elucidated. Several minor metabolites have been found, but not identified yet. Enzymes involved in certain steps in the pathway and their role in busulphan kinetics and drug-drug interactions have not been recognized yet. Thus, considerable amount of work remains to be done before the personalization of the treatment with busulphan will be possible. Meanwhile, TDM may compensate for the unknown factors and a limited sampling model can help, to some extent, in personalizing the dose.

TDM is an important issue in personalization of busulphan treatment [141]. The need for a simplified method of monitoring drug pharmacokinetics in clinical practice is obvious. Co-medications, induction or inhibition of busulphan metabolism and drug-drug interactions indicate the need for repeated assessments of Bu concentrations during conditioning regimen [47, 142]. Moreover, the clinical outcome of HSCT including the transplantation-related mortality and morbidity has been reported to correlate with the conditioning regimens [143]. Repeated assessments of the kinetics with the full profile sampling in this patient group are not feasible as common practice. Limited sampling strategies help to overcome the issue of the amount of blood withdrawn over the period of 4 days.

LSM should have some robustness against changes in population factors so that it can be used safely by different institutions and independently verified. In a recent study using Monte-Carlo simulation, a tendency towards underestimation with multiple linear regression and overestimation with curve fitting algorithms was reported [144].

Monitoring of drug kinetics should be complemented with identification of at-risk subpopulations such as patients with hepatic or renal impairment [145]. It is not easy to find an algorithm that could perfectly recreate the information lost when sampling is limited to fewer time points.

Three LSMs and the standard rich sampling WinNonlin adaptive compartment modeling have been studied. Results indicated that LSMs can produce clinically useful estimates. In particular, a combination of a curve fitting model and a simplified single compartment model seems to give good results. The low deviation in the present model would rarely affect the dose adjustment and would not impair the clinical benefit gained from TDM. Thanks to LSMs, monitoring can be performed repeatedly during the conditioning at the same cost and

with the same effort as monitoring one single dose with full-kinetics sampling protocol. This could provide another chance to correct the outliers in absorption or metabolism.

Using an ordinary Windows desktop computer without any specialized software, a compartment and a non-compartment curve fitting method can be easily employed for the AUC estimates. The possibility of presenting a graph for the simulated concentration curve further facilitates the interpretation. Additional sampling points increase accuracy, and then decision on which model to choose must be based on individual needs and means. Our study clearly showed that LSM is likely to be of a significant benefit.

For better understanding of busulphan metabolism, a new and reproducible method has been developed for the detection of busulphan and four of its major metabolites in both plasma and urine in one analysis, regardless of different methods of extraction. The method has been subjected to the standard validation criteria [129, 130] and applied to a clinical case where the patient received high dose busulphan as a part of his conditioning regimen.

The method can be also utilized for the detection of Bu metabolites which are used in other non-medical fields such as agriculture and environmental medicine.

The analytical method has been applied to quantify busulphan metabolites *in vitro* in experiments on enzymes involved in Bu metabolic pathway. We have found that FMO3 and to lesser extent CYPs do play a major role in the metabolism of busulphan. Busulphan is a lipophilic drug which limits its excretion in the urine. Only 2% of busulphan is excreted as the unchanged drug [28]. In the body the drug is oxidized to more hydrophilic metabolites which can easily be excreted in the urine. FMO3 and CYPs catalyzed the oxidation of busulphan through its first core metabolite THT. It is likely that these enzymes also play a role in the further downstream oxidation of THT-1-oxide to sulfolane, and in turn, sulfolane to 3-OH sulfolane.

Incubation of THT with HLM showed that THT concentrations have rapidly decreased with gradual formation of the subsequent metabolites. Inhibition of FMO3 has suppressed THT disappearance which was after FMO3 inhibition 48% compared to 72% in samples devoid of FMO3 inhibition. On the other hand, THT concentrations decreased to 67% after CYPs inhibition. These results showed that THT is metabolized by the microsomal enzymes and FMO3 is the main enzyme in this process.

THT incubation with recombinant microsomes confirmed the previous results. FMO3 had the highest initial THT disappearance rate ( $v_0$ ) and  $CL_{int}$  value followed by CYPs 3A4, 4A11, 2C8 and 2C9. Comparing CYPs based on the initial THT disappearance rate ( $v_0$ )/(POR/CYP ratio), CYP2C8 had the highest rate for THT metabolism followed by CYPs 2C9, 2C19, 2E1 and 3A4.

It has been reported that the administration of Bu concurrently with drugs known to be metabolized by FMO3 or CYP led to abnormally high Bu plasma concentrations. FMO3 was reported to be involved in metabolism of many drugs including voriconazole, ketoconazole,

methimazole, tamoxifen, codeine and nicotine [40-42]. Most of these drugs are given routinely during busulphan conditioning due to the high risk of infection in the immune-compromised patients. Thus, FMO3 inhibition by these drugs may explain the high Bu levels in those patients.

A case study on a 7 year old boy with AML confirmed which significance the drug-drug interactions have for busulphan exposure [146]. Oral metronidazole was given 3 times daily to treat the patient for a clostridium infection along with busulphan administration. The daily predicted AUC was exceeded by 86% [146]. Other CYP dependent drugs such as itraconazole and ketobemidone also lead to higher plasma concentrations of busulphan [33, 35]. Our results are in agreement with the report on the role of CYP2C9 in THT oxidation. Moreover, its polymorphism has been shown to affect Bu metabolism [147].

In our study, another patient undergoing stem cell transplantation was treated with high dose busulphan (2 mg/kg, bid) for four days and voriconazole co-dosing. This patient had very high busulphan levels compared to the administered. Measuring THT concentrations in the same plasma samples showed that THT was detectable 1 h after busulphan first dose with higher accumulation and slower clearance compared to has been reported previously for a patient treated with Bu alone ( $P < 0.05$ ) [119]. Yanni *et al.*, have reported that 25% of voriconazole is metabolized by FMO3 [40]. In this patient, voriconazole was withdrawn completely after the first dose of busulphan. Later busulphan concentrations were reduced to the expected values.

Investigation of *FMO3* gene expression in patients undergoing stem cell transplantation revealed a significant up-regulation ( $P < 0.05$ ) after Bu conditioning compared to levels before Bu conditioning. *FMO3* up-regulation had the same pattern as that observed for *GSTAI* ( $P < 0.05$ ).

Studies on the drugs kinetics in mice have corroborated our findings. Mice treated with PTU had a significant ( $P < 0.05$ ) increase in Bu plasma concentrations and AUC compared to mice injected with Bu alone. Moreover, simulated accumulation of THT by injecting THT concomitantly with Bu has also resulted in higher levels of Bu. Also THT concentrations and AUC were significantly ( $P < 0.05$ ) increased after PTU injection compared to those measured in mice injected with THT alone. In mice injected with Bu and PTU, THT concentrations and AUC were significantly ( $P < 0.05$ ) higher compared to those injected with Bu only. All the above results showed that THT accumulation, either by FMO3 inhibition or injecting THT with Bu has increased Bu concentrations and AUC.

Our group has previously reported that the time interval between Bu and Cy in Bu/Cy conditioning regimen affected the frequency of liver toxicity and pharmacokinetics of Cy [36]. Cy is known to be metabolized through CYPs, and their consumption in Bu metabolism can affect its kinetics and increase the toxicity.

Our results showed that CYP2B6 is one of the enzymes involved in busulphan metabolism while it is the main bioactivator for cyclophosphamide. This may imply that protocols for Bu/Cy conditioning might be modified.

The expression levels of *CYP2B6* in patients conditioned with Cy and TBI didn't show any significant variation over a 2-days Cy conditioning period. However, CYP2B6 is mainly a hepatic enzyme while the expression levels were assessed in mononuclear cells from peripheral blood.

In these patients, high inter-individual variability in kinetics of Cy was observed. Also levels of 4-OH-Cy/Cy were elevated at 6 h after the second infusion compared to levels at 6 h after the first infusion; thus, confirming auto-induction of CYP2B6-dependent metabolism of Cy as previously reported.[148]

POR is the main electron donor for all microsomal cytochrome P450 monooxygenases and its polymorphisms have been shown to affect CYP-mediated drug metabolism as well as direct bioactivation of prodrugs [149].

*POR* expression was significantly ( $P < 0.01$ ) up-regulated before and 6 h after the second Cy dose. High inter-individual variation in gene expression after Cy infusion was observed. This variation may explain the high variation in Cy kinetics [118].

*POR\*28* is the only reported polymorphism that increases CYP activity *in vivo* [96]. PCR results for *POR\*28* genotype showed that almost half of the patients were carriers for *POR\*28*. Five out of these 6 patients had significantly higher *POR* expression after Cy conditioning. However, 2 other patients also had high *POR* expression, possibly due to other *POR* polymorphisms not yet described or effects on nuclear receptors or other factors involved in *POR* regulation, also resulting in high inducibility.

Chen *et al.* studied the effect of the *POR* genotype on CYP2B6 bupropion metabolism. Their results showed a 70-74% reduction in CYP2B6 activity with certain *POR* polymorphisms *in vitro* [94]. That was in agreement with another study, which also reported that *S*-Mephenytoin *N*-demethylation by CYP2B6 varied with the *POR* polymorphism in human liver [95].

*POR* variability affects also CYPs other than CYP2B6, such as CYP2C9 activities when incubated with flurbiprofen, diclofenac, and tolbutamide. These drugs, like Cy, are metabolized rapidly [92]. The effect of *POR* variants and expression levels varies with the substrate and the CYP enzyme variant, for example *POR* polymorphisms A287P and R457H variants are associated with no detectable CYP2D6 metabolism of 7-ethoxymethoxy-3-cyanocoumarin (EOMCC), while Q153R polymorphism had increased CYP2D6 activity with EOMCC *in vitro* [91].



Steroidogenic activity is depending mainly on CYP1A2 and CYP2C19 and POR variants affected their activities to different extents. *POR* polymorphisms A287P and R457H have reduced CYP1A2 and CYP2C19 catalytic activities. The A503V polymorphism gave 85% of wild-type activity with CYP1A2 and 113% of wild-type activity with CYP2C19, while Q153R polymorphism increased both CYP1A2 and CYP2C19 activities [90].

CYP3A4 had completely lost its function *in vitro* by two of the *POR* polymorphisms, Y181D and A287P. Other *POR* polymorphisms, such as K49N, A115V and G413S, resulted in increased POR activity for testosterone with up to 65% [94]. Tacrolimus is metabolized by CYP3A5 and *POR*\*28 resulted in a significantly higher level of tacrolimus exposure [93].

A study on human liver samples showed that four *POR* polymorphisms have reduced both POR and drug-metabolizing CYP activity. The same study also showed intronic polymorphisms that altered POR activity [150].

In our *in vitro* study, the relative amount of POR has been shown to play a major role in the metabolic activity of different alleles of CYP2B6. Nevertheless, *CYP2B6* polymorphism can still affect the drug kinetics.

The intrinsic clearance of Cy was clearly proportional to the POR/CYP ratio in recombinant human CYP2B6.1 ranging between 3.12 and 33.66  $\mu\text{L}/\text{min}/\text{nmol}$  CYP despite that  $K_m$  was almost constant in all batches. In these experiments, we first used microsomes with constant amount of CYP and variable amounts of POR, and then confirmed in other experiments in microsomes with constant amount of POR and variable amounts of CYP.

Despite that CYP2B6 is the main enzyme in Cy bioactivation, studies on *CYP2B6* polymorphisms and their effects on Cy kinetics are contradictory.

Polymorphic human CYPs expression levels for the C1459T mutation (alleles \*5 and \*7) have been reported to be significantly lower than for *CYP2B6*\*1 [63], while it has a higher intrinsic clearance both for Cy *in vitro* and *in vivo* [70, 76]. In Caucasians, the SNP frequency has been reported to be 33% and 29% for A785G and G516T, respectively. [63]. These SNPs are present in several *CYP2B6* allelic variants such as (*2B6*\*4, *2B6*\*6, *2B6*\*7 and *2B6*\*9).

Ariyoshi *et al.* have reported that *CYP2B6*\*6 has higher activity in 4-hydroxylation of Cy, but lower activity in 8-hydroxylation of efavirenz. This *in vitro* study used microsomes including *CYP2B6*\*1, \*4 and \*6 and containing the same amount of measured POR activity [151].

On the other hand, Raccor *et al.* have reported that *CYP2B6* genotype is not related to 4-OH-Cy formation both *in vitro* or *in vivo* [58]. Moreover, other studies have confirmed that genotyping of CYP2B6 and other CYPs involved in Cy metabolism didn't affect its kinetics and clinical factors such as patients' age and cancer grade affected Cy kinetics to greater extent [59, 60, 78].

Recently, epigenetic mechanisms were reported to be important for drug treatment. Epigenetic modifiers contribute to the inter-individual variations in drug metabolism. A novel class of drugs, termed epidrugs, has been reported from clinical trials to intervene in the epigenetic control of gene expression. Moreover, epigenetic biomarkers can be used in monitoring patients' disease prognosis and treatment [152].

Expression levels of several other CYPs were assessed over a two days Cy conditioning period. Out of them, only CYP2J2 had a strong correlation to Cy conditioning.

*CYP2J2* gene was highly expressed in patients before Cy conditioning start as compared to healthy individuals. Similarly to blood and solid cancer cells; mononuclear cells from patients with hematological malignancies also expressed high levels of *CYP2J2* [109-112, 122-124].

Gene array analysis demonstrated that the expression of *CYP2J2* was further up-regulated in patients upon treatment with Cy, indicating that *CYP2J2* is induced by Cy. However, *CYP2J2* up-regulation showed high inter-individual variation after the first Cy infusion. Genotyping patients for *CYP2J2* SNP "rs1056596" (A/T) revealed that only one patient was carrier for his mutation. Lower *CYP2J2* expression was detected in this patient.

Our group has previously reported that Cy induced concentration- and time-dependent cytotoxicity in HL-60 cells *in vitro* despite the fact that these cells lack CYP2B6 and other enzymes involved in Cy bioactivation [113]. HL-60 cells predominantly express CYP1A1 and CYP1B1, [113, 153] but, up to our knowledge, neither is involved in Cy bioactivation. In the present study, reduction of 4-OH-Cy formation in HL-60 cells by the *CYP2J2* inhibitor, telmisartan, and concomitant increase in cell viability strongly support the role of *CYP2J2* in Cy bioactivation [109].

4-OH-Cy was formed following incubation of Cy with recombinant *CYP2J2*. This finding provides confirmation that *CYP2J2* is capable of bioactivating Cy. The apparent  $K_m$  and  $V_{max}$  were within the range 3.7–6.6 mM and 2.9–10.3 pmol/(min·pmol) CYP, respectively. This resulted in a  $V_{max}/K_m$  of 0.5–2.3  $\mu\text{L}/(\text{min}\cdot\text{pmol})$  CYP. A similar  $K_m$  value was obtained from wild type CYP2B6 (4.9 mM) [154]. Further,  $V_{max}/K_m$  of *CYP2J2* was even higher than some CYP2B6 polymorphisms [154], suggesting that *CYP2J2* may be a predominant enzyme responsible for Cy bioactivation in certain patients.

Furthermore, *CYP2J2* was found to be up-regulated during *in vivo* treatment with Cy. Several studies have reported that *CYP2J2* is an important enzyme in the extrahepatic metabolism of drugs and highly expressed in several tissues, including urinary bladder, intestine, and heart.

Recently, *CYP2J2* was reported as a major enzyme involved in the metabolism of drugs and other xenobiotics, and plays an important role in intestinal first-pass metabolism of antihistamines [101-103]. One study that investigated the effect of Cy on the intestinal barrier function reported modification of intestinal permeability and diarrhea during and after Cy conditioning [155].

Involvement of CYP2J2 in Cy bioactivation may explain its acute cardiotoxic effect reported by Gharib *et al.*[156] since CYP2J2 is expressed in the human heart where it is responsible for the epoxidation of endogenous arachidonic acid. Our results may explain in part the cardio-, uro-, and gut toxicity observed during high dose treatment with Cy in transplanted patients. Moreover, this toxicity in combination with the alloreactivity may intensify graft versus host disease observed in transplanted patients.

In order to better understand the mechanisms involved in cyclophosphamide action, global gene expression profiling (other than CYPs) was studied in the patients conditioned with Cy and TBI. The data analysis has generated comprehensive knowledge that can be employed in understanding the rationales by which Cy is used as a conditioning or immunosuppressive /immunoregulatory or agent.

Treatment with Cy down-regulated the expression of several genes mapped to immune/autoimmune activation, allograft rejection and GVHD. This finding strongly confirms that this alkylating agent is a potent immunosuppressive agent. The most noticeable down-regulated genes are *CD3*, *CD28*, *CTLA4*, *MHC II*, *PRF1*, *GZMB* and *IL-2R*.

CD3 molecule is a complex protein that is expressed as a co-receptor in all mature T lymphocytes and a subset of NK cells [157]. It is important in T cell activation. CD3 is targeted by several drugs, including monoclonal antibodies, and thus, suitable for the treatment of different autoimmune diseases [158, 159]. Down-regulation of *CD3* gene expression implies that the initial event of T cell activation, which requires the formation of a complex consisting of CD3 and T cell receptor, is impaired upon treatment with Cy.

CD28 and CTLA4 are two surface molecules that are important in activation and subsequent regulation of cell-mediated immune responses [160]. CD28 is constitutively expressed on the surface of T cells and provides a key co-stimulatory signal upon interaction with CD80 (B7-1) and CD86 (B7-2) on antigen-presenting cells [161]. In contrast, CTLA4 is expressed transiently in the activated T cells. CTLA4, by binding to CD80 or CD86, delivers negative signals, which leads to T cell inactivation [161]. Treatment with Cy has down-regulated the expression of both *CD28* and *CTLA4* suggests that this drug exerts dual effects on T cells as it suppresses the early phase of T cell activation as well as prolongs the activity of effector T cells.

MHC II molecules (major histocompatibility complex class II molecules) are the key molecules involved in presenting antigens to CD4+ T cells. These molecules are constitutively expressed in professional (macrophages, dendritic and B cells) and non-professional (thymic epithelial cells) antigen presenting cells [162]. By binding to foreign peptides, these molecules provide “signal 1” for activation of CD4+ T cells. Thus, down-regulation of the expression of *MHC II* implies that Cy prevents T cell activation by impairing the process of MHC II mediated antigen presentation. Furthermore, this can also explain the efficacy of Cy in the treatment of autoimmune diseases.

Due to its immunosuppressive effects in autoimmune diseases, cyclophosphamide has recently been used in high doses after HSCT to prevent graft rejection and GVHD [20]. In these settings, HLA matching does not seem to be important if the patient receives Cy post-transplantation, which is a great importance for the patients lacking conventional stem cell donors [163, 164].

The *PRF1* (perforin-1) gene encodes a cytolytic protein, which is found in cytotoxic T cells and NK cells. PRF1 shares structural and functional similarities with complement component 9 (C9) [165]. Like BRF1, GZMB (granzyme B) is a protease expressed by cytotoxic T lymphocytes and NK cells and induces apoptosis on target cells [166]. Granzyme can access its target cells through pores formed by perforin [167]. The expression of *BRF1* and *GZMB* genes is down-regulated upon treatment with Cy. This finding strongly suggests that cytotoxic activity of the immune cells mainly mediated by CD8+ T and NK cells is also lessened by Cy.

IL-2R (Interleukin-2 receptor) is expressed on the activated T cells as well as regulatory T (Treg) cells (also known as suppressor T cells). Upon binding to IL-2, IL-2R promotes cell cycle progression through phase G1 of the cell cycle, which leads to the onset of DNA synthesis and replication [168]. Therefore, down-regulation of *IL-2R* gene expression in Cy treated patients may prevent alloreactivity against donor hematopoietic stem cells. Furthermore, the reduction in IL-2R expression might also attenuate the number of Treg cells, which are known to play an unfavourable role in malignancies [169, 170]. Recently, it was reported that Cy can suppress Treg cells and allow more effective induction of antitumor immune responses [171].

In addition to the genes related to the immune system, treatment with Cy down-regulated the expression of several genes (e.g., *Ras*, *LMO2*, *MCM4* and *MCM7*) that are related to cancer development and cell cycle progression. For instance, Ras (rat sarcoma) oncoproteins are known to be responsible for signal transmission inside the cells and for participating in cell growth, differentiation and survival [172]. Oncogenic mutations in *Ras* genes have been detected in several human cancers [173, 174].

The *LMO2* (LIM domain only 2) gene encodes a cysteine-rich, two protein structural domain that plays an important role in hematopoietic development; moreover, its ectopic expression in T cells leads to the onset of acute lymphoblastic leukemia (ALL) [175]. In mice, LMO2 induced precancerous stem cells and initiated leukemia (T-ALL) by inducing thymocyte self-renewal [176, 177].

Finally, minichromosome maintenance proteins (MCM) 4 and 7 are known to be essential for the initiation of genomic replication [178] and their down-regulation during Cy treatment confirms the ability of this drug to reduce cancer size by slowing cell replication. MCM4 and MCM7 were found to be involved in both DNA replication and cell cycle pathways. Thus, Cy induced down regulation in *Ras*, *LMO2*, *MCM4* and *MCM7* genes might shed light on the mechanisms underlying the anti-cancer effects of Cy.

Several genes were up-regulated during treatment with Cy. Most of these genes are immune-related receptor genes, e.g. *IL1R2* (interleukin 1 receptor, type II or CD121b), *IL18R1* (interleukin-18 receptor 1 or CDw218a) and *FLT3* (Fms-like tyrosine kinase 3, or CD135). *IL1R2* is a protein expressed on B cells, monocytes and neutrophils and functions as a molecular decoy that sequesters IL-1 $\beta$  and blocks the initiation of downstream signaling, thereby preventing inflammation [179].

Moschella *et al.* have reported that IL-1 $\beta$  was increased and the maximum concentration was reached at day 3 after Cy administration which is in good agreement with our finding [180]. On the other hand, *IL18R1* is a cytokine receptor that specifically binds interleukin 18 (IL18) and is essential for IL18 mediated signal transduction. IFN- $\alpha$  as well as IL12 are reported to induce the expression of this receptor in NK and T cells. Interestingly, *IL18R1* and *IL1R2* genes along with three other members of the interleukin 1 receptor family, including *IL1R1*, *IL1RL2* (IL-1Rrp2), and *IL1RL1* (T1/ST2) form a gene cluster on chromosome 2q [181].

Thus, Cy induced increase in expression of *IL1R2* and *IL18R1* meaning that cytokine receptor genes located on chromosome 2q are susceptible to Cy. In a recent publication, Moschella *et al.* have reported that Cy has activated IFN- $\alpha$  signature and IFN- $\alpha$  -induced proinflammatory mediators. Moreover, Cy also has induced expansion and activation of *IL18R1* and other receptors [182]. These results confirm our finding; however, further studies are warranted to confirm mechanisms underlying this hypothesis.

*FLT3* is a protein expressed on the surface of many hematopoietic progenitor cells and plays an important role in the development of B and T progenitor cells [183]. However, it remains to be elucidated if increased expression of *FLT3* implies that treatment with Cy might lead either directly or indirectly to mobilization of hematopoietic progenitor cells to the periphery.

Our results showed a significant increase in the expression of angiopoietin-related protein 1 (*ANGPTL1*) and c-JUN proto-oncogene (*c-JUN*) genes in all patients. The high expression was independent of Cy treatment. These two genes are known to play an important role in cancer, i.e. *ANGPTL1*, which is a member of the vascular endothelial growth factor family, was reported to mediate a defense mechanism against cancer growth and metastasis. Kuo *et al.* reported the inverse correlation between the expression of *ANGPTL1* and cancer invasion and lymph node metastasis in lung cancer patients and experimental cancer models [184].

Overexpression of *c-JUN* has been shown in several human cancer types such as non-small cell lung cancer, breast cancer, colon cancer and lymphomas [185-188]. Moreover, *c-JUN* was reported to be associated with proliferation and angiogenesis in invasive breast cancer [189]. Jiao *et al.* have reported that c-JUN induced epithelial cellular invasion in breast cancer [190]. Cancer cells are rapidly dividing and c-JUN is important for progression through the G1 phase of the cell cycle [191]. c-JUN antagonizes P53 expression which is a cell cycle arrest inducer [192]. Moreover, c-JUN is an apoptosis down-regulator, which is important for cancer cell survival [191]. c-JUN was reported to promote BCR-ABL induced lymphoid

leukemia [193]. Furthermore, the expression of *c-JUN* was reported to be enhanced in chemotherapy resistant tumors [194-196].

Thus, based on our findings and the reported studies, we propose that these genes might be considered as potential markers for therapeutic efficacy in hematological malignancies. In addition, we strongly believe that targeting the gene expression of *c-JUN* might have therapeutic potential in these diseases [197, 198].

## 6 CONCLUSION

A new, reproducible and robust method for the detection of busulphan and four of its major metabolites was developed, using gas chromatography in combination with mass spectrometry. The quantification of busulphan and its metabolites was an essential contributing factor in achieving a better understanding of the metabolic pathway of busulphan.

FMO3, and to a lesser extent CYPs, are involved in busulphan clearance through metabolism of the busulphan primary core metabolite, THT. Drugs metabolized through FMO3 and CYPs may affect busulphan kinetics and thus alter its pharmacodynamics.

The use of limited sampling in clinical TDM for oral busulphan is robust and reproducible. The method showed that adequate algorithms and sampling times are important elements in order to reach reliable results. This model can be used for dose adjustment of busulphan for adult as well as pediatric patients.

Cyclophosphamide induces both down- and up-regulation of genes belonging predominantly to the immune system. This knowledge can be further expanded by studies on how cyclophosphamide can be used to target specific subpopulations of cells connected to certain diagnoses.

*ANGPTL1* and *c-JUN* were overexpressed in patients with hematological malignancies undergoing HSCT independently from cyclophosphamide treatment. This implies that these genes may be used as markers for target treatment of hematological malignancies.

POR and its polymorphic variants affect the bioactivation of cyclophosphamide. Determination of patient POR genotype and expression levels in addition to CYP2B6 genotype and activity before commencement of cyclophosphamide therapy may have high impact on clinical dose adjustment, and hence on treatment efficacy and outcome.

To the best of our knowledge, this is the first report about the involvement of CYP2J2 in cyclophosphamide metabolism. *In vitro* studies in HL-60 and recombinant enzymes showed that cyclophosphamide was metabolized by CYP2J2. Inhibition of CYP2J2 in HL-60 cells increased cell viability and survival. *CYP2J2* was up-regulated *in vivo* during treatment with cyclophosphamide. Moreover, *CYP2J2* gene expression was significantly up-regulated in patients with hematological malignancies compared to healthy controls.

CYP2J2 is reported to be highly expressed in several tissues including urinary bladder, intestine and heart, which may in part explain cardiotoxicity, urotoxicity and gut toxicity observed during high dose treatment with cyclophosphamide in transplanted patients due to local cyclophosphamide bioactivation in these tissues. Further studies are warranted to confirm the role of CYP2J2 in organ toxicity.

The present results have improved our understanding of Bu/Cy metabolism and may help in developing new strategies for personalized medicine.

## 7 FUTURE PERSPECTIVES

- Further studies should address the effect of each microsomal enzyme on busulphan metabolism and kinetics. These studies should include the enzyme gene polymorphisms and their impact on treatment efficacy.
- Since CYPs are involved in busulphan metabolism, Bu/Cy conditioning protocols should be revised regarding drug administration sequence, time interval between both drugs and concomitant supportive therapy.
- Studies on other SNPs affecting POR activity *in vivo* and subsequently affecting cyclophosphamide kinetics will be of high importance for dose adjustment of cyclophosphamide.
- Other as yet unidentified CYP enzymes might be involved in cyclophosphamide metabolism, and their discovery would help in dose adjustment and in reducing adverse effects.



## 8 ACKNOWLEDGEMENTS

Finally we reach this stage, the end of the journey and the start of a new unknown journey. The entirety of this work was done at *Karolinska Institutet* at the Department of Laboratory Medicine, Division of Clinical Research Center (KFC), Experimental Cancer Medicine (ECM). I really appreciate the opportunity I have been given to study at this place. *NOVUM* is a great research center and I am proud to have worked in this building for more than four years. Since I moved to Sweden, I have spent more time in NOVUM than I have at home and this is how it should be for whoever is interested in “Research”.

First of any acknowledgements goes to **God** (Allah) for the innumerable blessings, support and mercy I had during my PhD journey.

*Professor Moustapha Hassan*, my main supervisor: (Dear Prof.) before anything you know that you were, for me, not only a supervisor. I will never forget all your help and all the great tips for living in Sweden especially to move in, to fix my car in addition to many other tips and support. I really enjoyed your endless invitations and the specially the day we had ice cream with the seagull ☺. I hope I get a chance to pay you back for some part of what you did with me. I hope that you didn't regret replying to my first email. Thank you.

*Associate Professor Zuzana Potáčová*, my co-supervisor: I still remember the first day we met. It was my first day in NOVUM and you came late in the evening after finishing hard day in the clinic. I really appreciate all the effort you put in for me especially during the correcting of my writing. I always enjoyed the scientific discussions with you which end up with new and brilliant ideas. I owe you my appreciations.

*Dr. Ylva Terelius*, my co-supervisor: no more “Tabasco”☺ Thank you for all your guidance and support during my studies. You introduced me to a new world full of kinetics and linearity. I will never forget our VERY late evening meetings and I will miss your nice conversations we had during the pizza time. I hope to stay in contact with you.

*Associate Professor Manuchehr Abedi-Valugerdi*: it was really great to meet you. You always have enriched our discussions. You have saved my studies several times and thank you for all your help in the collaborating and writing.

*Dr. Ali Moshfegh*: Thank you for all your collaboration and help. I know that I gave you headache several times but I appreciate your helpful answers. I enjoyed visiting you in Solna especially in the winter when you offered me “Hot Chocolate”.

*Dr. Ann-Louise Hagbjörk*: Thank you for introducing me to the microsomal world. You taught me the base of many experiments which were the corner stone for most of my studies. The day I spent at your company was one of my best days ever.

*Associate Professor Jonas Mattsson*: Thank you for helping me in all clinical studies with patients. Your input from the clinical point of view was very valuable and enriched my work. Thank you for all quick answers to my emails.

**Jennifer Usterud**, the great secretary: Thank you for all your help in revising my writing and preparing the manuscripts for submission. I would like to additionally thank you for you taking care of all my papers and applications. You are the most active person I have ever met.

**Professor Andrej Weintraub**: thank you for all your guidance and positive support during all my studies. I will never forget your encouragement before my half time control.

**Professor Mats Eriksson**, my mentor: thank you for taking such responsibility. I'm happy that we didn't have any troubles over the four years of study. All my best wishes to you.

All people at the administration of **Clinical Research Center** (KFC): **Hanna**, you helped me so much with all administrative issues from the first to the last day. **Kathrin**, you came late but it was great to meet such a nice and smiley person, all best wishes for your marriage. **Kirsti**, thank you for your help, especially with all cards requirements. **Lottie**, it is enough to say that I will never forget your birthday as we share the same day, thank you for everything. Till **Eissa, Nelsson** och **Sara**, tack för din chatt med mig på Svenska ☺.

**Marita Ward**, the smiley helpful lady: I really enjoyed visiting your office and meeting you. Your smile always told me that everything will be fine. Thank you for your help with my LADOK and all my applications from admission till dissertation.

**Professor Alaa Saad**, professor of Clinical Pathology, Faculty of Medicine, Suez Canal University: thank you for opening the door for me and my colleagues to have the chance to study at Karolinska Institutet. I appreciate all your effort, contact and care during my studies.

I would like to thank **Professor Emad Ismail**, **Professor Samir Abdel Monem** and **Professor Moushira Abdel Wahab** as well as all of my professors and colleagues at the Department of Biochemistry and Molecular Biology, Faculty of Medicine, Suez Canal University, Egypt for all contact and support I had from them. I also want to thank **Professor Enas El Sheikh** and **Professor Maivel Ghattas** from the new Faculty of Medicine, Port-Said University, good luck with the new project and all my best wishes to you.

**Dr. Brigitte Twelkmeyer**: thank you for introducing me to the mass spectrometry world. Congratulations for your baby ☺. My collaborators, **Dr. Alina**, **Dr. Sofia** and **Dr. Tommy**; thank you for all help and hard work we had together. Everyone at **CAST** and **PKL**, thank you for your help during long days and nights. Special thanks to **Anette Hallander**.

To our collaborators at KTH, **Professor Mamoun** and **Dr. Fei**; thank you for all the meetings and collaboration we had. I really enjoyed visiting your lab.

To my friends at **ECM** group, former and present members who I spent with them more than what I spent with my family; I would like to thank all of you for the endless pleasure and happiness we have endured together, and for all days we spent to raise up the name of our group. I will never forget all fun times we had during picnics, lunches and Christmas tables. Thank you in person; **Dr. Behnam** and his lovely family, our young boss at office especially when it is lunch time. **Dr. Sulaiman** and his lovely family, miss you all so much and miss all

our talks in the kitchen. **Mona** and her lovely family, looking forward for your dissertation soon “InshaALLah”. **Dr. Maria** and **Dr. Jose**, I really enjoyed all the funny discussion about philosophy. **Dr. Maryam** and **Dr. Raoul**, I will never forget the “Sushi” day and thank you for all the picnics you planned. **Dr. Åsa**, finally we had a Swedish member in the group. Both **Heba** and **Fadwa**, It is not wise to write your names at the same line as you will never stop talking. Good luck with your PhD. **Dr. Randa**, **Dr. Heevy**, **Svetlana**, **Ladan** and our new member **Mohamed Alaa**, good luck with all your future. Finally, to my students and friends, **David** and **Sean**; it was really great to meet both of you. I enjoyed our work together so much. From the bottom of my heart I wish you the best in your future.

I want to dedicate my thesis to the memory of **Dr. Hatem Sallam**; the person who was waiting for me upon arrival to Arlanda airport for the first time and who helped me to establish my life in Sweden. I can't imagine that I can't invite you to my dissertation. I'm thankful for all that you have done for me and may God bless your family.

Thank you to all my friends and corridor mates especially the anesthesia group: **Christina**, **Maria**, **Eva**, **Towe**, **Nicolas**, **Henrik**, **Katrin** and **Siva**. MCG group; **Dara**, **Abdel Rahman**, **Alamdar**, **Burcu** and **Sylvian** and to smiley **Risul** and to our lab guest; **Ylva**. It was nice to meet you all; I enjoyed all our talks in the corridor and in the kitchen and my best wishes go to you. To my Persian friends, **Dr. Mohsen**; thank you for BBQ organizations. **Yaser**, looking forward to your next movie. **Ghazaleh** and **Amir**, it was a pleasure to meet you.

My friends, **Dr. Rami Genead**: I will never forget all our nice times together. Good luck with **Dr. Manal** and God bless your lovely **Adam**. **Dr. Mohamed Yousry** and **Dr. Sally**, thank you for all invitations at your home. All best wishes to you and your cute **Jannah** and **Abdullah**. **Dr. Hamdy Omar**, the nice person I knew since I was studying medicine. It was fun to join your political discussions with the boss. Good luck to you and your family. **Dr. Mohamed Saliem**, thank you for all your advice, especially in the beginning, I wish the best to you and your family. **Dr. Eman Zaghloul**, one day we will meet in Egypt “InshaAllah”, good luck with your future and your kids. **Ramy Helal**, Good luck with your studies. **Dr. Kariem Ezzat**, looking forward to seeing you and your lovely family. **Dr. Lauy Al Anati**, it was nice to meet you and your family and good luck with all your future prospects. To all my friends in Egypt and on Facebook, thank you for all your contact and support.

**Mr. Ossama Khalaf**: thank you for all your help, I felt that I have had a real support since I met you. **Mr. Medhat Shenouda**, thank you for all the nices time and visits with your lovely family, it was really great to meet you. **Mr. Yahia Farh**, visiting you always gives me the feeling that I'm back home to “Port-Said”, thank you for helping me especially with my car. **Mr. Ahmed**, It was pleasure to meet you, thank you for keeping in touch. **Mr. Atef**, I will never forget the times we spent at your restaurant, hope you get well soon.

**Eng. Ramez ElSisi** and **Mrs. Sara**: thank you for all fun we had together. I won a real friend abroad. Take care of my cute “**Yassino**”. **Dr. Ahmed Reda** and **Dr. Marwa**, it was pleasure to know such a great family, good luck with your PhD and your lovely kids “**Omar & Ali**”. Last

but not least, my childhood friend: **Dr. Moustafa El Masry** and **Dr. Maie**, it was great when you moved to Sweden. I will never forget our crazy days in Stockholm when our wives were away ☺. Take care of your cute **Nour**.

I would like to thank the Egyptian Ambassador in Stockholm, **Mr. Ambassador Wael Nasr**, for all his support and effort to upgrade the research in Egypt. It was really a great day when he visited our lab.

**My family**, all my aunts, uncles, cousins and their families (sorry that I don't have space to write all your names ☺); thank you all for all the contact, support and care during my studies. I also enjoyed all the times we had together in my short vacations at home. **Grandma**; I wish you were here today.

My parents in-law, **Dr. Abdel Wahab El Masry** and **Dr. Fawzeya El Mahalawy**, and my family in-law; **Dr. Mohamed**, **Dr. May**, **Dr. Menna** and **Eng. Mohamed Hossam**; thank you for all love and care I received for more than 10 years. I have built so many memories during the days you were visiting us. I'm looking forward to seeing my lovely **Mouaz** and **Yassin**. Thank you for the best gift I ever had, my wife, **Reem**.

My only brother, **Dr. Ahmed El Serafi** and **Dr. Raniah**; thank you for all the happy days and memories we had together and for all your calls and support. I hope that we can enjoy more vacations as one big family and finally I will be able to see my lovely **Rahma** and **Omar**.

My parents, **Prof. Taher El Serafi** and **Dr. Fardous Rezk**; simply, I can't find the words, but without both of you I would never be in such a position. The support you have given to me I have never seen in any other families. I owe you A LOT that I can't pay back, but at least I will do my best to make you happy and proud of your son. I love you and may Allah bless your lives with health and happiness.

Last but not least, to my wife (and life), **Dr. Reem El Masry**; we started our journey together from the very first day in the middle of the freezing January and here we are now. Thank you for the endless love and support and for understanding my need to work during the weekends. Now it is the highest time to take a break and I'm looking forward to more cruises together. I love you and I can't imagine my life without you. And to my only and lovely son **Youssef**, when we came to Sweden you were just taking your first walking steps. I hope that one day you will understand what your father did and that you will be proud of him. You are the only one in the world that I wish to see one day as better than me. I love you.

This thesis was kindly supported by generous grants from the **Swedish Cancer Society** (CancerFonden), the **Swedish Childhood Cancer Foundation** (Barncancerfonden) and **Karolinska Institutet foundation** (KI Fonder).

## 9 REFERENCES

1. Sudhakar, A., *History of Cancer, Ancient and Modern Treatment Methods*. J Cancer Sci Ther, 2009. **1**(2): p. 1-4.
2. Reeds, K., *Dioscorides unriddled. "Dioscorides on pharmacy and medicine"*. By John M. Riddle. Essay review. Isis, 1987. **78**(291): p. 85-8.
3. Farber, S. and L.K. Diamond, *Temporary remissions in acute leukemia in children produced by folic acid antagonist, 4-aminopteroyl-glutamic acid*. N Engl J Med, 1948. **238**(23): p. 787-93.
4. DeVita, V.T., Jr. and E. Chu, *A history of cancer chemotherapy*. Cancer Res, 2008. **68**(21): p. 8643-53.
5. Sabattini, E., et al., *WHO classification of tumours of haematopoietic and lymphoid tissues in 2008: an overview*. Pathologica, 2010. **102**(3): p. 83-7.
6. Thomas, E.D., et al., *Intravenous infusion of bone marrow in patients receiving radiation and chemotherapy*. N Engl J Med, 1957. **257**(11): p. 491-6.
7. Riley, R.S., et al., *Hematologic aspects of myeloablative therapy and bone marrow transplantation*. J Clin Lab Anal, 2005. **19**(2): p. 47-79.
8. Burt, R.K., et al., *Clinical applications of blood-derived and marrow-derived stem cells for nonmalignant diseases*. JAMA, 2008. **299**(8): p. 925-36.
9. Copelan, E.A. and H.J. Deeg, *Conditioning for allogeneic marrow transplantation in patients with lymphohematopoietic malignancies without the use of total body irradiation*. Blood, 1992. **80**(7): p. 1648-58.
10. Deeg, H.J., *Delayed complications and long-term effects after bone marrow transplantation*. Hematol Oncol Clin North Am, 1990. **4**(3): p. 641-57.
11. Gupta, T., et al., *Cyclophosphamide plus total body irradiation compared with busulfan plus cyclophosphamide as a conditioning regimen prior to hematopoietic stem cell transplantation in patients with leukemia: a systematic review and meta-analysis*. Hematol Oncol Stem Cell Ther, 2011. **4**(1): p. 17-29.
12. Wingard, J.R., et al., *Growth in children after bone marrow transplantation: busulfan plus cyclophosphamide versus cyclophosphamide plus total body irradiation*. Blood, 1992. **79**(4): p. 1068-73.
13. Peters, W.P., et al., *Clinical and pharmacologic effects of high dose single agent busulfan with autologous bone marrow support in the treatment of solid tumors*. Cancer Res, 1987. **47**(23): p. 6402-6.
14. Bacigalupo, A., et al., *Defining the intensity of conditioning regimens: working definitions*. Biol Blood Marrow Transplant, 2009. **15**(12): p. 1628-33.
15. Santos, G.W., et al., *Marrow transplantation for acute nonlymphocytic leukemia after treatment with busulfan and cyclophosphamide*. N Engl J Med, 1983. **309**(22): p. 1347-53.

16. Tutschka, P.J., E.A. Copelan, and J.P. Klein, *Bone marrow transplantation for leukemia following a new busulfan and cyclophosphamide regimen*. *Blood*, 1987. **70**(5): p. 1382-8.
17. Eberly, A.L., et al., *Optimal prevention of seizures induced by high-dose busulfan*. *Pharmacotherapy*, 2008. **28**(12): p. 1502-10.
18. Kondo, N., et al., *DNA damage induced by alkylating agents and repair pathways*. *J Nucleic Acids*, 2010. **2010**: p. 543531.
19. Binotto, G., L. Trentin, and G. Semenzato, *Ifosfamide and cyclophosphamide: effects on immunosurveillance*. *Oncology*, 2003. **65**(Suppl 2): p. 17-20.
20. Luznik, L. and E.J. Fuchs, *High-dose, post-transplantation cyclophosphamide to promote graft-host tolerance after allogeneic hematopoietic stem cell transplantation*. *Immunol Res*, 2010. **47**(1-3): p. 65-77.
21. Guengerich, F.P., *Common and uncommon cytochrome P450 reactions related to metabolism and chemical toxicity*. *Chem Res Toxicol*, 2001. **14**(6): p. 611-50.
22. Guengerich, F.P., *Cytochrome p450 and chemical toxicology*. *Chem Res Toxicol*, 2008. **21**(1): p. 70-83.
23. Evans, W.E. and J.A. Johnson, *Pharmacogenomics: the inherited basis for interindividual differences in drug response*. *Annu Rev Genomics Hum Genet*, 2001. **2**: p. 9-39.
24. Nelson, D.R., et al., *Comparison of cytochrome P450 (CYP) genes from the mouse and human genomes, including nomenclature recommendations for genes, pseudogenes and alternative-splice variants*. *Pharmacogenetics*, 2004. **14**(1): p. 1-18.
25. Pastore, A., et al., *Determination of blood total, reduced, and oxidized glutathione in pediatric subjects*. *Clin Chem*, 2001. **47**(8): p. 1467-9.
26. Pompella, A., et al., *The changing faces of glutathione, a cellular protagonist*. *Biochem Pharmacol*, 2003. **66**(8): p. 1499-503.
27. Hassan, M. and H. Ehrsson, *Metabolism of 14C-busulfan in isolated perfused rat liver*. *Eur J Drug Metab Pharmacokinet*, 1987. **12**(1): p. 71-6.
28. Hassan, M. and H. Ehrsson, *Urinary metabolites of busulfan in the rat*. *Drug Metab Dispos*, 1987. **15**(3): p. 399-402.
29. Hassan, M., et al., *Pharmacokinetic and metabolic studies of busulfan in rat plasma and brain*. *Eur J Drug Metab Pharmacokinet*, 1988. **13**(4): p. 301-5.
30. Hassan, M., et al., *Pharmacokinetic and metabolic studies of high-dose busulphan in adults*. *Eur J Clin Pharmacol*, 1989. **36**(5): p. 525-30.
31. Gibbs, J.P., M. Czerwinski, and J.T. Slattery, *Busulfan-glutathione conjugation catalyzed by human liver cytosolic glutathione S-transferases*. *Cancer Res*, 1996. **56**(16): p. 3678-81.
32. Hassan, M. and B.S. Andersson, *Role of pharmacogenetics in busulfan/cyclophosphamide conditioning therapy prior to hematopoietic stem cell transplantation*. *Pharmacogenomics*, 2013. **14**(1): p. 75-87.
33. Hassan, M., et al., *Ketobemidone may alter busulfan pharmacokinetics during high-dose therapy*. *Ther Drug Monit*, 2000. **22**(4): p. 383-5.

34. Nilsson, C., et al., *The effect of metronidazole on busulfan pharmacokinetics in patients undergoing hematopoietic stem cell transplantation*. Bone Marrow Transplant, 2003. **31**(6): p. 429-35.
35. Buggia, I., et al., *Itraconazole can increase systemic exposure to busulfan in patients given bone marrow transplantation*. GITMO (Gruppo Italiano Trapianto di Midollo Osseo). Anticancer Res, 1996. **16**(4A): p. 2083-8.
36. Hassan, M., et al., *The effect of busulphan on the pharmacokinetics of cyclophosphamide and its 4-hydroxy metabolite: time interval influence on therapeutic efficacy and therapy-related toxicity*. Bone Marrow Transplant, 2000. **25**(9): p. 915-24.
37. Cashman, J.R., *Structural and catalytic properties of the mammalian flavin-containing monooxygenase*. Chem Res Toxicol, 1995. **8**(2): p. 166-81.
38. Lawton, M.P., et al., *A nomenclature for the mammalian flavin-containing monooxygenase gene family based on amino acid sequence identities*. Arch Biochem Biophys, 1994. **308**(1): p. 254-7.
39. Hernandez, D., et al., *Organization and evolution of the flavin-containing monooxygenase genes of human and mouse: identification of novel gene and pseudogene clusters*. Pharmacogenetics, 2004. **14**(2): p. 117-30.
40. Yanni, S.B., et al., *Role of flavin-containing monooxygenase in oxidative metabolism of voriconazole by human liver microsomes*. Drug Metab Dispos, 2008. **36**(6): p. 1119-25.
41. Yamazaki, H. and M. Shimizu, *Survey of variants of human flavin-containing monooxygenase 3 (FMO3) and their drug oxidation activities*. Biochem Pharmacol, 2013. **85**(11): p. 1588-93.
42. Bloom, A.J., et al., *Effects upon in-vivo nicotine metabolism reveal functional variation in FMO3 associated with cigarette consumption*. Pharmacogenet Genomics, 2013. **23**(2): p. 62-8.
43. Hassan, M., et al., *Busulfan bioavailability*. Blood, 1994. **84**(7): p. 2144-50.
44. Grochow, L.B., et al., *Pharmacokinetics of busulfan: correlation with veno-occlusive disease in patients undergoing bone marrow transplantation*. Cancer Chemother Pharmacol, 1989. **25**(1): p. 55-61.
45. Bartelink, I., et al., *Association between Busulfan Exposure and Outcome in Children Receiving Intravenous Busulfan before Hematologic Stem Cell Transplantation*. Biology of Blood and Marrow Transplantation, 2009: p. 231-241.
46. Bartelink, I., et al., *TARGETING TO AN OPTIMAL AUC OF INTRAVENOUS BUSULFAN PREVENTS GRAFT FAILURE IN TRANSPLANTATION IN CHILDREN WITH NON-MALIGNANT DISEASES*. Biology of Blood and Marrow Transplantation, 2009: p. 76-77.
47. McCune, J.S. and L.A. Holmberg, *Busulfan in hematopoietic stem cell transplant setting*. Expert Opin Drug Metab Toxicol, 2009. **5**(8): p. 957-69.
48. Robertson, G.R., C. Liddle, and S.J. Clarke, *Inflammation and altered drug clearance in cancer: transcriptional repression of a human CYP3A4 transgene in tumor-bearing mice*. Clin Pharmacol Ther, 2008. **83**(6): p. 894-7.

49. Ljungman, P., et al., *High busulfan concentrations are associated with increased transplant-related mortality in allogeneic bone marrow transplant patients*. Bone Marrow Transplant, 1997. **20**(11): p. 909-13.
50. Vassal, G., *Pharmacologically-guided dose adjustment of busulfan in high-dose chemotherapy regimens: rationale and pitfalls (review)*. Anticancer Res, 1994. **14**(6A): p. 2363-70.
51. Chattergoon, D.S., et al., *An improved limited sampling method for individualised busulphan dosing in bone marrow transplantation in children*. Bone Marrow Transplant, 1997. **20**(5): p. 347-54.
52. Hassan, M., et al., *Busulphan kinetics and limited sampling model in children with leukemia and inherited disorders*. Bone Marrow Transplant, 1996. **18**(5): p. 843-50.
53. Sandström, M., et al., *Population pharmacokinetic analysis resulting in a tool for dose individualization of busulphan in bone marrow transplantation recipients*. Bone Marrow Transplant, 2001. **28**(7): p. 657-64.
54. Sladek, N.E., *Metabolism of oxazaphosphorines*. Pharmacol Ther, 1988. **37**(3): p. 301-55.
55. Cho, J.Y., et al., *Haplotype structure and allele frequencies of CYP2B6 in a Korean population*. Drug Metab Dispos, 2004. **32**(12): p. 1341-4.
56. Chang, T.K., et al., *Differential activation of cyclophosphamide and ifosfamide by cytochromes P-450 2B and 3A in human liver microsomes*. Cancer Res, 1993. **53**(23): p. 5629-37.
57. Ren, S., et al., *Oxidation of cyclophosphamide to 4-hydroxycyclophosphamide and deschloroethylcyclophosphamide in human liver microsomes*. Cancer Res, 1997. **57**(19): p. 4229-35.
58. Raccor, B.S., et al., *Potential contribution of cytochrome P450 2B6 to hepatic 4-hydroxycyclophosphamide formation in vitro and in vivo*. Drug Metab Dispos, 2012. **40**(1): p. 54-63.
59. Afsar, N.A., et al., *Relationship of drug metabolizing enzyme genotype to plasma levels as well as myelotoxicity of cyclophosphamide in breast cancer patients*. Eur J Clin Pharmacol, 2012. **68**(4): p. 389-95.
60. Fernandes, B.J., et al., *Pharmacokinetics of cyclophosphamide enantiomers in patients with breast cancer*. Cancer Chemother Pharmacol, 2011. **68**(4): p. 897-904.
61. Ekins, S. and S.A. Wrighton, *The role of CYP2B6 in human xenobiotic metabolism*. Drug Metab Rev, 1999. **31**(3): p. 719-54.
62. Gervot, L., et al., *Human CYP2B6: expression, inducibility and catalytic activities*. Pharmacogenetics, 1999. **9**(3): p. 295-306.
63. Lang, T., et al., *Extensive genetic polymorphism in the human CYP2B6 gene with impact on expression and function in human liver*. Pharmacogenetics, 2001. **11**(5): p. 399-415.
64. Miksys, S., et al., *Smoking, alcoholism and genetic polymorphisms alter CYP2B6 levels in human brain*. Neuropharmacology, 2003. **45**(1): p. 122-32.
65. Yengi, L.G., et al., *Quantitation of cytochrome P450 mRNA levels in human skin*. Anal Biochem, 2003. **316**(1): p. 103-10.



66. Ward, B.A., et al., *The cytochrome P450 2B6 (CYP2B6) is the main catalyst of efavirenz primary and secondary metabolism: implication for HIV/AIDS therapy and utility of efavirenz as a substrate marker of CYP2B6 catalytic activity.* J Pharmacol Exp Ther, 2003. **306**(1): p. 287-300.
67. Zanger, U.M. and K. Klein, *Pharmacogenetics of cytochrome P450 2B6 (CYP2B6): advances on polymorphisms, mechanisms, and clinical relevance.* Front Genet, 2013. **4**: p. 24.
68. Jaquenoud Sirot, E., et al., *Multicenter study on the clinical effectiveness, pharmacokinetics, and pharmacogenetics of mirtazapine in depression.* J Clin Psychopharmacol, 2012. **32**(5): p. 622-9.
69. Ribaud, H.J., et al., *Pharmacogenetics of plasma efavirenz exposure after treatment discontinuation: an Adult AIDS Clinical Trials Group Study.* Clin Infect Dis, 2006. **42**(3): p. 401-7.
70. Xie, H., et al., *Pharmacogenetics of cyclophosphamide in patients with hematological malignancies.* Eur J Pharm Sci, 2006. **27**(1): p. 54-61.
71. Klein, K., et al., *Genetic variability of CYP2B6 in populations of African and Asian origin: allele frequencies, novel functional variants, and possible implications for anti-HIV therapy with efavirenz.* Pharmacogenet Genomics, 2005. **15**(12): p. 861-73.
72. Rotger, M., et al., *Influence of CYP2B6 polymorphism on plasma and intracellular concentrations and toxicity of efavirenz and nevirapine in HIV-infected patients.* Pharmacogenet Genomics, 2005. **15**(1): p. 1-5.
73. Tsuchiya, K., et al., *Homozygous CYP2B6 \*6 (Q172H and K262R) correlates with high plasma efavirenz concentrations in HIV-1 patients treated with standard efavirenz-containing regimens.* Biochem Biophys Res Commun, 2004. **319**(4): p. 1322-6.
74. Hesse, L.M., et al., *Pharmacogenetic determinants of interindividual variability in bupropion hydroxylation by cytochrome P450 2B6 in human liver microsomes.* Pharmacogenetics, 2004. **14**(4): p. 225-38.
75. Ariyoshi, N., et al., *A single nucleotide polymorphism of CYP2b6 found in Japanese enhances catalytic activity by autoactivation.* Biochem Biophys Res Commun, 2001. **281**(5): p. 1256-60.
76. Xie, H.J., et al., *Role of polymorphic human CYP2B6 in cyclophosphamide bioactivation.* Pharmacogenomics J, 2003. **3**(1): p. 53-61.
77. Lang, T., et al., *Multiple novel nonsynonymous CYP2B6 gene polymorphisms in Caucasians: demonstration of phenotypic null alleles.* J Pharmacol Exp Ther, 2004. **311**(1): p. 34-43.
78. Yao, S., et al., *Gene polymorphisms in cyclophosphamide metabolism pathway, treatment-related toxicity, and disease-free survival in SWOG 8897 clinical trial for breast cancer.* Clin Cancer Res, 2010. **16**(24): p. 6169-76.
79. Reynolds, M. and S.R. McCann, *A comparison between regimens containing chemotherapy alone (busulfan and cyclophosphamide) and chemotherapy (V. RAPID) plus total body irradiation on marrow engraftment following allogeneic bone marrow transplantation.* Eur J Haematol, 1989. **43**(4): p. 314-20.

80. Eroglu, C., et al., *Comparison of total body irradiation plus cyclophosphamide with busulfan plus cyclophosphamide as conditioning regimens in patients with acute lymphoblastic leukemia undergoing allogeneic hematopoietic stem cell transplant*. *Leuk Lymphoma*, 2013.
81. de Jonge, H.J., G. Huls, and E.S. de Bont, *Gene expression profiling in acute myeloid leukaemia*. *The Netherlands journal of medicine*, 2011. **69**(4): p. 167-76.
82. Mills, K., *Gene expression profiling for the diagnosis and prognosis of acute myeloid leukaemia*. *Front Biosci*, 2008. **13**: p. 4605-16.
83. Khokher, S., et al., *Association of immunohistochemically defined molecular subtypes with clinical response to presurgical chemotherapy in patients with advanced breast cancer*. *Asian Pac J Cancer Prev*, 2013. **14**(5): p. 3223-8.
84. Rimsza, L.M., et al., *Gene expression predicts overall survival in paraffin-embedded tissues of diffuse large B-cell lymphoma treated with R-CHOP*. *Blood*, 2008. **112**(8): p. 3425-33.
85. Wang, S.L., et al., *Genetic variation of human cytochrome p450 reductase as a potential biomarker for mitomycin C-induced cytotoxicity*. *Drug Metab Dispos*, 2007. **35**(1): p. 176-9.
86. Pandey, A.V., C.E. Fluck, and P.E. Mullis, *Altered heme catabolism by heme oxygenase-1 caused by mutations in human NADPH cytochrome P450 reductase*. *Biochem Biophys Res Commun*, 2010. **400**(3): p. 374-8.
87. Fluck, C.E., et al., *Mutant P450 oxidoreductase causes disordered steroidogenesis with and without Antley-Bixler syndrome*. *Nat Genet*, 2004. **36**(3): p. 228-30.
88. Huang, N., et al., *Diversity and function of mutations in p450 oxidoreductase in patients with Antley-Bixler syndrome and disordered steroidogenesis*. *Am J Hum Genet*, 2005. **76**(5): p. 729-49.
89. Merla, G., et al., *Submicroscopic deletion in patients with Williams-Beuren syndrome influences expression levels of the nonhemizygous flanking genes*. *Am J Hum Genet*, 2006. **79**(2): p. 332-41.
90. Agrawal, V., N. Huang, and W.L. Miller, *Pharmacogenetics of P450 oxidoreductase: effect of sequence variants on activities of CYP1A2 and CYP2C19*. *Pharmacogenet Genomics*, 2008. **18**(7): p. 569-76.
91. Sandee, D., et al., *Effects of genetic variants of human P450 oxidoreductase on catalysis by CYP2D6 in vitro*. *Pharmacogenet Genomics*, 2010. **20**(11): p. 677-86.
92. Subramanian, M., et al., *Effect of P450 oxidoreductase variants on the metabolism of model substrates mediated by CYP2C9.1, CYP2C9.2, and CYP2C9.3*. *Pharmacogenet Genomics*, 2012. **22**(8): p. 590-7.
93. Zhang, J.J., et al., *Effect of the P450 oxidoreductase \*28 polymorphism on the pharmacokinetics of tacrolimus in Chinese healthy male volunteers*. *Eur J Clin Pharmacol*, 2012.
94. Chen, X., et al., *Influence of Various Polymorphic Variants of Cytochrome P450 Oxidoreductase (POR) on Drug Metabolic Activity of CYP3A4 and CYP2B6*. *Plos One*, 2012. **7**(6).
95. Wortham, M., et al., *Expression of constitutive androstane receptor, hepatic nuclear factor 4 alpha, and P450 oxidoreductase genes determines interindividual variability*

- in basal expression and activity of a broad scope of xenobiotic metabolism genes in the human liver.* Drug Metabolism and Disposition, 2007. **35**(9): p. 1700-1710.
96. de Jonge, H., et al., *The P450 oxidoreductase \*28 SNP is associated with low initial tacrolimus exposure and increased dose requirements in CYP3A5-expressing renal recipients.* Pharmacogenomics, 2011. **12**(9): p. 1281-91.
  97. Ma, J., et al., *Mapping of the CYP2J cytochrome P450 genes to human chromosome 1 and mouse chromosome 4.* Genomics, 1998. **49**(1): p. 152-5.
  98. Delozier, T.C., et al., *Detection of human CYP2C8, CYP2C9, and CYP2J2 in cardiovascular tissues.* Drug Metab Dispos, 2007. **35**(4): p. 682-8.
  99. Node, K., et al., *Anti-inflammatory properties of cytochrome P450 epoxygenase-derived eicosanoids.* Science, 1999. **285**(5431): p. 1276-9.
  100. Xu, X., X.A. Zhang, and D.W. Wang, *The roles of CYP450 epoxygenases and metabolites, epoxyeicosatrienoic acids, in cardiovascular and malignant diseases.* Adv Drug Deliv Rev, 2011. **63**(8): p. 597-609.
  101. Hashizume, T., et al., *Involvement of CYP2J2 and CYP4F12 in the metabolism of ebastine in human intestinal microsomes.* J Pharmacol Exp Ther, 2002. **300**(1): p. 298-304.
  102. Lee, C.A., et al., *Identification of novel substrates for human cytochrome P450 2J2.* Drug Metab Dispos, 2010. **38**(2): p. 347-56.
  103. Matsumoto, S., et al., *Involvement of CYP2J2 on the intestinal first-pass metabolism of antihistamine drug, astemizole.* Drug Metab Dispos, 2002. **30**(11): p. 1240-5.
  104. Noshita, N., et al., *Copper/zinc superoxide dismutase attenuates neuronal cell death by preventing extracellular signal-regulated kinase activation after transient focal cerebral ischemia in mice.* J Neurosci, 2002. **22**(18): p. 7923-30.
  105. Bhatnagar, A., *Beating ischemia: a new feat of EETs?* Circ Res, 2004. **95**(5): p. 443-5.
  106. Gross, G.J., et al., *Cytochrome P450 and arachidonic acid metabolites: role in myocardial ischemia/reperfusion injury revisited.* Cardiovasc Res, 2005. **68**(1): p. 18-25.
  107. Seubert, J.M., et al., *Role of epoxyeicosatrienoic acids in protecting the myocardium following ischemia/reperfusion injury.* Prostaglandins Other Lipid Mediat, 2007. **82**(1-4): p. 50-9.
  108. Li, R., et al., *Cytochrome P450 2J2 is protective against global cerebral ischemia in transgenic mice.* Prostaglandins Other Lipid Mediat, 2012. **99**(3-4): p. 68-78.
  109. Chen, C., et al., *Cytochrome P450 2J2 is highly expressed in hematologic malignant diseases and promotes tumor cell growth.* J Pharmacol Exp Ther, 2011. **336**(2): p. 344-55.
  110. Freedman, R.S., et al., *Comparative analysis of peritoneum and tumor eicosanoids and pathways in advanced ovarian cancer.* Clin Cancer Res, 2007. **13**(19): p. 5736-44.
  111. Jiang, J.G., et al., *Cytochrome p450 epoxygenase promotes human cancer metastasis.* Cancer Res, 2007. **67**(14): p. 6665-74.

112. Chen, C., et al., *Selective inhibitors of CYP2J2 related to terfenadine exhibit strong activity against human cancers in vitro and in vivo*. J Pharmacol Exp Ther, 2009. **329**(3): p. 908-18.
113. Xie, H.J., et al., *Effect of cyclophosphamide on gene expression of cytochromes p450 and beta-actin in the HL-60 cell line*. Eur J Pharmacol, 2002. **449**(3): p. 197-205.
114. Ehrsson, H., et al., *Busulfan kinetics*. Clinical pharmacology and therapeutics, 1983. **34**(1): p. 86-9.
115. Ringden, O., et al., *Methotrexate, cyclosporine, or both to prevent graft-versus-host disease after HLA-identical sibling bone marrow transplants for early leukemia?* Blood, 1993. **81**(4): p. 1094-101.
116. Przepiorcka, D., et al., *1994 Consensus Conference on Acute GVHD Grading*. Bone Marrow Transplant, 1995. **15**(6): p. 825-8.
117. Remberger, M., et al., *A high antithymocyte globulin dose increases the risk of relapse after reduced intensity conditioning HSCT with unrelated donors*. Clin Transplant, 2013. **27**(4): p. E368-74.
118. El-Serafi, I., et al., *Cyclophosphamide alters the gene expression profile in patients treated with high doses prior to stem cell transplantation*. Plos One, 2014. **9**(1): p. e86619.
119. El-Serafi, I., et al., *Gas chromatographic-mass spectrometry method for the detection of busulphan and its metabolites in plasma and urine*. J Chromatogr B Analyt Technol Biomed Life Sci, 2013. **913-914**: p. 98-105.
120. Sadeghi, B., et al., *GVHD after chemotherapy conditioning in allogeneic transplanted mice*. Bone Marrow Transplant, 2008. **42**(12): p. 807-18.
121. Smith, P.B. and C. Crespi, *Thiourea toxicity in mouse C3H/10T1/2 cells expressing human flavin-dependent monooxygenase 3*. Biochem Pharmacol, 2002. **63**(11): p. 1941-8.
122. Ren, S., et al., *Discovery and characterization of novel, potent, and selective cytochrome P450 2J2 inhibitors*. Drug Metab Dispos, 2013. **41**(1): p. 60-71.
123. Afsharian, P., et al., *The effect of ciprofloxacin on cyclophosphamide pharmacokinetics in patients with non-Hodgkin lymphoma*. Eur J Haematol, 2005. **75**(3): p. 206-11.
124. Griskevicius, L., L. Meurling, and M. Hassan, *Simple method based on fluorescent detection for the determination of 4-hydroxycyclophosphamide in plasma*. Ther Drug Monit, 2002. **24**(3): p. 405-9.
125. Hassan, M. and H. Ehrsson, *Gas chromatographic determination of busulfan in plasma with electron-capture detection*. J Chromatogr, 1983. **277**: p. 374-80.
126. Ehrsson, H. and M. Hassan, *Determination of busulfan in plasma by GC-MS with selected-ion monitoring*. J Pharm Sci, 1983. **72**(10): p. 1203-5.
127. Ritter, C.A., et al., *Determination of tetrahydrothiophene formation as a probe of in vitro busulfan metabolism by human glutathione S-transferase A1-1: use of a highly sensitive gas chromatographic-mass spectrometric method*. J Chromatogr B Biomed Sci Appl, 1999. **730**(1): p. 25-31.

128. Xie, H.J., et al., *Alteration of pharmacokinetics of cyclophosphamide and suppression of the cytochrome p450 genes by ciprofloxacin*. Bone Marrow Transplant, 2003. **31**(3): p. 197-203.
129. Shah, V.P., et al., *Analytical methods validation: bioavailability, bioequivalence and pharmacokinetic studies. Conference report*. Eur J Drug Metab Pharmacokinet, 1991. **16**(4): p. 249-55.
130. Shah, V.P., et al., *Bioanalytical method validation--a revisit with a decade of progress*. Pharm Res, 2000. **17**(12): p. 1551-7.
131. Schuler, U., et al., *Busulfan pharmacokinetics in bone marrow transplant patients: is drug monitoring warranted?* Bone Marrow Transplant, 1994. **14**(5): p. 759-65.
132. Vassal, G., et al., *Is 600 mg/m<sup>2</sup> the appropriate dosage of busulfan in children undergoing bone marrow transplantation?* Blood, 1992. **79**(9): p. 2475-9.
133. Balasubramanian, P., et al., *Evaluation of existing limited sampling models for busulfan kinetics in children with beta thalassaemia major undergoing bone marrow transplantation*. Bone Marrow Transplant, 2001. **28**(9): p. 821-5.
134. Nieto, Y. and W.P. Vaughan, *Pharmacokinetics of high-dose chemotherapy*. Bone Marrow Transplant, 2004. **33**(3): p. 259-69.
135. Purves, R.D., *Optimum numerical integration methods for estimation of area-under-the-curve (AUC) and area-under-the-moment-curve (AUMC)*. J Pharmacokinet Biopharm, 1992. **20**(3): p. 211-26.
136. Nerella, N.G., L.H. Block, and P.K. Noonan, *THE IMPACT OF LAG TIME ON THE ESTIMATION OF PHARMACOKINETIC PARAMETERS .I. ONE-COMPARTMENT OPEN MODEL*. Pharmaceutical Research, 1993. **10**(7): p. 1031-1036.
137. Ferraty, F., P. Hall, and P. Vieu, *Most-predictive design points for functional data predictors*. Biometrika, 2010. **97**(4): p. 807-24.
138. Sjo, F., et al., *Comparison of algorithms for oral busulphan area under the concentration-time curve limited sampling estimate*. Clin Drug Investig, 2014. **34**(1): p. 43-52.
139. Naidong, W., et al., *Novel liquid chromatographic-tandem mass spectrometric methods using silica columns and aqueous-organic mobile phases for quantitative analysis of polar ionic analytes in biological fluids*. J Chromatogr B Biomed Sci Appl, 2001. **754**(2): p. 387-99.
140. Karalis, V. and P. Macheras, *Current regulatory approaches of bioequivalence testing*. Expert Opin Drug Metab Toxicol, 2012. **8**(8): p. 929-42.
141. Chunduri, S., et al., *Fludarabine/i.v. BU conditioning regimen: myeloablative, reduced intensity or both?* Bone Marrow Transplant, 2008. **41**(11): p. 935-40.
142. Lindley, C., et al., *Intraindividual variability in busulfan pharmacokinetics in patients undergoing a bone marrow transplant: assessment of a test dose and first dose strategy*. Anticancer Drugs, 2004. **15**(5): p. 453-9.
143. Grochow, L.B., *Busulfan disposition: the role of therapeutic monitoring in bone marrow transplantation induction regimens*. Semin Oncol, 1993. **20**(4 Suppl 4): p. 18-25; quiz 26.

144. Tsuruta, H., et al., *Limited sampling strategies to estimate the area under the concentration-time curve. Biases and a proposed more accurate method.* Methods Inf Med, 2012. **51**(5): p. 383-94.
145. Canal, P., E. Chatelut, and S. Guichard, *Practical treatment guide for dose individualisation in cancer chemotherapy.* Drugs, 1998. **56**(6): p. 1019-38.
146. Gulbis, A.M., et al., *Busulfan and metronidazole: an often forgotten but significant drug interaction.* Ann Pharmacother, 2011. **45**(7-8): p. e39.
147. Uppugunduri, C.R., et al., *The association of cytochrome P450 genetic polymorphisms with sulfolane formation and the efficacy of a busulfan-based conditioning regimen in pediatric patients undergoing hematopoietic stem cell transplantation.* Pharmacogenomics J, 2013.
148. Xie, H., et al., *Cyclophosphamide induces mRNA, protein and enzyme activity of cytochrome P450 in rat.* Xenobiotica, 2005. **35**(3): p. 239-51.
149. Hart, S.N. and X.B. Zhong, *P450 oxidoreductase: genetic polymorphisms and implications for drug metabolism and toxicity.* Expert Opin Drug Metab Toxicol, 2008. **4**(4): p. 439-52.
150. Hart, S.N., et al., *Genetic polymorphisms in cytochrome P450 oxidoreductase influence microsomal P450-catalyzed drug metabolism.* Pharmacogenet Genomics, 2008. **18**(1): p. 11-24.
151. Ariyoshi, N., et al., *Q172H replacement overcomes effects on the metabolism of cyclophosphamide and efavirenz caused by CYP2B6 variant with Arg262.* Drug Metab Dispos, 2011. **39**(11): p. 2045-8.
152. Ivanov, M., I. Barragan, and M. Ingelman-Sundberg, *Epigenetic mechanisms of importance for drug treatment.* Trends Pharmacol Sci, 2014.
153. Nagai, F., et al., *Cytochrome P450 (CYP) expression in human myeloblastic and lymphoid cell lines.* Biol Pharm Bull, 2002. **25**(3): p. 383-5.
154. Nguyen, T.A., et al., *Improvement of cyclophosphamide activation by CYP2B6 mutants: from in silico to ex vivo.* Mol Pharmacol, 2008. **73**(4): p. 1122-33.
155. Russo, F., et al., *The effects of fluorouracil, epirubicin, and cyclophosphamide (FEC60) on the intestinal barrier function and gut peptides in breast cancer patients: an observational study.* BMC Cancer, 2013. **13**: p. 56.
156. Gharib, M.I. and A.K. Burnett, *Chemotherapy-induced cardiotoxicity: current practice and prospects of prophylaxis.* Eur J Heart Fail, 2002. **4**(3): p. 235-42.
157. Soudais, C., et al., *Independent mutations of the human CD3-epsilon gene resulting in a T cell receptor/CD3 complex immunodeficiency.* Nat Genet, 1993. **3**(1): p. 77-81.
158. Chatenoud, L. and J.A. Bluestone, *CD3-specific antibodies: a portal to the treatment of autoimmunity.* Nat Rev Immunol, 2007. **7**(8): p. 622-32.
159. Kaufman, A. and K.C. Herold, *Anti-CD3 mAbs for treatment of type 1 diabetes.* Diabetes Metab Res Rev, 2009. **25**(4): p. 302-6.
160. Magistrelli, G., et al., *A soluble form of CTLA-4 generated by alternative splicing is expressed by nonstimulated human T cells.* European journal of immunology, 1999. **29**(11): p. 3596-602.

161. Waterhouse, P., et al., *Lymphoproliferative disorders with early lethality in mice deficient in Ctla-4*. Science (New York, N Y ), 1995. **270**(5238): p. 985-8.
162. Ting, J.P. and J. Trowsdale, *Genetic control of MHC class II expression*. Cell, 2002. **109 Suppl**: p. S21-33.
163. Bashey, A., et al., *T-cell-replete HLA-haploidentical hematopoietic transplantation for hematologic malignancies using post-transplantation cyclophosphamide results in outcomes equivalent to those of contemporaneous HLA-matched related and unrelated donor transplantation*. J Clin Oncol, 2013. **31**(10): p. 1310-6.
164. Luznik, L., P.V. O'Donnell, and E.J. Fuchs, *Post-transplantation cyclophosphamide for tolerance induction in HLA-haploidentical bone marrow transplantation*. Semin Oncol, 2012. **39**(6): p. 683-93.
165. Rosado, C.J., et al., *A common fold mediates vertebrate defense and bacterial attack*. Science (New York, N Y ), 2007. **317**(5844): p. 1548-51.
166. Trapani, J.A., *Target cell apoptosis induced by cytotoxic T cells and natural killer cells involves synergy between the pore-forming protein, perforin, and the serine protease, granzyme B*. Australian and New Zealand journal of medicine, 1995. **25**(6): p. 793-9.
167. Lopez, J.A., et al., *Perforin forms transient pores on the target cell plasma membrane to facilitate rapid access of granzymes during killer cell attack*. Blood, 2013. **121**(14): p. 2659-68.
168. Martino, A., et al., *Stat5 and Sp1 regulate transcription of the cyclin D2 gene in response to IL-2*. Journal of Immunology, 2001. **166**(3): p. 1723-9.
169. Cao, J., et al., *DNA vaccines targeting the encoded antigens to dendritic cells induce potent antitumor immunity in mice*. BMC Immunol, 2013. **14**: p. 39.
170. Matias, B.F., et al., *Influence of immunotherapy with autologous dendritic cells on innate and adaptive immune response in cancer*. Clin Med Insights Oncol, 2013. **7**: p. 165-72.
171. Le, D.T. and E.M. Jaffee, *Regulatory T-cell modulation using cyclophosphamide in vaccine approaches: a current perspective*. Cancer Research, 2012. **72**(14): p. 3439-44.
172. Wennerberg, K., K.L. Rossman, and C.J. Der, *The Ras superfamily at a glance*. J Cell Sci, 2005. **118**(Pt 5): p. 843-6.
173. Goodsell, D.S., *The molecular perspective: the ras oncogene*. Stem Cells, 1999. **17**(4): p. 235-6.
174. Bos, J.L., *ras oncogenes in human cancer: a review*. Cancer Research, 1989. **49**(17): p. 4682-9.
175. El Omari, K., et al., *Structure of the leukemia oncogene LMO2: implications for the assembly of a hematopoietic transcription factor complex*. Blood, 2011. **117**(7): p. 2146-56.
176. McCormack, M.P. and D.J. Curtis, *The thymus under siege: Lmo2 induces precancerous stem cells in a mouse model of T-ALL*. Cell Cycle, 2010. **9**(12): p. 2267-8.

177. McCormack, M.P., et al., *The Lmo2 oncogene initiates leukemia in mice by inducing thymocyte self-renewal*. Science (New York, N Y ), 2010. **327**(5967): p. 879-83.
178. Kearsley, S.E. and K. Labib, *MCM proteins: evolution, properties, and role in DNA replication*. Biochimica et biophysica acta, 1998. **1398**(2): p. 113-36.
179. Mantovani, A., et al., *Tuning of innate immunity and polarized responses by decoy receptors*. Int Arch Allergy Immunol, 2003. **132**(2): p. 109-15.
180. Moschella, F., et al., *Unraveling cancer chemoimmunotherapy mechanisms by gene and protein expression profiling of responses to cyclophosphamide*. Cancer Res, 2011. **71**(10): p. 3528-39.
181. Dale, M. and M.J. Nicklin, *Interleukin-1 receptor cluster: gene organization of IL1R2, IL1R1, IL1RL2 (IL-1Rrp2), IL1RL1 (T1/ST2), and IL18R1 (IL-1Rrp) on human chromosome 2q*. Genomics, 1999. **57**(1): p. 177-9.
182. Moschella, F., et al., *Cyclophosphamide induces a type I interferon-associated sterile inflammatory response signature in cancer patients' blood cells: implications for cancer chemoimmunotherapy*. Clin Cancer Res, 2013. **19**(15): p. 4249-61.
183. Rosnet, O., et al., *Human FLT3/FLK2 gene: cDNA cloning and expression in hematopoietic cells*. Blood, 1993. **82**(4): p. 1110-9.
184. Kuo, T.C., et al., *Angiopoietin-like protein 1 suppresses SLUG to inhibit cancer cell motility*. The Journal of clinical investigation, 2013. **123**(3): p. 1082-95.
185. Szabo, E., et al., *Altered cJUN expression: an early event in human lung carcinogenesis*. Cancer Research, 1996. **56**(2): p. 305-15.
186. Smith, L.M., et al., *cJun overexpression in MCF-7 breast cancer cells produces a tumorigenic, invasive and hormone resistant phenotype*. Oncogene, 1999. **18**(44): p. 6063-70.
187. Zhang, Y., et al., *Critical role of c-Jun overexpression in liver metastasis of human breast cancer xenograft model*. BMC Cancer, 2007. **7**: p. 145.
188. Zhang, H.S., et al., *PAX2 protein induces expression of cyclin D1 through activating AP-1 protein and promotes proliferation of colon cancer cells*. Journal of Biological Chemistry, 2012. **287**(53): p. 44164-72.
189. Vleugel, M.M., et al., *c-Jun activation is associated with proliferation and angiogenesis in invasive breast cancer*. Hum Pathol, 2006. **37**(6): p. 668-74.
190. Jiao, X., et al., *c-Jun induces mammary epithelial cellular invasion and breast cancer stem cell expansion*. J Biol Chem, 2010. **285**(11): p. 8218-26.
191. Wisdom, R., R.S. Johnson, and C. Moore, *c-Jun regulates cell cycle progression and apoptosis by distinct mechanisms*. The EMBO journal, 1999. **18**(1): p. 188-97.
192. Schreiber, M., et al., *Control of cell cycle progression by c-Jun is p53 dependent*. Genes & development, 1999. **13**(5): p. 607-19.
193. Kollmann, K., et al., *c-JUN promotes BCR-ABL-induced lymphoid leukemia by inhibiting methylation of the 5' region of Cdk6*. Blood, 2011. **117**(15): p. 4065-75.
194. Ritke, M.K., et al., *Increased c-jun/AP-1 levels in etoposide-resistant human leukemia K562 cells*. Biochem Pharmacol, 1994. **48**(3): p. 525-33.



195. Rubin, E., et al., *cis-Diamminedichloroplatinum(II) induces c-jun expression in human myeloid leukemia cells: potential involvement of a protein kinase C-dependent signaling pathway*. *Cancer Res*, 1992. **52**(4): p. 878-82.
196. Zhou, J., et al., *Paclitaxel-resistant human ovarian cancer cells undergo c-Jun NH2-terminal kinase-mediated apoptosis in response to noscapine*. *J Biol Chem*, 2002. **277**(42): p. 39777-85.
197. Gurzov, E.N., et al., *Targeting c-Jun and JunB proteins as potential anticancer cell therapy*. *Oncogene*, 2008. **27**(5): p. 641-52.
198. Xia, Y., et al., *Differential Regulation of c-Jun Protein Plays an Instrumental Role in Chemoresistance of Cancer Cells*. *Journal of Biological Chemistry*, 2013. **288**(27): p. 19321-9.